ISTANBUL TECHNICAL UNIVERSITY ★ EURASIA INSTITUTE OF EARTH SCIENCES

UNDERSTANDING THE SOURCES AND THE EXTEND OF ATMOSPHERIC PARTICULATE MATTER PROBLEM OVER TURKEY USING MESOSCALE CHEMICAL TRANSPORT MODEL

Ph.D. THESIS

Metin BAYKARA

Department of Climate and Marine Sciences

Earth System Sciences Programme

DECEMBER 2018

ISTANBUL TECHNICAL UNIVERSITY ★ EURASIA INSTITUTE OF EARTH SCIENCES

UNDERSTANDING THE SOURCES AND THE EXTEND OF ATMOSPHERIC PARTICULATE MATTER PROBLEM OVER TURKEY USING MESOSCALE CHEMICAL TRANSPORT MODEL

Ph.D. THESIS

Metin BAYKARA
(601132002)

Department of Climate and Marine Sciences

Earth System Sciences Programme

Thesis Advisor: Prof. Dr. Alper ÜNAL

DECEMBER 2018

İSTANBUL TEKNİK ÜNİVERSİTESİ ★ AVRASYA YER BİLİMLERİ ENSTİTÜSÜ

ORTA ÖLÇEKLİ KİMYASAL TAŞINIM MODELİ İLE TÜRKİYE'DEKİ PARTİKÜL MADDE PROBLEMİ VE KAYNAKLARININ ARAŞTIRILMASI

DOKTORA TEZİ

Metin BAYKARA
(601132002)

İklim ve Deniz Bilimleri Anabilim Dalı

Yer Sistem Bilimleri Programı

Tez Danışmanı: Prof. Dr. Alper ÜNAL

ARALIK 2018

Metin BAYKARA, a Ph.D. student of ITU Eurasia Institute of Earth Sciences, student ID 601132002, successfully defended the dissertation entitled "UNDERSTANDING THE SOURCES AND THE EXTEND OF ATMOSPHERIC PARTICULATE MATTER PROBLEM OVER TURKEY USING MESOSCALE CHEMICAL TRANSPORT MODEL", which he prepared after fulfilling the requirements specified in the associated legislations, before the jury whose signatures are below.

Thesis Advisor :	**Prof. Dr. Alper ÜNAL** İstanbul Technical University	.....
Jury Members :	**Prof. Dr. Tayfun KINDAP** Istanbul Technical University	.....
	Prof. Dr. Mete TAYANÇ Marmara University	.....
	Prof. Dr. Göksel DEMİR Kırklareli University	.....
	Doç. Dr. Hüseyin Kurtuluş ÖZCAN Istanbul University-Cerrahpaşa	.....

Date of Submission : 3 December 2018
Date of Defense : 21 December 2018

To my family,

FOREWORD

I would like to express my special appreciation to my advisor Professor Dr. Alper Ünal. His advice on both research as well as on my career have been invaluable.

I'd also like to thank Professor Dr. Tayfun Kındap and Professor Dr. Mete Tayanç for their guidance. Special thanks to Associate Professor Oğuz Kurdoğlu for believing in my abilities.

I appreciate all the support I have received from my colleagues in Eurasia Institute of Earth Sciences and Istanbul Technical University. They were great to me and helped me widen my scientific perspective on many subjects.

I'd like to thank my family, my father Mustafa Baykara, my mother Hülya Baykara, and my sister Ahu Baykara Çelik for their support. I am forever grateful.

December 2018 Metin BAYKARA

TABLE OF CONTENTS

Page

ABBREVIATIONS

AQM	: Air Quality Model
BCON	: Boundary Condition Processors
CB6	: The Carbon Bond-VI photochemical mechanism
CMAQ	: The Community Multiscale Air Quality Modeling System
CO	: Carbon Monoxide
EMEP	: The European Monitoring and Evaluation Program
EU	: The European Union
GFS	: NCEP Global Forecast System
HDD	: Heating Degree Days
ICON	: The Initial Concentration
IMM	: Istanbul Metropolitan Municipality
IPCC	: Intergovernmental Panel on Climate Change
I/O API	: Input/Output Applications Programming Interface
KAMAG	: National Emissions Inventory Management System for Turkey
MACC	: Monitoring and Atmospheric Composition and Climate
NCAR	: National Center for Atmospheric Research
NCEP	: The National Centers for Environmental Prediction
NMVOC	: Non Methane Volatile Organic Compounds
NO_x	: Nitrogen Oxides
O_3	: Ozone
PM	: Particulate Matter
RRTM	: The Rapid Radiative Transfer Model
SMOKE	: Sparse Matrix Operator Kernel Emissions
SO_2	: Sulfur Dioxide
SO_x	: Sulfur Oxides
TNO	: Netherlands Organization for Applied Scientific Research
USEPA	: The U. S. Environmental Protection Agency
WHO	: The World Health Organization
WRF	: Weather Research and Forecasting

SYMBOLS

µg	: Microgram
µg/m^3	: Microgram per cubicmeter
km	: Kilometer
◦C	: Celcius Degree
%	: Percentage
mb	: Milibar

LIST OF TABLES

Page

LIST OF FIGURES

Page

UNDERSTANDING THE SOURCES AND THE EXTEND OF ATMOSPHERIC PARTICULATE MATTER PROBLEM OVER TURKEY USING MESOSCALE CHEMICAL TRANSPORT MODEL

SUMMARY

Turkey, with a population climbing to 80 million, has its own challenging air pollution issues, especially particulate matter pollution. Local emission sources are generally the main contributors of particulate matter levels due to their nature. Among these local emission sources, residential heating is one of the emission sectors that contribute to emissions of harmful air pollutants in highly populated urban areas.

As the capital of Turkey's industry, megacity Istanbul has been experiencing air pollution problems that has reached to significant levels since 1980's, in which the pollutant concentrations have exceeded the air quality standards for several times. In Istanbul, local anthropogenic sources comprise nearly 60% of particulate matter levels. According to the air quality monitoring report of the Ministry of Environment and Urbanization, the daily mean particulate matter (<10 μg, PM_{10}) concentrations exceeded the limit with more than 100 $\mu g/m^3$ at several provinces in winter of 2015 in Istanbul.

Representation of major emission sources such as road transportation and residential heating are crucial for the air quality modeling and policy making. Modeling concentrations of particulate matter have a number of important roles, some of which are complementary to measurement. These roles include assessing concentrations at locations without monitors and answering questions such as how will particulate matter levels change in the future. Results of modeling studies can be directly compared to the appropriate ambient air quality standards because all relevant sources of pollution in the modeling domain are included in this type of model. The US EPA Community Multiscale Air Quality (CMAQ v5.2) model, a three-dimensional Eulerian atmospheric chemistry and transport model, was used to evaluate the air quality of Turkey, focusing on Marmara Region and Istanbul for the winter of 2015 using three-level nested domains with an up to date spatially distributed high-resolution emissions inventory based on local activity data.

Emissions is one of the two main inputs of CMAQ model. In order to process the high-resolution emissions inventory used in this thesis, a regional emission model, called DUMANpy, similar to Sparse Matrix Operator Kernel Emissions (SMOKE) Modeling System of the US EPA was adapted and customized to create temporally and spatially distributed emission for Turkey. One of the main purpose of DUMANpy is to convert the resolution of the emission inventory data to the resolution needed by an air quality model.

Other main input of CMAQ model is the meteorology input because sophisticated air quality models require meteorological fields and incorporate complex chemical

reaction schemes. The meteorological modeling inputs are important due to complications caused by complex terrain conditions, where measurement is not an option. The meteorological inputs for air quality modeling were generated using the Weather Research and Forecasting (WRF v3.8.1) model.

CMAQ model results showed that using high-resolution emissions for the residential heating sector significantly improve the spatial distribution and concentration of air pollutants (SO_2, PM_{10}, $PM_{2.5}$) for Istanbul. Air quality model simulations with our high-resolution emissions underestimated PM_{10} concentrations throughout the study episode on average by only 4.16% with a mean bias of 2.23 $\mu g/m^3$ while base inventory underestimated PM_{10} concentrations on average by 35.1% with a mean bias of 18.91 $\mu g/m^3$. Results show that our spatially distributed high-resolution emissions inventory produces more realistic results for Istanbul during wintertime when residential heating has the most influence on local air pollution. These results show the necessity and importance of high-resolution local emissions for anthropogenic emissions sectors for urban areas which in turn would help improve our understanding and extend of the air pollution problem in Turkey.

ORTA ÖLÇEKLİ KİMYASAL TAŞINIM MODELİ İLE TÜRKİYE'DEKİ PARTİKÜL MADDE PROBLEMİ VE KAYNAKLARININ ARAŞTIRILMASI

ÖZET

Türkiye, nüfusu 80 milyona yaklaşırken hava kirliliği ve özellikle partikül madde kirliliği sorunu ile başa çıkmaya çalışmaktadır. Özellikle nüfusun yoğun olarak ikamet ettiği büyük şehirlerde yerel emisyon kaynakları, uzak mesafeli taşınıma göre, hava kirleticilerinin ana kaynağıdır. Yerel emisyon kaynakları arasında ise evsel ısınma özellikle kış aylarında hava kirliliği üzerinde en çok etkiye sahip olan kaynaktır.

Türkiye'nin endüstri merkezinde konumlanmış olan İstanbul'da 1980'li yıllardan günümüze birçok sefer kritik seviyelere ulaşan hava kirliliği problemleri devamlılığını sürdürmektedir.

İstanbul'daki hava kirliliğinin ana sebeplerinden biriside yerel insan-kaynaklı emisyonların partikül madde seviyesinin 60%'ını oluşturmasıdır. T.C. Çevre ve Şehircilik Bakanlığı (ÇŞB)'nın raporuna göre 2015 kış ayında İstanbul ilinde partikül madde konsantrasyonları birçok günde ÇŞB partikül madde standardı olan 70 $\mu g/m^3$ değerinin üzerinde ölçülmüştür. Hava kirliliği üzerine olan etkilerinden dolayı ana emisyon kaynaklarının modellenmesi büyük önem teşkil etmektedir. Bu kaynakların modellenmesi kirletici ölçümlerini desteklediği gibi farklı faydalarıda bulunmaktadır. En önemli faydalardan birisi ölçüm istasyonlarının bulunmadığı noktalarda hesaplanan kirletici konsantrasyonları ve gelecekteki farklı senaryoların sonuçlarını tahmin etmek gibi.

Bu çalışmada hava kalitesi modellemesi için üç boyutlu Eulerian atmosfer kimyası ve taşıma modeli olan The US EPA Community Multiscale Air Quality (CMAQ v5.2) modeli kullanılmıştır. Modelleme alanı iç içe üç model alanından oluşmaktadır. En dış alan Avrupa ve Orta Doğu'yu içerirken, orta alan tüm Türkiye'yi, en iç model alanı ise Marmara Bölgesini içerisine almaktadır.

Modelleme periyodu 2015 kış aylarıdır. Seçilmiş olan bu zaman aralığında yerel kirletici kaynaklarının etkisinin bulunması amacı ile uzun mesafeden taşınım olmayan günler saptanmıştır ve bu günler üzerine çalışmalar yoğunlaştırılmıştıre. Türkiye bulunduğu konumdan dolayı bir çok farklı partikül madde kaynağına komşudur. Atmosferik sistemlerlere bağlı olarak bu kaynaklardan (örn: Sahara çölü) Türkiye'ye yüksek miktarlarda paritkül madde taşınımı gerçekleşmektedir. Uzun mesafeli taşınım olduğu günlerde taşınan kirleticiler yerel kirletici kaynaklarını bastırmakta ve etkilerini maskelemektedir. Çalışma periyodu için sıcaklık ve paritkül madde konsantrasyonları gözlem verileri incelenmiş ve yerel kirleticilerin hava kirliliği üzerine olan etkilerinin en iyi temsil edilebileceği zaman aralığı çalışmada kullanılmıştır.

Hava kalitesi modellemesinin iki ana girdisi bulunmaktadır; emisyon ve meteoroloji girdileri. Çalışmada kullanılan emisyonlar Türkiye'yi içeren Avrupa tabanlı emisyon envanterleri (TNO ve EDGAR) ile yerel emisyon verileri yüksek çözünürlüklü İstanbul ili için hazırlanmış olan emisyon envanterinden alınmıştır. CMAQ modeli

emisyon girdisi olarak saatlik ve kimyasal türleştirme yapılmış emisyonları kullanmaktadır. Emisyon envanterleri emisyon miktarlarını yıllık olarak sakladıkları için bu emisyonları hava kalitesi modelinde kullanmadan önce bir takım işlemlerden geçmek zorundadırlar. Kuzey Amerika için yazılmış olan Sparse Matrix Operator Kernel Emissions (SMOKE) emisyon işleme modeli Avrupa ve Türkiye için mevcut değildir. Bu yüzden CMAQ modeli emisyon girdisinin oluşturulması amacı ile SMOKE modeli benzeri bir emisyon işleme programı, DUMANpy, Türkiye için bu tez çerçevesinde yazılmış ve emisyon hazırlama işlemlerinde kullanılmıştır. Bu program emisyon envanterinden elde ettiği bilgileri zamanda ve mekanda dağıtarak emisyonları hava kalitesi modeli tarafından istenilen biçime getirmektedir.

DUMANpy, Python programlama dilinde yazılmıştır. Emisyon girdileri öncellikle gridlenmekte, daha sonra zamansal profileller kullanılarak yıl bazından saatlik veriler oluşturulmaktadır. Daha sonra hava kalitesinde kullanılan kimyasal mekanizmaya göre emisyonlardaki kirleticiler kimyasal bileşenlerine ayrılmaktadır. Emisyonların kaynağına göre düşeydeki dağılımları yapılarak CMAQ modeline hazır olan son çıktılar üretilmektedir. Diğer bir ana girdi olan meteoroloji girdileri için ise çevrim dışı olarak Weather Research and Forecasting (WRF v3.8.1) modelinin çıktıları kullanılmıştır. Meteoroloji girdileri kimyasal reaksiyonlar ve kimyasal taşınım gibi kompleks işlemlerin arkasındaki en önemli etkenleri hava kalitesi modeline sağlamaktadır. Meteoroloji modeli hava kalitesi modeli ile çevrim dışı olarak eşleştirilmiş ve çalıştırılmıştır.

Meteoroloji modeli çıktılarının kullanılmasının önemli bir sebebi ise ölçüm yapılamayan alanlardaki meteorolojik değerleride hava kalitesi modeline sağlamasıdır. Meteoroloji modeli CMAQ modelleme alanının genişletilmiş halini kullanmaktadır. Hem emisyonlar hem de meteoroloji çıktıları CMAQ modeline verilmeden önce kalite kontrolü ve ölçüm verileri ile karşılartırılarak güvenilirlikleri değerlendirilmektedir.

Girdiler tamamlandıktan sonra hava kalitesi modeli CMAQ tüm model alanları ve farklı emisyon envanterleri için çalıştırılmıştır. Modelleme alanları arasındaki boyut farkı çalışma alanın odaklandığı bölge için araştırılmıştır. Bu alanlardaki hava kalitesi modeli performansları daha sonra ölçüm verileri ile karşılaştırılmıştır. Model en iyi performansı en iç modelleme alanında gösterdiği belirlenmiştir.

Marmara bölgesini kapsayan en iç modelleme alanı için hem genel emisyon envanteri hem de yüksek çözünürlüklü yerel emisyon kaynaklarından hesaplanmış olan envanter kullanılarak model performansı ve senaryo analizleri yapılmıştır.

Hava kalitesi model sonuçları yüksek çözünürlüklü emisyon envanteri ile yapılmış olan senaryo analizinin genel envantere göre daha iyi sonuç verdiğini göstermiştir. Yüksek çözünürlüklü envanter sayesinde özellikle evsel ısınma sektörü kaynaklı emisyonların kış dönemideki kirletici konsantrasyonlarının (SO_2, PM_{10}, $PM_{2.5}$) etkisi İstanbul ili için daha iyi olduğu görülmektedir.

Yerel kirletici kaynaklarının etkilerinin baskın olduğu günlerde emisyon sektörlerinin hava kirliliği üzerine olan etkilerinin ortaya konulması önemlidir. Hava kalitesini iyileştirmeye yönelik planlamaları ve verilecek olan kararları daha sağlıklı bir şekilde verebilmek için kaynakların etkisini doğru ve yüksek çöznürlüklü olarak görmek önemlidir.

Bu çalışma sonucunda sadece konsantrasyonların temsiliyetinde miktar olarak iyileştirme yapılmış olmasının yanı sıra emisyon kaynaklarının mekansal olarak temsiliyetide iyileştirilmiştir. Bu tez içerisinde yapılmış olan modelleme çalışmaları göstermektedir ki İstanbul gibi nüfusun yoğun olduğu şehirlerde insan kaynaklı emisyonların temsiliyeti hem toplum sağlığı hem de yasa yapıcılar için bir araç oluşturması bakımından büyük bir önem arz etmektedir.

1. INTRODUCTION

Air pollution is determined by the level of pollutants in the air. Above their normal ambient levels, they produce adverse effects on animals, vegetation, and humans. Air pollution is a major environmental and social problem affecting everyone be it in developed or in developing countries. In order to reduce the adverse impacts caused by air pollution there have been various legislations to address air pollution problem going back as early as mid 20th century but gained more attention in 1990s.

Generally, air quality standards are set for six common "criteria pollutants": carbon monoxide (CO), ozone (O_3), lead (Pb), sulfur dioxide (SO_2), nitrogen dioxide (NO_2), particulate matter (also known as particle pollution) (PM). These air pollutants are called “criteria” air pollutants because they are being regulated by certain criteria based on human/environmental health. Air pollutants can be either emitted directly as particles into the atmosphere (primary pollutants) or formed in the atmosphere (secondary pollutants). Primary pollutants include sulfur dioxide, oxides of nitrogen, carbon monoxide, volatile organic compounds, and carbonaceous and non-carbonaceous primary particles. Secondary pollutants arise from chemical reactions of primary pollutants in the atmosphere. Prominent secondary pollutants in the air include ozone, particulate matter, etc.

Tropospheric (Ground level) Ozone, the primary constituent of urban smog, is a secondary pollutant created by chemical reactions between nitrogen oxides (NO_x) and volatile organic compounds (VOC) in the presence of sunlight. Emissions from industrial facilities, motor vehicle exhaust, gasoline vapors, and chemical solvents are some of the sources of NO_x and VOC. In particular, nature originated volatile organic compounds are released from different plant species (isoprenoid, terpenoids) and anthropogenic VOCS are released from burning fuel (gasoline, oil, coal, wood, charcoal, natural gas, etc.); solvents, paints, glues, and other products. Additionally, they include such chemicals as benzene, toluene, methylene chloride, and methyl chloroform.

As ozone is a powerful oxidant it can react with a wide range of cellular components and biological materials. Ozone is a known pulmonary irritant affecting the respiratory mucous membranes, other lung tissues, and respiratory functions. Relatively low amounts can cause chest pain, coughing, shortness of breath and throat irritation while existing chronic respiratory diseases such as bronchitis, emphysema, and asthma may be worsened. Even healthy people can experience breathing problems when exposed to ozone. Harmful effects of short-term exposure to low levels of ozone may be recoverable but health effects may become more damaging at higher levels or longer exposures. Long-term exposures to higher concentrations may also cause permanent lung damage, and in children may lead to abnormal lung development (US EPA, 1996).

CO is an odorless, colorless gas formed by incomplete combustion of carbon in fuel that can be harmful when inhaled in large amounts. The greatest sources of CO to outdoor air are methane oxidation by OH radical along with combustion and industrial processes, and biomass burning. CO affects human health by impairing the ability of the blood to bring O_2 to body tissues. Breathing air with a high concentration of CO reduces the amount of oxygen that transported in the blood stream to critical organs (e.g. heart and brain). At very high levels, which are possible in enclosed environments, CO can be fatal. The acute effects of CO poisoning are well understood (Raub et al. 2000). However, the outcomes of long-term, low-concentration CO exposures are less well understood. Because of the critical nature of blood flow and O_2 delivery to the heart and brain, these organ systems, as well as the lungs (the first organ to come into contact with the pollutant), have received the most attention.

Sulfur dioxide (SO_2) is the predominant anthropogenic sulfur containing air pollutant. SO_2 as a gas formed when sulfur is exposed to oxygen at high temperatures during processes. Emissions that lead to high concentrations of SO_2 generally also lead to the formation of other SO_x. The largest sources of SO_2 emissions are from fossil fuel combustion at power plants, oil and gas industry, pipeline operations. Lesser sources of SO_2 emissions include: industrial processes such as extracting metal from ore, pulp and paper production, natural sources, and ships, trains, other vehicles, and heavy equipment that burn fuel with a high sulfur content. Other sources include large ships and off-road equipment which burn high sulphur containing fuels. Sulphur dioxide may also be released from natural sources such as volcanic eruptions, and in low

quantities, from forest fires. SO_2 can harm the human respiratory system and make breathing difficult. Children, the elderly, and those who suffer from asthma. At high concentrations, gaseous SO_x can harm trees and plants by damaging foliage and decreasing growth. SO_2 and other sulfur oxides can contribute to acid rain which can harm sensitive ecosystems.

Nitrogen Dioxide (NO_2) is among the highly reactive gases known as nitrogen oxides (NO_x). Nitrogen oxides (NO_x, sum of NO and NO_2) are formed when oxygen and nitrogen react at high temperatures. Other nitrogen oxides include nitrous acid and nitric acid. NO_2 is used as the indicator for the larger group of nitrogen oxides. NO_x primarily gets in the air from the burning of fuel. NO_x forms from emissions from cars, trucks and buses, power plants, and off-road equipment. It is eventually oxidized to nitric acid (HNO_3). Nitric acid contributes to acid deposition and to aerosol formation. The nitrate particles that result from NO_x make the air hazy and difficult to see though. NO_x in the atmosphere contributes to nutrient pollution in coastal waters. High concentration of NO_2 can irritate airways in the human respiratory system. Such exposures over short periods can aggravate respiratory diseases, particularly asthma, leading to respiratory symptoms. Long exposure duration to NO_2 concentrations may increase chance of getting respiratory infections and weaken respiratory structure which may result in development of asthma.

Particles in the atmosphere are originated from natural and anthropogenic sources. Natural sources are volcanoes, sea spray, and windborne dust, anthropogenic sources are anthropogenic activities, such as combustion of fuels. Secondary particles are products of atmospheric transformation of nitrogen oxides (mainly emitted by traffic and some industrial processes) and sulfur dioxide resulting from the combustion of sulfur-containing fuels. The anthropogenic contribution to particulate matter takes place through primary emissions of particulates and through secondary particulate formation in the atmosphere from gaseous sulphur dioxide, nitrogen oxides, ammonia, and from volatile organic compounds (VOC).

PM less than 2.5 μm in diameter are referred to as “fine”, while those greater than 2.5 μm diameter as “coarse”. The distinction between “fine” and coarse particles is crucial because these particles modes are removed from the atmosphere by different mechanisms, have different chemical composition, distinctly different characteristics, and more importantly differ significantly in their deposition patterns in the respiratory

tract. Life time of particulate matter larger than 10 μm generally has its lifetime limited to the order of hours by rapid removal due to its size. Particles are often assumed to be spherical, whereas this is only the case for non-aggregated, liquid particles. Particle shape and phase can influence radiative properties and health impacts. Fine particles ($PM_{2.5}$), consists of secondary pollutants created by the condensation of gaseous pollutants (e.g. sulfur dioxide and nitrogen dioxide), are serious threats because they can penetrate and accumulate deep inside the lungs while being small enough to be absorbed deeply into the lungs, and sometimes even into the bloodstream. Some types of $PM_{2.5}$ include diesel exhaust particles, wood smoke, mineral dusts, such as coal, asbestos, limestone, and metal dusts and fumes. The size of 2.5 μm was chosen because of its significance for the penetration of human lungs, set out by the high risk respirable convention. For comparison, coarse particles (PM_{10}) corresponds to the thoracic convention the size of inhaled particles that penetrate beyond the larynx. PM affects more people than any other pollutant, and studied in most cases for its intense effects on human health and economy (Akhtar et al., 2014). Correlations between the PM inhalation and respiratory/cardiovascular mortality were indicated in epidemiological studies (Brook et al., 2004; Puett et al., 2014).

Modification of $PM_{2.5}$-related effects by $PM_{2.5}$ species themselves have been found by previous studies (Dai, Zanobetti, Koutrakis, & Schwartz, 2014; Middleton et al., 2008). PM consists of many chemical components that originate from various sources. Determining the different levels of toxicity of PM species and identifying species is important to general strategies and regulations. There is currently no clear understanding of which particle properties, such as their size or the presence of specific chemical substances, are most responsible for the toxic effects because PM is measured by mass as opposed to different sources or components of PM and as airborne particles differ greatly from place to place in size and chemical composition. There are limited number of studies that have investigated the toxicity of PM components due to the sophistications and difficulties in measuring particulate matter species. These investigations have reported numerous components that may be responsible for particle toxicity, such as elemental and organic carbon, sulfate, nitrate, and metals including zinc, nickel, iron, potassium, and chromium (Atkinson et al., 2001; Franklin, Koutrakis, & Schwartz, 2008; Ghio, Carraway, & Madden, 2012; Ito et al., 2011; Ye et al., 2018).

Air quality management's primary objective is the protection of human health and the environment from the aforementioned harmful effects of air pollution and pollutants. The areas of air quality science and air quality management are closely coupled, the tools developed by scientists carry out the tasks help controlling air pollution.

Management of air quality involves several steps of inter-related elements such as establishing air quality goals, analyses and evaluations, and implementation of mitigation measures. Analysis procedure is one of the most crucial step of air quality management cycle. Analysis provide critical information to air quality managers. Air quality managers use emissions inventories, air monitoring, air quality modeling and other assessment tools to understand the air quality problem fully.

Air quality managers use models to identify source contributions to air quality problems and assist in the design of effective strategies to reduce harmful air pollutants. Managers also apply models to simulate ambient pollution concentrations under different policy scenarios, as a tool to make and justify decisions. Models are also used to determine the relative contributions from different sources in tracking trends, monitoring compliance, and making policy decisions. Modeling helps estimate the relationship between sources of pollution and their effects on ambient air quality.

Air quality management cycle is a dynamic process which is a continuous review and assessment of goals and strategies based on their effectiveness. A wide range of external factors beyond the scientific and technical aspects of air quality can drive the effectiveness of an air quality management system, however, it is beyond the scope of this thesis to comprehensively analyze these external factors (Figure 1.1).

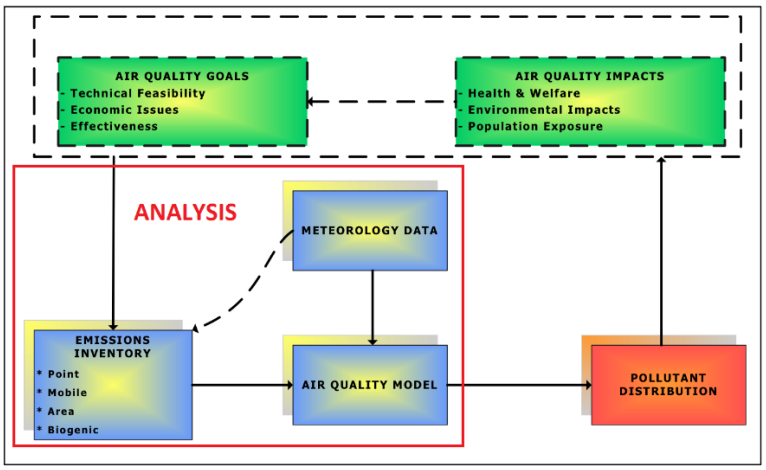

Figure 1.1 : Air quality management outline.

The use of computational models is essential to the environmental regulatory process. The complex relationship between emissions, and human and ecological impacts are linked by modeling in the regulatory process.

The atmospheric models are overall end products of our current scientific understanding of the different physical and chemical processes which determine the fate of species in the atmosphere and help us understand how these different processes interact. Models of the atmosphere built from fundamental conservation laws governing the physical behavior of the atmosphere, and use numerical methods to obtain the solution to the system of coupled governing equations.

Air quality modeling is a numerical tool used to describe the relationship between emissions, meteorology, atmospheric concentrations, deposition, and other factors. Air pollution modeling give a deterministic description of the air quality problem, including an analysis of factors.

Photochemical models are routinely utilized for regulatory analysis and assessment of the effectiveness of the control strategies. The most widely used photochemical models are Eulerian models which are typically used for regional scale air quality modeling studies and employ five-dimensional data sets. The modeling domain is divided into three-dimensional grid cells. Pollutants are spread between grid cells in the x and y directions (horizontal) and the z-direction (vertical), time, and the chemical species.

The main reason for Eulerian models to be prefered in atmospheric chemistry, to investigate air quality issues related to tropospheric ozone, particulate matter formation, secondary organic aerosols, is that they include all relevant chemical species via chemical mechanisms.

Air quality models require meteorological fields and incorporate complex chemical reaction schemes. The meteorological modeling inputs are important due to complications caused by complex terrain conditions, where measured is not an option. The meteorological information regarding wind speed and direction, vertical mixing, temperature, and atmospheric moisture are vital for the air quality model. Some PM components, including nitrate species, organic species, and water, are directly depend on these environmental factors provided by the meteorology model. These meteorological parameters are calculated by the model over an area of interest which is called a grid. When these models are applied in past events (e.g. scenario analysis),

they are able to combine ambient data with model predictions via four-dimensional data assimilation yielding temporal and spatially complete data sets.

Modeling concentrations of PM have a number of important roles, some of which are complementary to measurement. These roles include assessing concentrations at locations without monitors and answering questions such as how will PM levels change in the future. Results of modeling studies can be directly compared to the appropriate ambient air quality standards because all relevant sources of pollution in the modeling domain are included in this type of model.

1.1 Literature Review

In his study (Tayanç, 2000) analyzed the SO_2 concentration levels in Istanbul to assess the air pollution during the heating seasons in which concentration of air pollutants reach high levels due to consumption of low quality fossil fuels. He analyzed the period between 1985 – 1991. Study results showed that there was an increasing trend in the concentration levels during this period. The results indicated that monthly averages of SO_2 problem was specific to the heating season periods of 1993-94 and 1994-95. The maximum concentration areas on both sides of the city were characterized by very high residential population densities. He also showed that shifting to natural gas in 1995-96 seasons led to considerable decrease in SO_2 concentrations.

In a study by (Theodosi et al., 2010), the chemical composition of aerosols over Istanbul was examined. This is the first study to chemically characterize the aerosols for Istanbul by measuring the major aerosol components. To achieve this, 325 (PM_{10}) aerosol samples were collected from November 2007 to June 2009. Samples were analysed for the main ions, trace metals, water-soluble organic carbon (WSOC), organic (OC), and elemental carbon (EC). PM_{10} levels were found to be in an agreement with those measured by the Istanbul Megacity Municipality (IMM) air quality network, indicating that the sampling site is representative of the Istanbul. Trace elements related to human activities (as Pb, V, Cd, and Ni) obtained peak values during winter due to residential heating. Results showed that the PM_{10} measurements at study site represent the mean PM_{10} levels above Istanbul (especially during the cold season). During winter additional sources like household heating contribute to the total carbon loadings. The water-soluble organic to organic carbon ratio is characteristic for

an urban area, demonstrating a higher ratio in the summertime, mostly due to the large fraction of secondary (oxidised and more soluble) organic species.

Urbanization effects on the temperature trends are investigated at the selected stations in the Anatolian Peninsula by (Ozdemir et al., 2012). Nonparametric Mann–Kendall test procedure was employed for the urban and rural stations of the selected cities to detect the long-term change in temperature trends. Statistical analysis of daily minimum temperatures for the period between 1965 and 2006 suggest that there is no statistically significant increase in rural areas. All the urban sites and difference between urban and rural pairs show significant increase in temperatures, a strong indication for the existence of urban heat island affect over the region.

In another study by (Ozdemir et al., 2014), the first black carbon (BC) concentrations measured in the megacity Istanbul. Two measurement campaigns have been conducted to measure BC and fine particulate matter ($PM_{2.5}$) concentrations at four locations, characterized by different traffic densities. In the first campaign, BC daily mean concentrations have been found to be between 4 - 10 $\mu g/m^3$. In the second campaign, BC and $PM_{2.5}$ have been measured at the site with the highest traffic density for an entire year. Diurnal variations of BC concentrations followed those of traffic density. Generally high BC concentrations are observed during daytime and lower concentrations during the night-time, with differences in the timing and the intensity of morning and evening peaks. During the weekends higher concentrations were measured at night, when social activities and traffic increases.

In a review study by (Kanakidou et al., 2011), a comprehensive overview of the actual knowledge on the atmospheric pollution sources, transport, transformation, and levels in the East Mediterranean was provided. This review paper focuses both on the background atmosphere and on the similarities and differences between the urban areas one of which is megacity Istanbul. Ground-based observations are combined with satellite data and atmospheric modeling. The overall evaluation pointed out that long and regional range transport of natural and anthropogenic pollution sources have about similar importance with local sources for the background air pollution levels in the area. Background O_3 observations show an increasing gradient towards the south that partially compensates O_3 titration by NO_x in the urban sites. Due to the non linear dependence of O_3 on NO_x and NMVOC levels, control of NO_x emissions is expected to lead to higher O_3 levels and thus O_3 exceedances in the cities. Available information

on NMVOC total amounts, reactivity and chemical speciation is scarce, although the NMVOC/NO_x ratio and VOC reactivity is critical for the build-up of air pollution. CO observations in rural areas are also limited, despite the key role of CO in O_3 production. There is a clear need of such reliable and systematic measurements of NMVOC, NOx and CO in the region to support modeling of air pollution and climate impacts. PM, even in the urban regions, is also shown to have a significant contribution by long-range transport of African dust or distance anthropogenic pollution sources over the region. Results of this study suggest that long range transport also plays an important role in particulate matter concentration levels in city of Istanbul.

There is a limited number of studies using three dimensional Eulerian air quality models to evaluate air quality in Turkey. In the following part, these studies given in detail.

In a study by (Kindap et al., 2006), MM5 meteorology model and CMAQ air quality model were employed to investigate the long-range transport of PM_{10} from Europe to Istanbul. They have used 2001 EMEP inventory for the emission inputs. The study results indicate that under certain meteorological conditions the influence of Eastern European emissions to PM_{10} levels in Istanbul might be significant. The overall results suggest the contribution of long-range transport from Europe should be considered in the evaluation of PM_{10} levels in Turkey.

Impact of the weather conditions on the SO_2 and NO_2 levels in Istanbul was investigated by (Kindap, 2008). In the study, MM5 model was used to generate the meteorology inputs for the air quality model CMAQ. They have also conducted tracer analyses over the modeling domain, for the period January 7-11, 2002, using the online tracer model of MM5, MM5T. The tracer model showed the pollutant transport route which was Bucharest-Kiev-Warsaw-Istanbul. These results are inline with the hypothesis that the transboundary transport from Eastern Europe can play an important role in pollutant events happen in Istanbul. Model and observation comparison revealed that model captures the temporal variation of surface SO_2 and NO_2 concentrations at monitoring stations, however, the magnitudes of disagreement between the simulation and the observations indicated significant problems. This may be attributed to the incomplete nature of emission inventory along with the uncertainities of the regional model. This shows the importance of high resolution emission inventories along with high resolution modeling configuration.

In more recent modeling case studies, high resolution emission inventories were used (Im et al., 2010, 2011, 2012; Markakis et al., 2012). The motivation of these studies was to examine the PM10 as well as the effects of anthropogenic emissions on these levels in Istanbul.

In a study (Im et al., 2011) on surface ozone concentrations at Istanbul during a summer episode, June 2008, were simulated using MM5 meteorology model and CMAQ models with a high resolution inventory of anthropogenic gaseous and PM pollutants emissions developed for the study. Two base case runs were performed for the city of Istanbul; an anthropogenic emissions only base case run and anthropogenic and biogenic emissions combined base case run. Both biogenic and anthropogenic NMVOC emissions showed similar results in terms of magnitude. The inclusion of biogenic emissions significantly improved the performance of the model. Biogenic NMVOC emissions enhanced ozone concentrations in Istanbul. The temporal variations of simulated ozone levels as well as the resolution of night time chemistry were improved. Sensitivity runs also showed that ozone is more sensitive to NOx emissions in these areas since ozone concentrations were found to be most sensitive to changes in anthropogenic NO emissions. Overall, this study showed that in order to take control measures on anthropogenic emissions in the Istanbul, high resolution chemistry and transport models that are coupled with meteorology models can be useful tools to provide information to the decision makers.

In order to simulate a winter episode (13-17 January 2008), Im et al. 2010 employed the meteorological model WRF and the air quality model CMAQ, this is the first study to employ a model-ready emission inventory developed for Istanbul and used in WRF/CMAQ modeling system. Particulate matter, sulfate, nitrate, and ammonium aerosol components have been investigated, as well as their sensitivities to emission changes, for the first time in this study. The uncertainties originated from the emissions and the possible effects were also discussed in the paper. A model-ready anthropogenic emission inventory on 2 km spatial resolution was developed for Istanbul. The model produced PM_{10} concentrations that were comparable with the observations in terms of magnitude. PM_{10} levels calculated by the model underestimated the observations with an average of 10% at Bogazici University sampling station, whereas an overestimation of 12% is calculated for all stations. Overall, it was concluded that the study results showed significantly improved results for Istanbul compared to earlier studies. Besides

the improvements in the anthropogenic emissions, more realistic results can also be attributed to the higher spatial resolution of the model used. A better representation of the meteorological fields in a higher spatial resolution may also lead to better results. Base case results together with the sensitivity studies pointed significant contribution of local sources, pointing to the need of control strategies focusing on primary particulate emissions. Due to the lack of activity data outside the populated urban and industrial areas ofthe city, the emissions are most probably underestimated, leading to low aerosol concentrations around these areas. The sensitivity simulations showed the highest increase in PM_{10} concentrations occurs in the city center around the coastal area where most of the population is located. As a conclusion, the study shows the necessity to develop emission controls strategies that target directly to the primary particulate emissions in the region.

In a study conducted by (Markakis et al., 2012), an emission processing program was used to compile a high resolution emission inventory for the anthropogenic sources covering the Istanbul for the year 2007. The emission processor is used to produce emissions for a 92 x 57 km area covering the Istanbul with 2 km grid resolution. The emission inventory has high temporal resolution, covering monthly, weekly and diurnal processing, PM_{10} and $PM_{2.5}$ are chemically split into organic carbon, elemental carbon, sulfates, nitrates, ammonium and other particles while NMVOCs are chemically speciated into 23 chemical compounds. The compilation process includes the use of various activity information and statistical data. The study results showed that the on road emissions is a major contributor to the emissions, whereas residential combustion (for SO_x) and solvent use (for NMVOCs) are also important source categories. Industrial combustion is found out to be the main SO_x emitter. The temporal calculations show that monthly distributions follow the seasonal variation for most of the pollutants with higher emissions in winter time. The results suggest that an important air quality issue, PM pollution, may highly be influenced locally from the road transport emissions. Thus, air pollution reduction strategies should be developed and implemented considering the sectoral distributions of emissions. The study also points out two major deficiencies for such studies in Turkey; the lack of emission factors, particularly produced for the local activities and the lack of temporal profiles. These parameters highly influence the estimations of emissions accurately.

1.2 Hypothesis

The main aim is to understand the contribution of emission source categories (specifically residential heating) on particulate matter problem over Turkey focusing on megacity Istanbul mainly due to its dense population and impact of emissions sources that effect public health. Air quality related pollution problems are a major issue of urban areas and solutions for such complex problems are not straight forward and requires intricate environmental policies to improve the existing air quality and its impact on people. In order to obtain the most effective protection of public health, policy makers have to be creative in their approach; creating and utilizing such systems that are cost efficient and dependable on air pollution control whenever possible.

Air quality managers should effectively put models into use to predict the impacts from potential new emission sources and apply these models to simulate ambient pollution concentrations under different policy scenarios, as a tool to make and justify decisions. Such a modeling approach was applied on the particulate matter problem over Turkey and Istanbul, to provide insights, technical means, and a way to understand the underlying problem so that policy makers may benefit from it and provide efficient solutions accordingly.

2. MATERIALS AND METHODS

Air quality modeling systems often incorporate data from emissions and meteorological modeling systems and several other data source through special interface processors into chemical transport models. This structure allows a flexibility to substitute other emissions processing systems and meteorological models. In this section, all components of our modeling framework are detailed under their respective subsections.

Modeling domains and the grid structure are the basis for emissions, meteorological, and chemical transport modeling. The modeling setup for this study utilizes nested domains (Figure 2.1). The outermost domain, mother domain, is the 36x36 km spatial resolution domain (180 by 100 grid cells) covers majority of Europe and partially North Africa and Middle East. The 12x12 km spatial resolution domain covers Turkey and neighboring countries (160 by 79 grid cells), and the innermost domain covering Marmara region including Istanbul with 4x4 km resolution (127 by 85 grid cells).

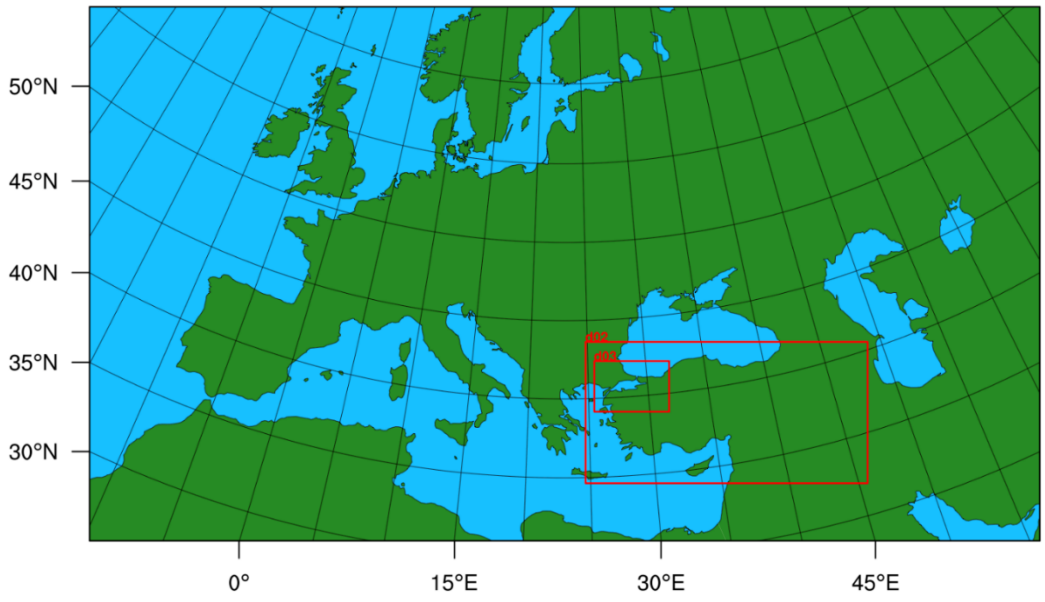

Figure 2.1 : Study modeling domain setup; d01(36 x 36 km), d02(12 x 12 km), d03(4 x 4 km).

2.1 Meteorological Modeling

Meteorological modeling is the first step of the air quality modeling system that will be described here. Mesoscale Advanced Research Weather Research and Forecasting (WRF-ARW) model (Skamarock et al., 2008), version 3.8.1 with advanced parameterization schemes was used in to prepare meteorology input for the Air Quality Model. The simulation of weather phenomena (e.g., temperature, winds, cloud formation, and precipitation rates) is crucial for air quality studies. The ARW dynamics solver together with other components of the WRF system used in producing a meteorological simulation. A dynamical solver performs a time (t) and space (x, y, and z) integration of the equations of motion. The equations cannot be solved analytically, so the equations discretized on a grid and approximate solutions are computed.

2.1.1 Vertical and Horizontal Grid Structures

The WRF-ARW core is based on an Eulerian solver, in order to solve the vertical momentum equation, hydrostatic approximation is not made, the equations are cast in flux (conservative), and a terrain-following mass vertical coordinate. In numerical models that utilize uneven terrain, whether the terrain is meant to represent the actual Earth or an idealized topographic surface, it is possible for the vertical surfaces of selected vertical coordinate systems to intersect the terrain. The coordinate definition is the traditional sigma coordinate used in many non-hydrostatic atmospheric models which is also called a mass vertical coordinate. In this study, 35 sigma layer vertical coordinates were used to evaluate closer to ground level phenomenon better. In air quality studies, 35 layers is the common practise due to better representation of the ground level meteorology.

2.1.2 Temporal discretization

Temporal discretization of the WRF-ARW uses a third-order Runge-Kutta time-integration scheme coupled with a split-explicit 2^{nd}-order time integration scheme for the acoustic and gravity-wave modes. 5^{th}-order upwind-biased advection operators are used in the fully conservative flux divergence integration; 2^{nd}-6^{th} order schemes are run-time selectable (Powers et al., 2017; Skamarock et al., 2008).

2.1.3 Map Projections

The ARW solver version 3.8.1 supports various projections that are described in (Haltiner, G.J. and Williams, 1980). In this thesis Lambert conformal projection was used for all the modeling map projections since it is the default projections for the models that have been used in this work. For ARW configurations using the Lambert conformal projection, the time step constraints is determined by the smallest physical horizontal grid spacing.

2.1.4 Initial and Boundary Conditions

Interpolated data forecast for real-data cases or user defined initial conditions can be used to run the ARW. The National Centers for Environmental Prediction (NCEP) Final Analyses (FNL) data of 1^{o} x 1^{o} were used for initial and boundary conditions requirements of the WRF model. The NCEP Global Forecast System (GFS) is a global spectral data assimilation and forecast model system giving 6 hourly atmospheric variables at 26 levels with a resolution of 0.5 degree.

The initial conditions are pre-processed through module named the WRF Preprocessing System (WPS). The WPS takes terrestrial and meteorological data, transforms them for input to the ARW pre-processor program and outputs, a complete 3-dimensional picture of the atmosphere, at the selected time periods, on the selected model grid. The WPS produced WRF-ARW input contains 3-dimensional fields (including the surface) of temperature (K), relative humidity, and the horizontal components of momentum (m/s). For nesting, all inner domains use the nest time-dependent lateral boundary condition where the outer row and column of the fine grid is specified from the parent domain.

2.1.5 Nesting

The ARW supports horizontal nesting that allows resolution to be focused over a region of interest. As of the version that was used in this thesis, no vertical nesting option is available. The grids are rectangular and are aligned with the coarser grid. Nested grid simulations can be produced using either 1-way nesting or 2-way nesting. The 1-way nesting option was used for the modeling purposes in this work since the study focus is on the innermost domain which has 4km resolution. The fine grid lateral

boundary conditions are interpolated from the coarse grid forecast. In a 1-way nest, this is the only information exchange between the grids (from the coarse grid to the fine grid).

2.1.6 Physics

The WRF physics options fall into several categories, each containing several choices. The physics categories are (1) micro-physics, (2) cumulus parameterization, (3) planetary boundary layer (PBL), (4) land-surface model, and (5) radiation. Four-dimensional data assimilation (FDDA) methods are also available in WRF-ARW and used for meteorological modeling simulations. These methods apply extra forcings to the model equations and are internally treated similarly to physics. The physics preparation involves filling arrays with physics-required variables. Physics packages compute velocity components, potential temperature, and moisture fields. The physics options that were used to run meteorological simulations are given in Table 2.1 and also further explained in their respective sections below. These options were chosen depending on their compatibility with the study domain and resolution of these domains.

2.1.6.1 Microphysics

Microphysics includes explicitly resolved water vapor, cloud, and precipitation processes. The WRF Single–moment 3–class and 5–class Schemes (Hong, Dudhia, & Chen, 2004) was used for all the meteorological model simulations (Table 2.1). The WRF single-moment microphysics scheme follows Schemes (Hong et al., 2004) including ice sedimentation and other new ice-phase parameterizations. A major difference from other approaches is that a diagnostic relation is used for ice number concentration that is based on ice mass content rather than temperature. The computational procedures are described in (Hong, Noh, & Dudhia, 2006). The order of the processes is also optimized to decrease the sensitivity of the scheme to the time step of the model. The WSM3 scheme predicts three categories of hydrometers: vapor, cloud water/ice, and rain/snow, which is a so-called simple-ice scheme.

2.1.6.2 Cumulus parameterization

These schemes are responsible for the sub-grid-scale effects of convective and/or shallow clouds. The schemes are intended to represent vertical fluxes due to

unresolved updrafts and downdrafts and compensating motion outside the clouds. They operate only on individual columns where the scheme is triggered and provide vertical heating and moistening profiles. Cumulus parameterizations are theoretically only valid for coarser grid sizes, (e.g., greater than 10 km), where they are necessary to properly release latent heat on a realistic time scale in the convective columns.

The Multi–scale Kain–Fritsch Scheme cumulus parameterization scheme (Zheng, Alapaty, Herwehe, Del Genio, & Niyogi, 2016) was used for all the meteorological model simulations (Table 2.1). The original Kain-Fritsch scheme is a mass flux parameterization and uses the Lagrangian parcel method. However, the multi-scale Kain-Fritsch scheme is an updated Kain-Fritsch scheme, including subgrid-scale cloud–radiation interactions (Alapaty et al., 2012; Herwehe, Alapaty, Spero, & Nolte, 2014), a dynamic adjustment time scale, a simple linear method using cloud updraft mass fluxes impacting grid-scale vertical velocity, and a lifting condensation level-based methodology for parameterizing entrainment, was developed for high-resolution simulations.

2.1.6.3 Planetary Boundary Layer

The planetary boundary layer (PBL) is responsible for vertical fluxes due to eddy transports in the whole atmospheric column, not just the boundary layer. Thus, when a PBL scheme is activated, explicit vertical diffusion is de-activated with the assumption that the PBL scheme will handle this process. Yonsei University Planetary Boundary Layer scheme (Hong et al., 2006) was used for all the meteorological model simulations (Table 2.1). The Yonsei University PBL (Hong et al., 2006) is the next generation of the Medium Range Forecast (MRF) PBL, also using the counter gradient terms to represent fluxes due to non-local gradients. Details are available in (Hong et al., 2006), including the analysis of the interaction between the boundary layer and precipitation physics.

2.1.6.4 Land-Surface Model

The land-surface models (LSMs) use atmospheric information from the surface layer scheme, radiative forcing from the radiation scheme, and precipitation forcing from the microphysics and convective schemes, together with internal information on the land's state variables and land-surface properties, to provide heat and moisture fluxes over land points and sea-ice points. The land-surface model provides no tendencies,

but does update the land's state variables which include the ground (skin) temperature, soil temperature profile, soil moisture profile, snow cover, and possibly canopy properties. There is no horizontal interaction between neighboring points in the LSM, so it can be regarded as a one-dimensional column model for each WRF land grid-point, and many LSMs can be run in a stand-alone mode.

The Unified Noah Land Surface Model (Tewari et al., 2004) was used for all the meteorological model simulations (Table 2.1). The scheme was developed by NCAR and NCEP, and is a unified code for research and operational purpose. This is a 4-layer soil temperature and moisture model with canopy moisture and snow cover prediction.

2.1.6.5 Atmospheric Radiation

The radiation schemes provide atmospheric heating due to radiative flux divergence and surface downward longwave and shortwave radiation for the ground heat budget. Longwave radiation includes infrared or thermal radiation absorbed and emitted by gases and surfaces. Upward longwave radiative flux from the ground is determined by the surface emissivity that in turn depends upon land-use type, as well as the ground (skin) temperature. Shortwave radiation includes visible and surrounding wavelengths that make up the solar spectrum. Hence, the only source is the Sun, but processes include absorption, reflection, and scattering in the atmosphere and at surfaces. For the longwave radiation scheme rapid radiative transfer model longwave radiation scheme (Mlawer, Taubman, Brown, Iacono, & Clough, 1997) was used while Dudhia shortwave radiation scheme (Dudhia, 1989) was used for shortwave radiation scheme for all the meteorological model simulations (Table 2.1).

Table 2.1 : WRF Physics options.

Micro Physics Options (mp_physics)	WRF Single–moment 3–class and 5–class Schemes (Hong et al., 2004)
Cumulus Parameterization Options (cu_physics)	Multi–scale Kain–Fritsch Scheme cumulus parameterization scheme (Zheng et al., 2016)
Planetary Boundary Layer (PBL) Physics Options (bl_pbl_physics)	Yonsei University Planetary Boundary Layer scheme (Hong et al., 2006)
Land Surface Options (sf_surface_physics)	Unified Noah Land Surface Model (Tweari et al., 2002)
Longwave Options (ra_lw_physics)	Rapid radiative transfer model longwave radiation scheme (Mlawer et al., 1997)
Shortwave Options (ra_sw_physics)	Dudhia shortwave radiation scheme (Dudhia, 1989)
Four dimensional data assimilation (FDDA)	(Liu et al., 2008; Stauffer and Seaman, 1994)

2.2 Emission Modeling

Emission modeling is the second step of the air quality modeling system that will be described here. This section contains two parts; emission inventories and emission processing. The inventories and other emission related data that was used in this study are given in the first part of this section. On the second part, emission processing and processors were described, and the new processor created for this study is explained. Providing information to quantify pollutant emission rates associated with specific sources and time periods are critical components of air quality modeling which leads into local and regional regulatory planning. Emission inventories must meet demands detailed chemical speciation, temporal and spatial resolution, data quality, data accessibility. Both anthropogenic activities and natural processes emit gases and particles into the atmosphere.

Anthropogenic sources are generally characterized as point, nonpoint or area, and mobile. Point sources are emitters located at fixed geographical coordinates that are large enough to be enumerated individually. A large facility may have many individual point sources. Stationary sources, such as such as dry cleaners, wood stoves, and home furnaces, whose individual emissions are too small to be considered as emission points in most analyses and uses are usually treated as nonpoint sources. Agricultural tilling, controlled burning, construction activities, and dust from mining also fall into this category. Some facilities such as refineries contain both point sources and nonpoint sources.

Emission inventories are developed to characterize these sources and to provide air quality managers, modelers, and other users with information on the sources of air pollutants and their precursors. Inventories are also essential for assessing whether or not air quality regulations are having the intended effect, a process often termed accountability.

Emission inventories were originally based on annual equivalent emission estimates and were developed on spatial and temporal scales. The emission inventory development process begins with emission measurements, compilation of activity data, development of emission factors and models, and collection of data from individual sources. Emission inventories are then compiled at the local, provincial,

regional, or national level, subjected to quality assurance checks and reviews, and enhanced as necessary for their particular use.

Emission inventories are subject to substantial levels of uncertainty. Better knowledge of these uncertainties provides the basis for improving air quality management. Most current inventories or models can provide quantitative estimates of emissions at national and county levels. These inventories and models can be used to compare the significance of different source categories. Emission estimates from current inventories and models can provide insights regarding air quality trends over time, they can be used to track pollution, and they can help decision-makers develop air quality management strategies.

2.2.1 Anthropogenic Emissions

In this study, the widely used emissions inventories TNO-MACC_III emission database (TNO) (Kuenen, Visschedijk, Jozwicka, & Denier Van Der Gon, 2014) and Emission Database for Global Atmospheric Research (EDGARv4.3.1) (Crippa et al., 2016) were employed.

The TNO-MACC_II emission inventory was developed for Europe by TNO for the years 2003–2009. It has a 1/8° longitude x 1/16° latitude resolution and covers NO_x, SO_2, NMVOC, NH_3, CO, PPM_{10}, $PPM_{2.5}$ and CH_4. The TNO-MACC_II inventory covers all of Europe including Turkey; however, it does not cover North Africa nor the Middle East. TNO-MACC_III (MACC-III Final Report) is the updated version of the TNO-MACCII product, which extended the time-series from year 2000 to year 2011. All years were revisited and the spatial distribution proxies updated and improved, often based on user comments.

EDGAR version v4.3.1, January 2016 (Crippa et al., 2016), hereafter referred to as EDGAR. This inventory provides global emissions for gaseous and particulate air pollutants (BC, CO, NH_3, NMVOC, NO_x, OC, PM_{10}, $PPM_{2.5}$, SO_2) per IPCC (Intergovernmental Panel on Climate Change) sector covering the whole time-series 1970–2010 at the global scale. Emissions are provided in tons of substance at 0.1 × 0.1° resolution. A highly detailed re-mapping of the sectors from the IPCC to the SNAP (Selected Nomenclature for Air Pollution) nomenclature has been made to allow comparing with the other databases. The EDGAR inventory was used for locations that aren't covered by the TNO emissions inventory.

These inventories are comparable in temporal terms, geographical extent and thematic resolution (sectors) but differences remain in terms of national total emission estimates and/or spatial gridding methodologies.

It should be noted that emissions data for Turkey in these emissions inventories are based on European Monitoring and Evaluation Programme (EMEP) (EMEP/CEIP, 2014) with a top-down approach. In this study, a bottom up approach was utilized for our residential heating emissions for the 4-km innermost domain. Bottom-up approach is combining available statistics on fuel combustion, industrial production, etc. with the most appropriate emission factors. For this approach, local activity data on annual consumption of all types of fuels were obtained from different regulatory bodies (i.e., Ministry of Environment and Urbanization (MoEU), Natural Gas providers, and local municipalities) and emission factors from the EMEP database were used in this study. Fifty-one countries in Europe and North America, including the EU as a whole, have to annually submit their emissions of air pollutants for the latest year and all historic years to EMEP. The reporting follows well-defined guidelines and asks countries to complete a pre-defined template with emissions by year, pollutant and sector that are defined by the Nomenclature for Reporting (NFR). These 43 sectors were defined based on the SNAP at level 1 with one additional level of detail for most sectors. Industrial combustion (SNAP 3) and industrial process 10 emissions (SNAP 4) have been aggregated to a new defined SNAP 34. This was done because there is often confusion between combustion and process emissions for a particular plant or facility, partly because countries may have slightly different definitions on where to draw the line or how to report.

2.2.1.1 SNAP Sector 1: Combustion in energy & transformation industries

Combustion in energy and transformation industries can be point sources or area sources depending on their capacities. Emitted pollutants are sulfur oxides (SO_x), nitrogen oxides (NO_x), carbon dioxide (CO_2), heavy metals, non-methane VOC and methane, nitrous oxide (N_2O), carbon monoxide (CO) and ammonia (NH_3).

Table 2.2 : Anthropogenic emissions sectors.

Sector No	Anthropogenic Sources
1	Energy industries
2	Non-industrial combustion
34	Industry (combustion + processes)
5	Extraction and distribution of fossil fuels
6	Product use
7	Road transport
8	Non-road transport and other mobile sources
9	Waste treatment
10	Agriculture

2.2.1.2 SNAP Sector 2: Non-industrial combustion

Non-industrial combustion plants cover commercial and institutional plants, residential plants and plants in agriculture, forestry and aquaculture. A specific methodology for these activities has not been prepared by EMEP, because the contribution to the total national emissions is thought to be currently insignificant, i.e. less than 1% of national emissions of any pollutant.

2.2.1.3 SNAP Sector 34: Industry (combustion + processes)

Combustion in manufacturing industry covers emissions released from that of combustion for furnaces with and without contact with different type of metals. Relevant pollutants are sulfur oxides (SO_x), nitrogen oxides (NO_x), carbon monoxide (CO), carbon dioxide (CO_2), nitrous oxide (N_2O) and heavy metals. Approximately, combustion in the manufacturing industry is responsible for 25 per cent SO_2, 24 per cent CO_2, 14 per cent NO_2 and 12 per cent CO of the all sectors.

Production processes include processes in petroleum industries; iron - steel industries - collieries, non – ferrous metal industries, inorganic chemical industries, wood, paper pulp, food, drink and other industries; production of halocarbons and sulfur hexafluoride. This sector covers emissions of SO_x (3 per cent of all sectors), NO_x (2 per cent of all sectors), CO (5 per cent of all sectors), CO_2 (4 per cent of all sectors), NMVOC (6 per cent of all sectors), N_2O (19 per cent of all sectors), NH_3 (3 per cent of all sectors), PM and heavy metals.

2.2.1.4 SNAP Sector 5: Extraction and distribution of fossil fuels

Extraction and distribution of fossil fuels include processes in extraction and the first treatment of solid/liquid/gas fossil fuels; liquid/gasoline fuel distribution; gas distribution networks. This sector covers emissions of NO_x, CO_2, VOC, NMVOC and CH_4.

2.2.1.5 SNAP Sector 6: Product use

Solvent use is a major contributor to NMVOC emissions. On a European scale its contribution is roughly a quarter of the total anthropogenic NMVOC emission. The contribution of the sector to anthropogenic NMVOC emissions varies between 15 per cent and 30 per cent. Also, solvent use contributes to the emissions of some heavy metals (Cd, Cu, Pb and Zn), CO, PM, SO_x and NO_x.

2.2.1.6 SNAP Sector 7: Road transport

Road Transport includes the emissions produced by the exhaust systems of road vehicles. It does not cover non-exhaust emissions such as fuel evaporation and component attrition. The vehicle category splits into base parts when we consider the report emissions from road transport to international bodies. However, from a technical point of view, it does not provide the level of detail considered necessary to collect emissions from road vehicles in a systematic way. This is because road vehicle power trains make use of a great range of fuels, engine technologies and after treatment devices. Thus, a more detailed vehicle category split is necessary and has been developed. Pollutants covered include all major emission contributions from road transportation: Ozone precursors (CO, NO_x, and NMVOC), greenhouse gases (CO_2, CH_4, and N_2O), acidifying substances (NH_3, SO_2), particulate matter (PM), carcinogenic species (PAHs & POPs), toxic substances (dioxins and furans) and heavy metals. In detail, the sector covers exhaust emissions of CO, NO_x, NMVOC, CH_4, CO_2, N_2O, NH_3, SO_x, diesel exhaust particulates (PM), PAHs and POPs, Dioxins and Furans and heavy metals contained in the fuel (Lead, Cadmium, Copper, Chromium, Nickel, Selenium and Zinc). A detailed NMVOC split is also included to distinguish hydrocarbon emissions as alkanes, alkenes, alkines, aldehydes, ketones and aromatics.

2.2.1.7 SNAP Sector 8: Non-road transport and other mobile sources

Other Mobile Sources and Machinery includes railways, inland waterways, agriculture, forestry, industry, household and gardening, other off-road, shipping activities and air traffic. These sectors cover emissions of NO_x, NMVOC, CH_4, CO, CO_2, NH_3, N_2O, PM, SO_x and some heavy metals.

On a European scale, SO_2 and NO_x emissions from national shipping can be important with respect to total national emissions. However, emissions from national shipping generally only represent a few percent of the emissions from shipping operating internationally. Globally, shipping is estimated to be responsible for around 5-12 per cent and 3-4 per cent respectively of anthropogenic NO_x and SO_2 emissions.

2.2.1.8 SNAP Sector 9: Waste treatment

Waste treatment and disposal includes waste incineration, solid waste disposal on land, open burning of agricultural wastes, cremation and other waste treatment. The relative proportion of emissions contributed by the sector varies between pollutants. The emissions of compounds such as non-methane volatile organic compounds (NMVOCs), NO_x, CO_2 and N_2O are unlikely to contribute significantly to total emissions. However, waste treatment and disposal have been a major source of emissions of CH_4 (19 per cent) and CO (6 per cent).

2.2.1.9 SNAP Sector 10: Agriculture

Agriculture is a branch of industry which cultivates land and keeps animals in order to produce food, fodder or raw materials used for industrial processes, and comprises arable agriculture, animal agriculture, horticulture, viniculture, etc., with a wide range of intensities. In principle, a sharp distinction between agriculture and natural systems is impossible, as even these systems are used intentionally for food, fodder or animal production and – at least in Europe – are almost everywhere subject to management measures.

2.3 Emission processing

Emissions data from emissions models and regulatory inventories are one of the most important inputs for the air quality models. In order to apply air quality modeling on

larger regions, at a finer grid resolution, with more emissions sources computationally efficient, user-friendly, a flexible emissions data processing system is a requirement.

The U.S. Environmental Protection Agency (EPA) Sparse Matrix Operator Kernel Emissions (SMOKE), an emission processor, is available since 1998, and an effective tool for emissions processing in a number of regional air quality modeling applications. In the following years, SMOKE has seen numerous improvements to its core design (e.g. emissions processing with user-selected chemical mechanisms, on-road mobile emission factors, include all toxic inventories, including point and nonpoint sources, etc.) further enhancing its use and efficiency. As of the current version 4.5 (2018) SMOKE supports the processing of global gridded emission inventories for input to chemistry-transport models. It should be noted that SMOKE was designed and being used for regulatory purposes in North America. In this study, we have written our own emission processor in Python programming language, hereinafter referred to as DUMANpy, based on the fundamentals of SMOKE.

One of the main purpose of DUMANpy is to convert the resolution of the emission inventory data to the resolution needed by an air quality model. Emission inventories are typically available with an annual total emissions value for each emissions source. However, air quality models often require emissions data on an hourly basis, for each model grid cell, and for each model species. In order to produce appropriate model-ready files, you must know the modeling parameters such as model grid and map projection, the episode dates, and the chemical mechanism to be used. DUMANpy is designed to create input data for Community Multiscale Air Quality (CMAQ) model, however, it can be modified to adapt any given air quality model. This CMAQ based approach uses a 3-D I/O API file that contains the gridded, hourly, speciated, and vertically distributed emissions.

For each processing category (i.e., area and point sources, other sources), DUMANpy performs the following tasks:

- read emissions inventory data files
- grow emissions from the inventory year to the modeled year
- transform inventory species into chemical mechanism species
- model the temporal and spatial distribution of the emissions
- merge the emissions source categories to form output files

DUMANpy, is using SMOKE's GSPRO speciation profile factors, EURODELTA-Trends (Colette et al., 2017) temporal factors for monthly, daily, weekdays and weekend diurnal variations, and EMEP vertical profiles (Status Report 1/2016, 2016) are used for vertical distribution of the emissions which is based on based upon plume rise calculations performed for different emission categories. Biogenic emissions were generated off-line using the Model of Emissions of Gases and Aerosols from Nature (MEGAN) version 2.10 version (Guenther et al., 2012) and included into model-ready emissions output by using our emission processor. DUMANpy can create the Network Common Data Form (NetCDF) output format needed by the AQM model.

DUMANpy is able to process all criteria pollutants such as carbon monoxide (CO), nitrogen oxides (NO_x), volatile organic compounds (VOC), ammonia (NH_3), sulfur dioxide (SO_2), PM_{10}, and $PM_{2.5}$; as well as toxic pollutants, such as mercury, benzene, and formaldehyde. Similar to SMOKE, DUMANpy has no limitation regarding the number or types of pollutants it can process.

DUMANpy supports variety of chemical mechanisms. The chemical mechanism is the mapping of the pollutants provided in the emissions inventory to the species needed by the AQM planned to use. Carbon Bond 6 (CB6) chemical mechanism with particulates was used in this study for the CMAQ model.

2.4 Chemical Transport Model (CTM)

Chemical Transport Models for atmospheric pollutants often are referred to by other names, including air-quality models, air quality simulation models, air-pollution models, emission-based models, source-based models, first principles models, and comprehensive models. CTMs are prognostic models that predict the atmospheric concentrations of desired pollutants based on a combination of fundamental and empirical representations of the relevant physicochemical atmospheric processes.

In this work, The U.S. EPA Community Multiscale Air Quality (CMAQ) model (version 5.2)(Development, 2017), a three-dimensional Eulerian atmospheric chemistry and transport model, was used. CMAQ is a multi-pollutant, multiscale air quality model that simulates all atmospheric and land processes that affect the transport, transformation, and deposition of atmospheric pollutants and/or their precursors on both regional and urban scales. It is designed as a science-based

modeling tool for handling all the major pollutant issues (including photochemical oxidants, particulate matter, acidic, and nutrient deposition).

CMAQ is written mainly in FORTRAN-90/95 and C languages. The CMAQ modeling system is comprised of the main CMAQ chemical transport model (CCTM) and several interface processors that link other model input data to the CCTM. The Meteorology-Chemistry Interface Processor (MCIP) processes meteorological model output to provide a complete set of meteorological data required for CCTM. MCIP is designed in such a way that other meteorological models can be linked with minimal effort. Initial and boundary conditions are generated with the ICON and BCON processors, respectively. A photolytic rate constant processor (JPROC) which is based on the RADM (Chang et al., 1987) approach, computes species specific photolysis rates for a set of predefined zenith angles, latitude, and altitudes.

2.4.1 The Meteorology-Chemistry Interface Processor (MCIP)

The main function of MCIP is to translate meteorological parameters from the output of a mesoscale model (WRF-ARW) to the Models 3 I/O API format (Coats Jr, 1996), which is required for CMAQ processors. MCIP links a meteorological model with CCTM to provide a complete set of meteorological data needed for air quality simulation. Because most meteorological models are not built for air quality modeling purposes, MCIP takes care of many issues related to data format translation, conversion of units of parameters, diagnostic estimations of parameters not provided, extraction of data for appropriate window domains, and reconstruction of meteorological data on different horizontal and vertical grid resolutions through interpolations as needed.

The required meteorological input fields in MCIP are used to define the physical, dynamic, and thermodynamic states of the troposphere and lower stratosphere for the CCTM. These fields include geospatial information, prognostic state variables, and several near-surface fields to sufficiently describe the atmospheric influence on the production, dispersion, transport, and deposition of chemical constituents, particularly

2.4.2 Initial Conditions Processor and Boundary Conditions Processor

The ICON processor generates species concentrations for every cell in the modeling domain, whereas the BCON processor generates species concentrations for the cells immediately surrounding the modeling domain. At present, the thickness of the

boundary cells is limited to one, which is the thickness required for all the transport algorithms currently included as part of the CCTM.

Both the ICON and BCON processors write the output ICs and BCs to standard Input/Output Application Programmer Interface (I/O API) files: 3-dimensional gridded files for the ICs and 3-dimensional boundary files for the BCs. The opening, formatting, and writing of these files are handled automatically by the ICON and BCON processors.

The ICON and BCON processors generate IC and BC files from one of three input sources. The first is a time invariant set of vertical concentration profiles. The second source of input data consists of existing Models-3 IO/API 3-dimensional concentration files, normally generated by the CCTM. The final source of IC and BC data involves the generation of special tracer species concentrations used to test numerical transport algorithms.

The CMAQ system contains a set of predefined profiles that can be used to generate the requisite ICs and BCs. These profiles give species concentrations as a function of height, and are spatially independent for the ICON processor and only minimally spatially dependent for the BCON processor. Both the ICON and BCON profile data are time independent.

2.4.3 Photolysis Rate Preprocessor (JPROC)

Many chemical reactions in the atmosphere are initiated by the photo-dissociation of numerous trace gases. These photo-dissociative reactions are responsible for most of the smog buildup detrimental to humans, animals, plant life and materials. In order to accurately model and predict the effects of air pollution, good photo-dissociation reaction rate (or photolysis rate) estimates must be made.

Preprocessor JPROC calculates a table of clear-sky photolysis rates (or J-values) for a specific date. The table is dimensioned by latitude, altitude, and time. Output from JPROC is an ASCII lookup table of photolysis rates that the CCTM uses to calculate gas-phase chemical transformations and pollutant concentrations.

2.4.4 CMAQ Chemistry-Transport Model (CCTM)

The CCTM simulates the relevant and major atmospheric chemistry, transport and deposition processes involved throughout the modeling domains. The science options

available to the user include the gas phase chemistry mechanisms, a set of numerical solvers for the mechanisms, options for horizontal and vertical advection schemes, algorithms for fine and coarse particulate matter predictions, photolysis rates, and a plume-in-grid approach. Through the Models-3 framework, CMAQ simulations can be developed using these different options without modifying source code.

Currently, nine science process classes are defined in CCTM; "drive" controls model data flows and synchronizes fractional time steps, "hadv" computes the effects of horizontal advection, "vadv" computes the effects of vertical advection, "adjcon" adjusts mixing ratio conservation property of advection processes, "hdiff" computes the effects of horizontal diffusion, "vdiff" computes the effects of vertical diffusion and deposition, "chem" computes the effects of gas-phase chemical reactions, "cloud" computes the effects of aqueous-phase reactions and cloud mixing, "aero" computes aerosol dynamics and size distributions; and "ping" computes the effects of plume chemistry.

2.4.4.1 Gas-Phase Chemistry

Atmospheric chemistry plays a major role in many air pollution problems, the representation of chemical interactions among atmospheric constituents is often an essential element of an air quality model.

A chemical mechanism is a collection of reactions that transforms reactants into products, including all important intermediates. Chemical mechanisms developed for air quality modeling are highly condensed, parameterized representations of a true chemical mechanism. Mechanism species can be divided into two categories: inorganic and organic. The number of important inorganic species is relatively small, and they are almost always represented explicitly in chemical mechanisms. The important inorganic species included in these mechanisms are ozone, nitric oxide, nitrogen dioxide, nitric acid, nitrous acid, hydrogen peroxide, sulfur dioxide, and several radicals formed through their interactions with other species. Gas-phase chemistry influences PM formation by producing aerosol precursors including sulfuric acid, nitric acid and semi-volatile organic compounds. Sulfur dioxide (can be oxidized to sulfuric acid by hydrogen peroxide and organic hydroperoxides.

In this study, Carbon Bond (CB) mechanism version 6 (CB6) (Yarwood et al., 2010) was used. CB6 describes tropospheric oxidant chemistry in a concise manner suitable

for use in complex 3-dimensional atmospheric models. CB6 includes several updates to peroxy radical chemistry that will improve formation of peroxides and therefore sulfate aerosol. Updates to reactions of dinitrogen pentoxide with water vapor will affect nighttime formation of nitric acid although heterogeneous reactions on aerosol (and other) surfaces may dominate nitric acid formation at night.

2.4.4.2 Advection and Diffusion

Several advection methods are implemented in the CMAQ; among these is the Yamartino-Blackman cubic algorithm which was used in this thesis. Options for computing subgrid vertical transport include eddy diffusion, and the Asymmetric Convective Model (ACM) (Pleim & Chang, 1992) applicable to convective conditions. Horizontal diffusion is modeled using a constant eddy diffusion coefficient.

2.4.4.3 Particle Modeling and Visibility

One of the major advancements in CMAQ is the modeling of fine and coarse mode particles, with the use of the fine particle model described in (Binkowski & Shankar, 1995). CMAQ predicts hourly gridded concentrations of fine particle mass whose size is equal to or less than 2.5 microns in diameter ($PM_{2.5}$), speciated to sulfate, nitrate, ammonium, organics and aerosol water. Secondary sulfate is produced when hydroxyl radicals react with sulfur dioxide to produce sulfuric acid that either condenses to existing particles or nucleates to form new particles. CMAQ model output includes number densities for both fine and coarse modes.

In another potential application, CMAQ can provide the basis for modeling the atmospheric transport and deposition of semi-volatile organic compounds (SVOC) with parameterizations for their rates of condensation to and/or volatilization from the modeled particles. The 6th generation CMAQ aerosol module (AERO6) takes chemical species concentrations and reactivity rates from the chemistry solvers and primary particulate concentrations from the emissions processor to compute fine and coarse particulate concentrations.

3. RESULTS AND DISCUSSIONS

In the first part of this section, ambient air quality data, processed through the quality assurance and quality measures, are presented. In the next part of the section, results of the WRF model and the emission model are presented. Finally, results obtained from the CMAQ model are given.

3.1 Ambient Air Quality Data

The observation data that were used in this study for particulate matter were obtained from the Turkish Ministry of Environment and Urbanization. In Istanbul, measurement device that is being used by the Istanbul Metropolitan Municipality (IMM) to measure PM_{10} in air quality monitoring stations is MP 101 M Beta Gauge device. This instrument is manufactured according to ISO 10473 standards, certified equivalent to reference method the U.S. EPA approved No. EQPM-0404-151 and EN 12341 and determines the particulate concentration by measuring the amount of radiation a sample absorbs when exposed to a radioactive source. Low energy beta rays are absorbed by collision with electrons, whose number is proportional to density. Absorption is, thus, a function of the mass of the irradiated material, independent of its physio-chemical nature. However, it should be noted that optical measurements have higher uncertainty compared to gravimetric methods due to occlusion of smaller particles behind larger particles.

Figure 3.1 shows station locations on the map. From this figure, it can be seen that while most of the stations are located in or close to city center stations such as Şile-MTHM, Silivri-MTHM, and Kartal are located further away from the city center. Location of stations are important since it is the deciding factor on the type of station due to their proximity to traffic, industry, and to other sources.

Figure 3.1 : Locations of Istanbul's air quality monitoring stations.

In this study, we have investigated the air quality data from 2012 to 2017 (Figure 3.2), standard calibration methods were applied to air quality observation data starting from 2012. For PM_{10} observations, monthly average for the selected period is 50.51 $\mu g/m^3$ with a standard deviation of 8.78 $\mu g/m^3$. The maximum value is measured as 68.35 $\mu g/m^3$ while minimum value is 32.25 $\mu g/m^3$, and median of the PM_{10} values is 51.12 $\mu g/m^3$. Statistics of the other pollutants are detailed in Table 3.1

Compared to the European and Turkish air quality standards; PM_{10} monthly averages for the study period is under Turkish standards (60 $\mu g/m^3$) but exceeds European standards (40 $\mu g/m^3$), $PM_{2.5}$ monthly averages are at European standard of 25 $\mu g/m^3$, it should be noted that there are no standards set for $PM_{2.5}$ in Turkey. For NO_x, monthly averages exceed both European (40 $\mu g/m^3$) and Turkish (60 $\mu g/m^3$) standards while SO_2 monthly averages are below both standards (125 and 250 $\mu g/m^3$, European and Turkish, respectively). In the following sections, steps of selecting the right episode for the study are given.

Table 3.1 : Observation statistics of pollutants.

Pollutant ($\mu g/m^3$)	Mean	Standard Deviation	Max	Min	Median
PM_{10}	50.51	8.78	68.35	32.25	51.12
$PM_{2.5}$	24.72	6.83	42.05	16.69	24.38
SO_2	7.71	3.12	15.15	2.88	7.03
O_3	37.85	12.98	72.47	13.84	38.11
NO_x	104.92	25.05	160.20	54.80	99.55
CO	763.37	192.85	1172.02	364.90	745.42

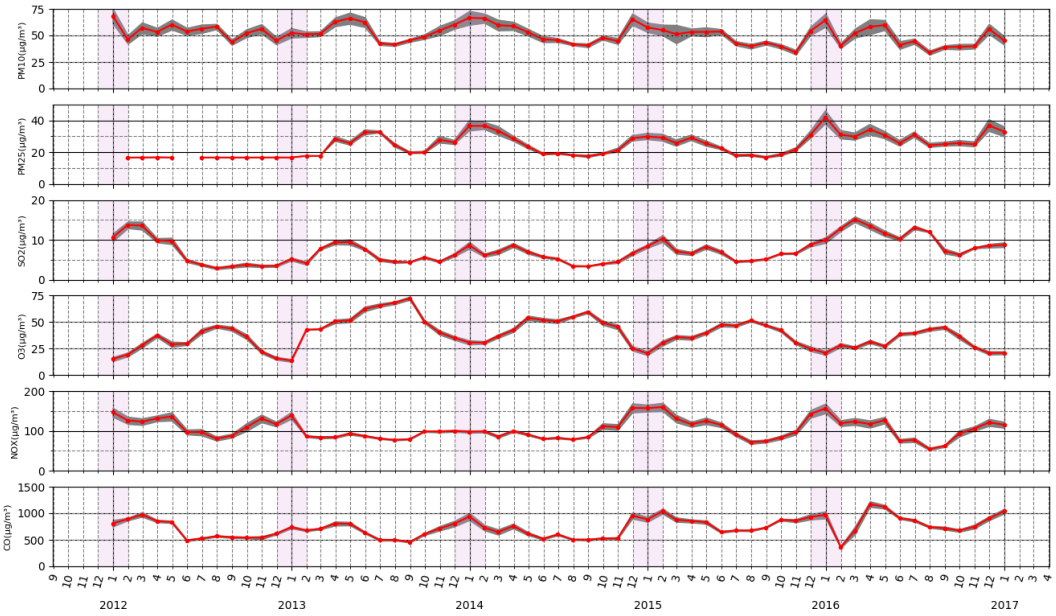

Figure 3.2 : Ambient Air Quality Data for Istanbul.

3.2 Episode Selection

One of the main goals of this study is to quantify the impact of residential heating on particulate matter levels in Istanbul. Therefore, the study period needs to focus on winter season, when residential heating emissions are highest and its impact is largest due to adverse meteorological condition during this time period.

In Figure 3.3, monthly temperature averages are given for years 2011-2016. According to the observation data, the year 2012 has the coldest winter while 2014 has the warmest winter for the 2011-2016 period. For this period suitable years to study the impact of residential heating are 2011-2012-2015 due to their low temperature averages. The temperature averages for 2011 winter months (December, January, February) are; 9 °C, 7 °C, and 6 °C, respectively. The temperature averages for 2012 winter months (December, January, February) are; 10 °C, 5 °C, and 4 °C, respectively. The temperature averages for 2015 winter months (December, January, February) are; 11 ^{0}C, 8 ^{0}C, and 7 ^{0}C, respectively.

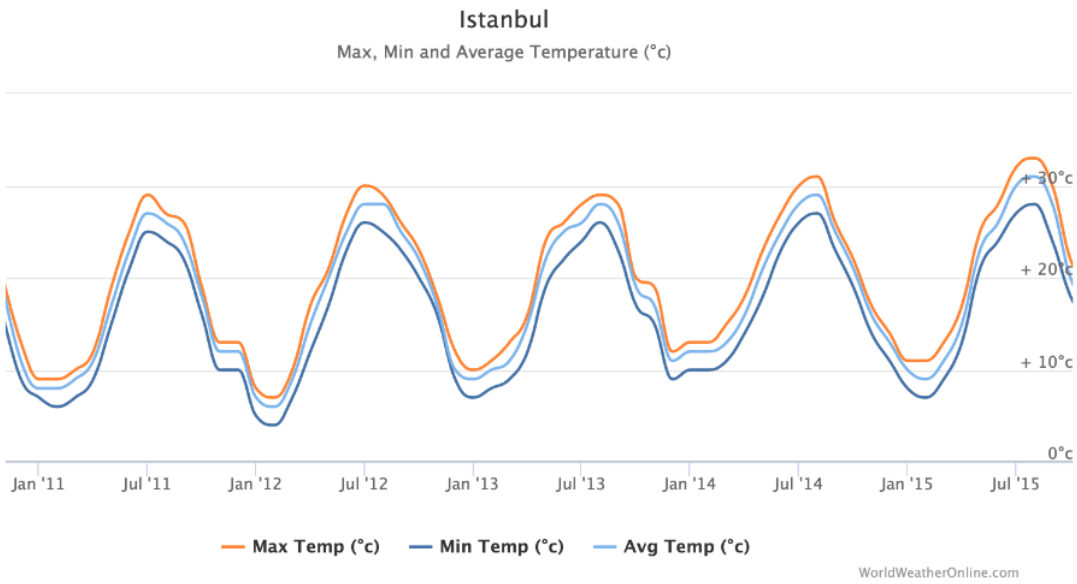

Figure 3.3 : Observation values of temperature for Istanbul (2011-2016).

As previously mentioned in the methodology section, in this study, emissions from TNO_MACC III emissions inventory is used. This emissions inventory cover years 2003-2011. Also, for the residential heating emissions we have used the only existed local activity data (coal, natural gas used) based on the KAMAG project (TUBITAK, 111G037) which covers 2014-2015 years.

We have selected the winter months of 2015 (2014 December, 2015 January, 2015 February) since this period is below the Heating Degree Day (HDD) baseline temperature (European baseline temperatures for heating degree days is 15.5^{o} C (Spinoni, Vogt, & Barbosa, 2015)) meaning that emissions from the residential heating sector has a significant influence on local outdoor air quality. For the modeling simulations, we have selected the first 18 days of December 2014 due its high variability and having values as high as over 100 µg/m^3.

3.2.1 December 2014

Figure 3.4 contains a time series plot of particulate matter concentrations measured by stations. For the December 2014, the average of all stations is 65.64 µg/m^3. Gray shaded area on the time series plot shows the 95% of values that are in $\mu \pm 2\sigma$ range. During the month, average particulate matter concentrations peaked three times; on December 3rd (195.52 µg/m^3), 15th (241.53 µg/m^3), 25th (195.38 µg/m^3). Peak days of average concentration coincide with dates of eight out of the total eighteen stations' maximum measurements. Five stations (Aksaray, Esenyurt-MTHM, Şirinevler-MTHM, Ümraniye-MTHM, Yenibosna) had their maximum PM_{10} concentration

measurements on December 15th and another three stations (Alibeyköy, Kadıköy, and Silivri-MTHM) had their maximum PM_{10} concentration measurements on December 25th. At the end of December, all stations fall under 50 µg/m^3, standard deviation is the lowest and the values of the day are bunched around the mean.

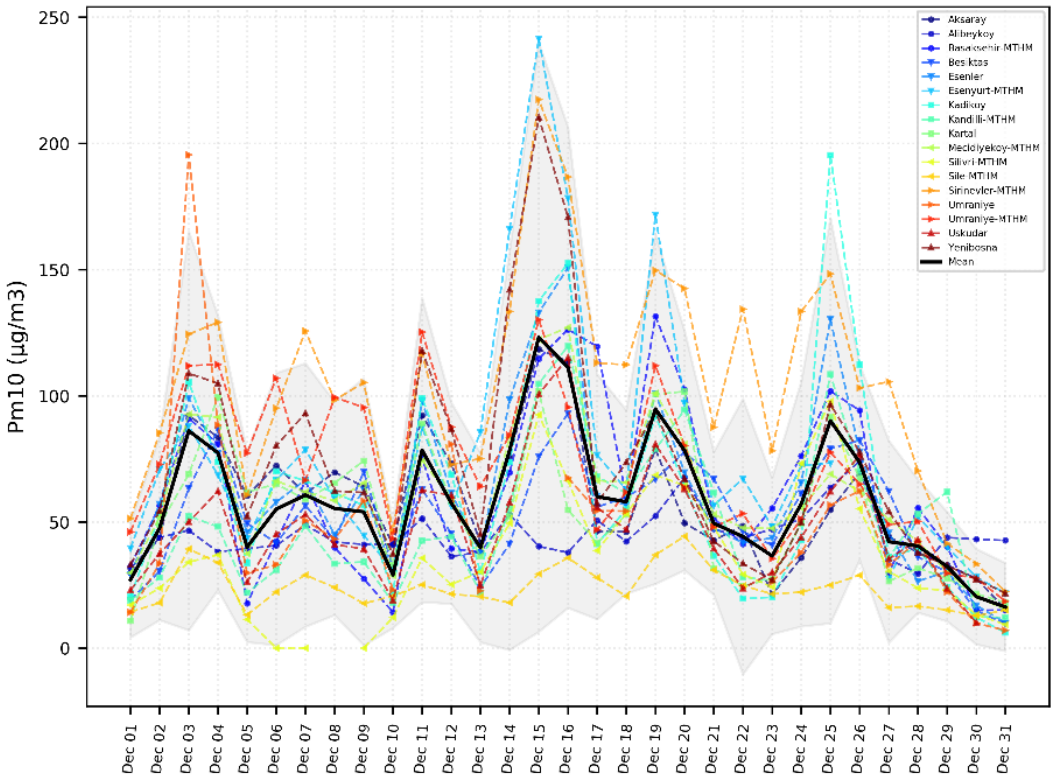

Figure 3.4 : PM_{10} (µg/m^3) values of air quality monitoring stations in Istanbul for December 2014.

In Figure 3.5, Empirical Cumulative Distribution Function (ECDF) plot of stations are given. ECDF was used to quantify the intra-variability among stations. The 25th percentile for the average distribution is approximately 30 µg/m^3 and it ranges between 15 – 60 µg/m^3. The 50th percentile of the average distribution is approximately 50 µg/m^3 and it ranges between 20 – 105 µg/m^3. For the 75th percentile average distribution is approximately 65 µg/m^3 and it ranges between 25 – 130 µg/m^3. For the 95th percentile average distribution is approximately 75 µg/m^3 and it ranges between 35 – 195 µg/m^3.

These values indicate that the intra-variability between stations increase as the percentile increases. This means that for higher values there seems to be higher variability in PM_{10} observations.

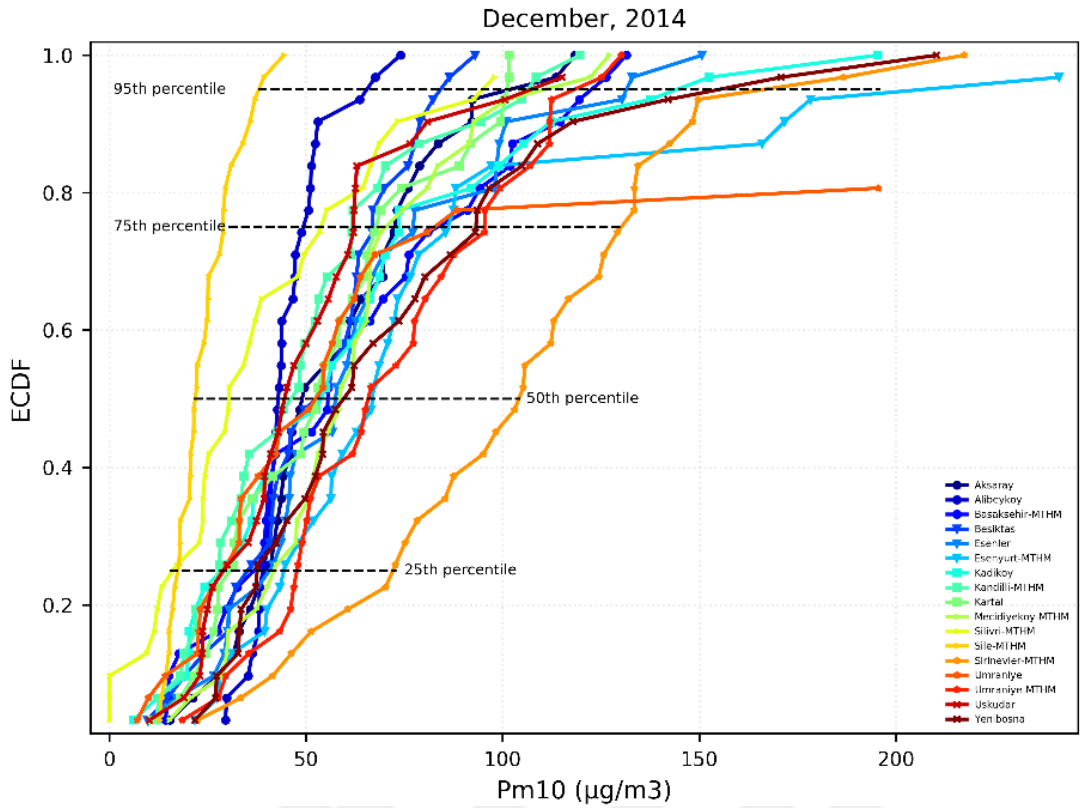

Figure 3.5 : ECDF values of all stations for December 2014.

3.2.2 January 2015

Figure 3.6 contains a time series plot of particulate matter concentrations measured by stations. For the January 2015, the average of all stations is 56.65 µg/m^3. Gray shaded area on the time series plot shows the 95% of values that are in $\mu \pm 2\sigma$ range. During the month, average particulate matter concentrations peaked three times; on January 3rd (89 µg/m^3), 17th (111.7 µg/m^3), 22nd (129.29 µg/m^3). Peak days of average concentration coincide with dates of fourteen out of the total eighteen stations' maximum measurements. Seven stations (Esenler, Kartal, Mecidiyeköy-MTHM, Şile-MTHM, Şirinevler-MTHM, Ümraniye-MTHM, Yenibosna) had their maximum PM_{10} concentration measurements on January 17th and another seven stations (Aksaray, Başakşehir-MTHM, Beşiktaş, Kadıköy, Kağıthane, Ümraniye, and Üsküdar) had their maximum PM_{10} concentration measurements on January 22nd. On January 28th, all stations dip under 50 µg/m^3, standard deviation is the lowest and the values of the day are bunched around the mean.

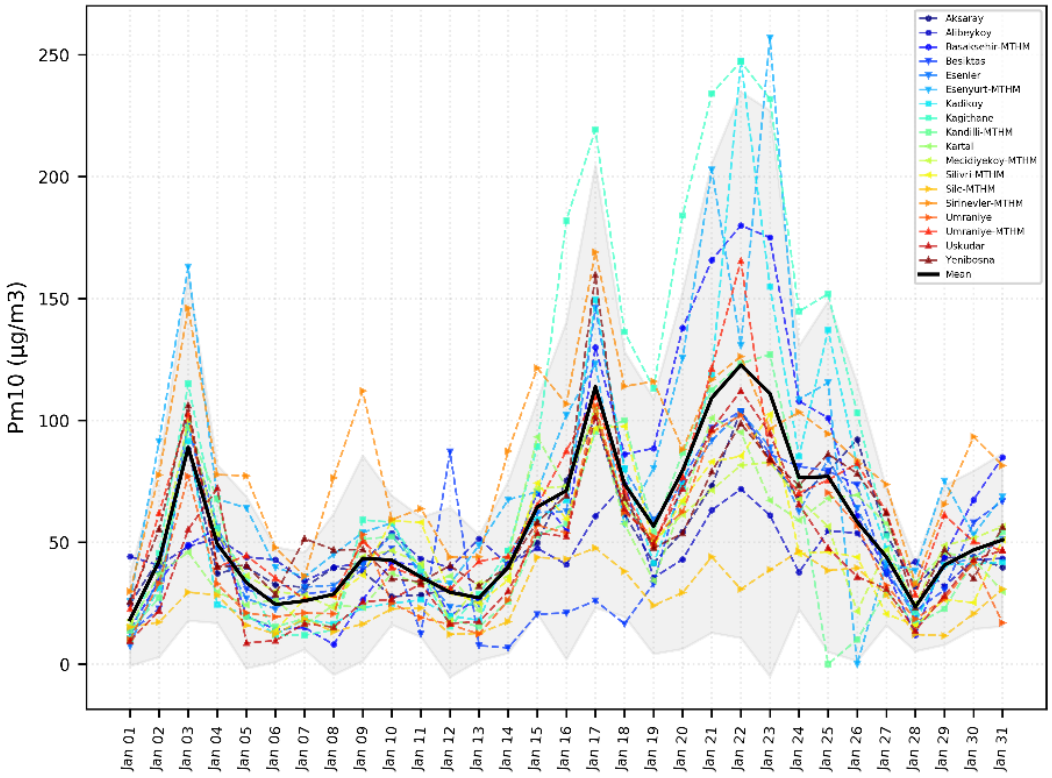

Figure 3.6 : PM_{10} ($\mu g/m^3$) values of air quality monitoring stations in Istanbul for January 2015.

In Figure 3.7, ECDF was used to quantify the intra-variability among stations. The 25th percentile for the average distribution is approximately 30 $\mu g/m^3$ and it ranges between 15 – 60 $\mu g/m^3$. The 50th percentile of the average distribution is approximately 40 $\mu g/m^3$ and it ranges between 24 – 85 $\mu g/m^3$. For the 75th percentile average distribution is approximately 55 $\mu g/m^3$ and it ranges between 40 – 160 $\mu g/m^3$. For the 95th percentile average distribution is approximately 85 $\mu g/m^3$ and it ranges between 45 – 165 $\mu g/m^3$.

These values indicate that the intra-variability between stations increase as the percentile increases. This means that for higher values there seems to be higher variability in PM_{10} observations.

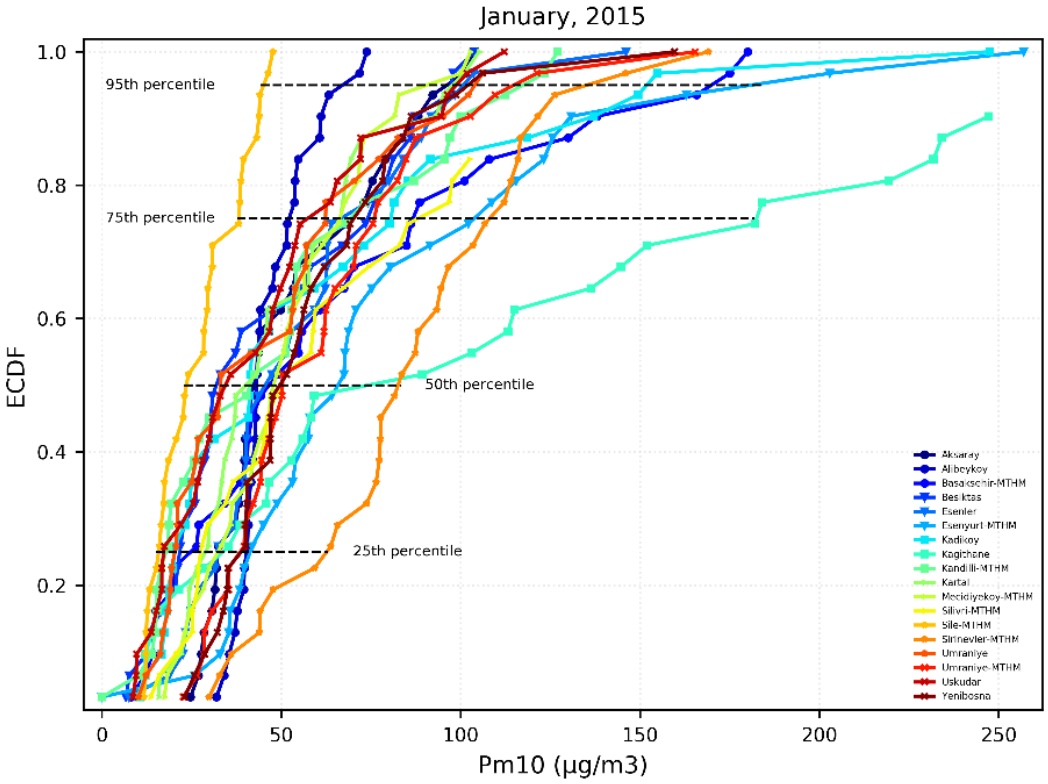

Figure 3.7 : ECDF values of all stations for January 2015.

3.2.3 February 2015

Figure 3.8 contains a time series plot of particulate matter concentrations measured by stations. For the February 2015, the average of all stations is 53.23 µg/m^3. Gray shaded area on the time series plot shows the 95% of values that are in $\mu \pm 2\sigma$ range. During the month, average particulate matter concentrations peaked three times; on February 1st (299.01 µg/m^3), 6th (285.04 µg/m^3), 27th (292.43 µg/m^3). Peak days of average concentration coincide with dates of eleven out of the total eighteen stations' maximum measurements. Eleven stations (Aksaray, Alibeyköy, Esenler, Kadıköy, Kartal, Kandilli, Mecidiyeköy-MTHM, Şile-MTHM, Şirinevler-MTHM, Ümraniye, Üsküdar) had their maximum PM_{10} concentration measurements on February 1st. On February 17th, all stations dip under 50 µg/m^3, standard deviation is the lowest and the values of the day are bunched around the mean, however, only Ümraniye-MTHM station had PM_{10} concentration measurements (107.08 µg/m^3) over 50 µg/m^3.

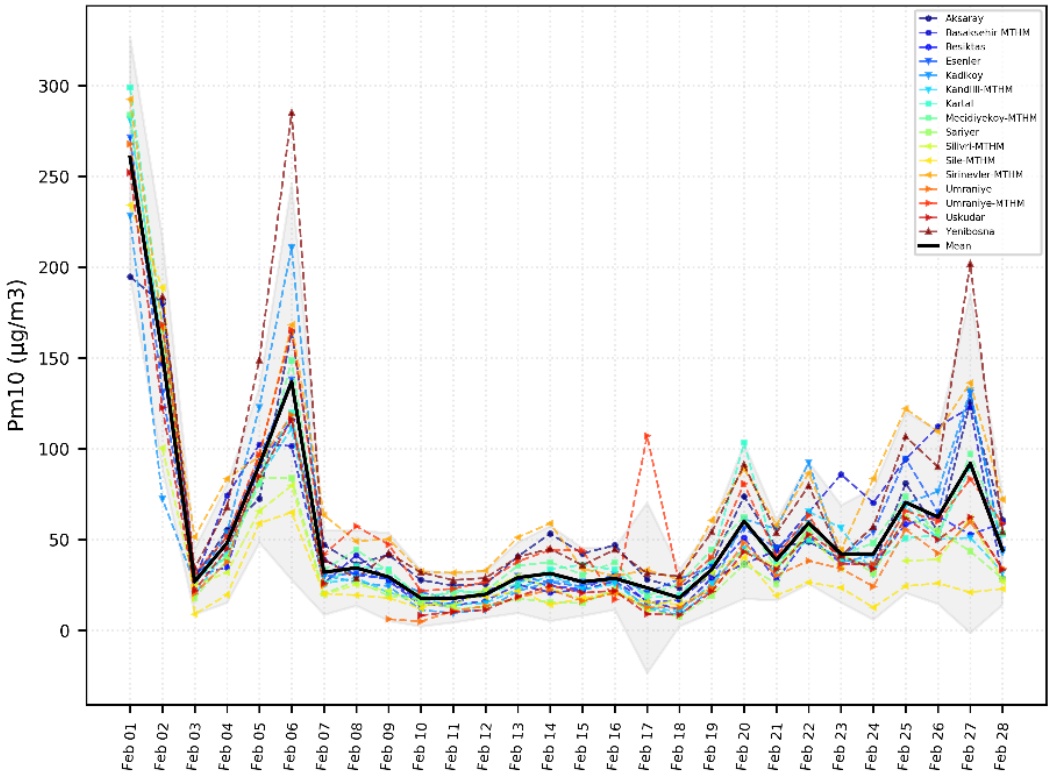

Figure 3.8 : PM_{10} (µg/m^3) values of air quality monitoring stations in Istanbul for February 2015.

In Figure 3.9, ECDF was used to quantify the intra-variability among stations. The 25th percentile for the average distribution is approximately 30 µg/m^3 and it ranges between 15 – 35 µg/m^3. The 50th percentile of the average distribution is approximately 50 µg/m^3 and it ranges between 20 – 55 µg/m^3. For the 75th percentile average distribution is approximately 50 µg/m^3 and it ranges between 22 – 75 µg/m^3. For the 95th percentile average distribution is approximately 175 µg/m^3 and it ranges between 120 – 245 µg/m^3.

These values indicate that the intra-variability between stations increase as the percentile increases. This means that for higher values there seems to be higher variability in PM_{10} observations.

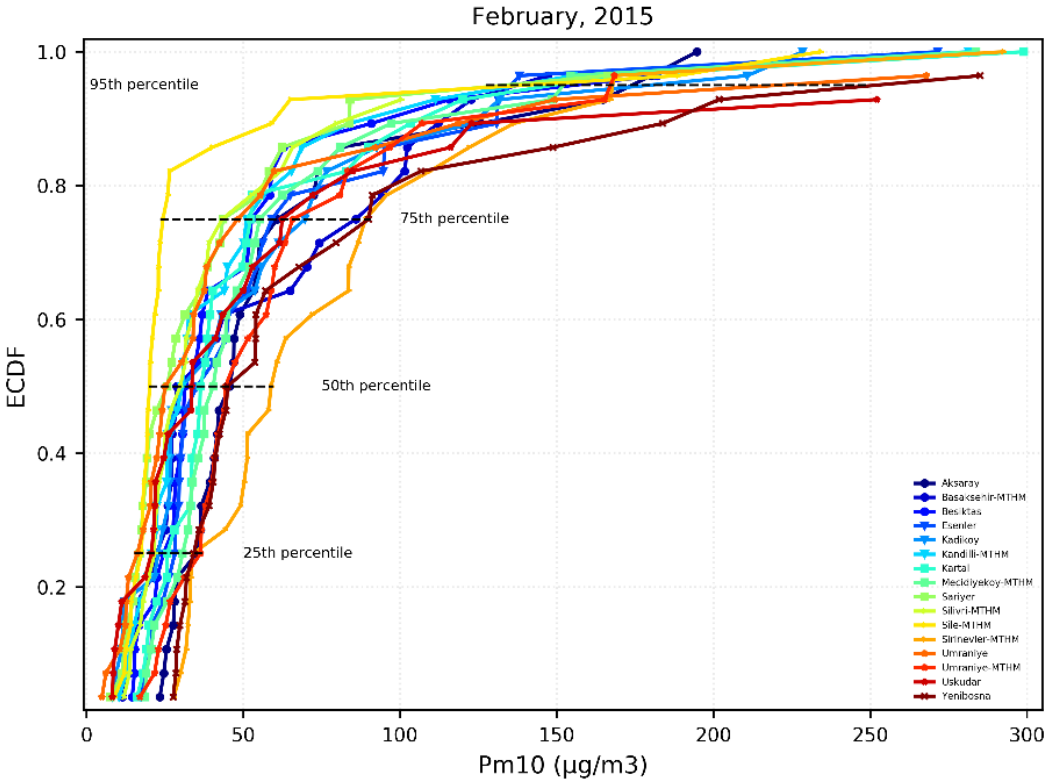

Figure 3.9 : ECDF values of all stations for February 2015.

Further detailed results of the observation station (Kartal station) is given in their respective sub-section. Kartal station is chosen as the representative observation station. This station is among stations that have higher chance of being affected by the residential heating and furthermore this is the only station with radiosounding observations. Kartal station observation values compared to model results to assess the model performance for the selected study period.

3.2.4 Kartal Station:

Kartal station is located in south eastern part of the city center (29° 12' 26", 40° 53' 24") (Figure 3.10).

3.2.4.1 December 2015:

Particulate matter concentrations exceeded national PM_{10} limit in seven days. These days are December 4^{th}, 9^{th}, 11^{th}, 15^{th}, 19^{th}, 20^{th}, 25^{th} (Figure 3.11). Maximum PM_{10} value is on December 20^{th} with 101.71 µg/m^3. The cleanest measured day was first day of the month with a concentration of 10.84 µg/m^3 (Figure 3.11). Particulate matter concentrations exceeded 100 µg/m^3 on three days. Monthly average of this station is 54.60 µg/m^3.

Figure 3.10 : Kartal station's location.

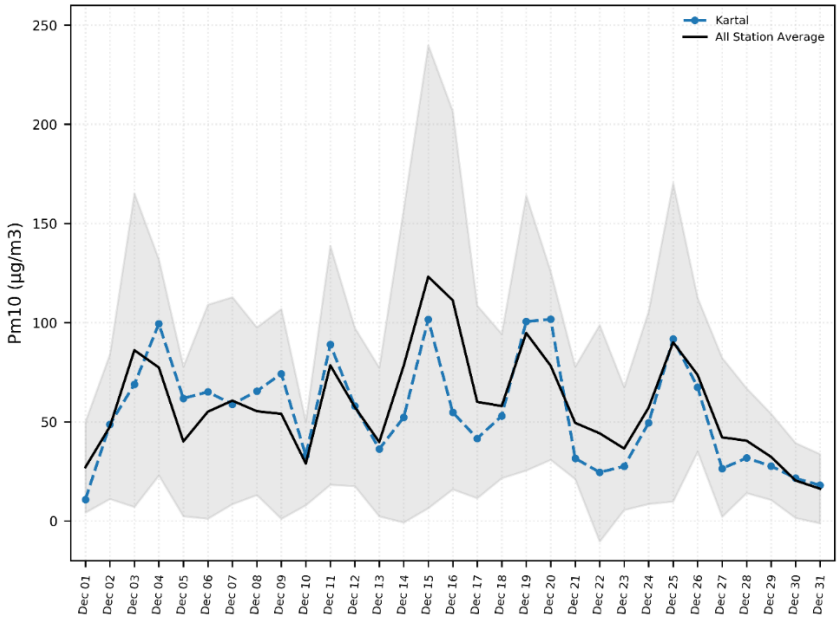

Figure 3.11 : Kartal station December 2014 observation values.

In Figure 3.12, ECDF plot of Kartal station shows that 77% of daily PM_{10} concentrations are under national daily PM_{10} limit. From the same figure it can be seen that 50th percentile is above European daily PM_{10} limit of 50 µg/m^3 meaning that for most days Kartal station has particulate matter pollution in December 2014 by European air quality standards.

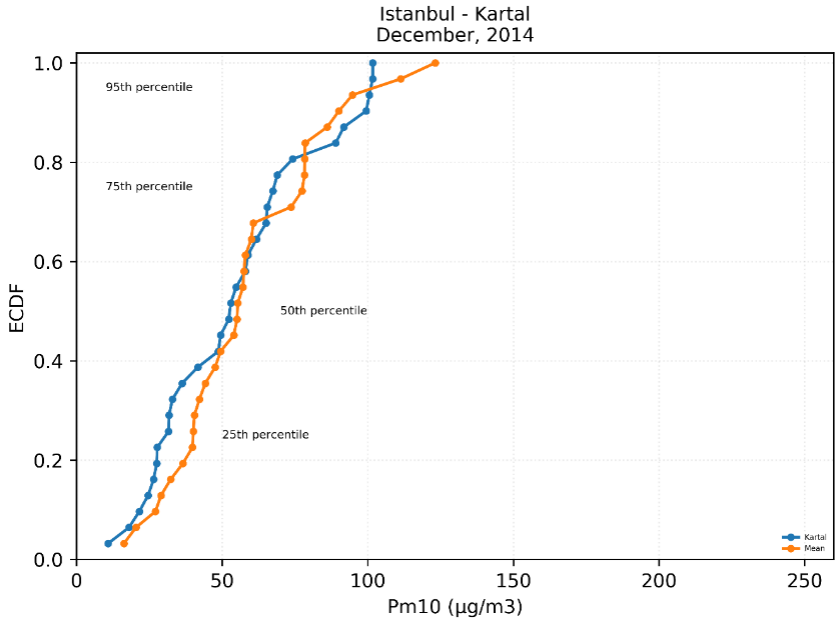

Figure 3.12 : ECDF values of Kartal station for December 2014.

3.2.4.2 January 2015:

Particulate matter concentrations exceeded national PM_{10} limit in five days. These days are January 15th, 16th, 17th, 21st, 22nd (Figure 3.13). Maximum PM_{10} value is on January 17th with 105.09 µg/m^3. The cleanest measured day was first day of the month with a concentration of 15.81 µg/m^3 (Figure 3.13). Particulate matter concentrations went over 100 µg/m^3 on two days. Monthly average of this station is 48.80 ug/m3.

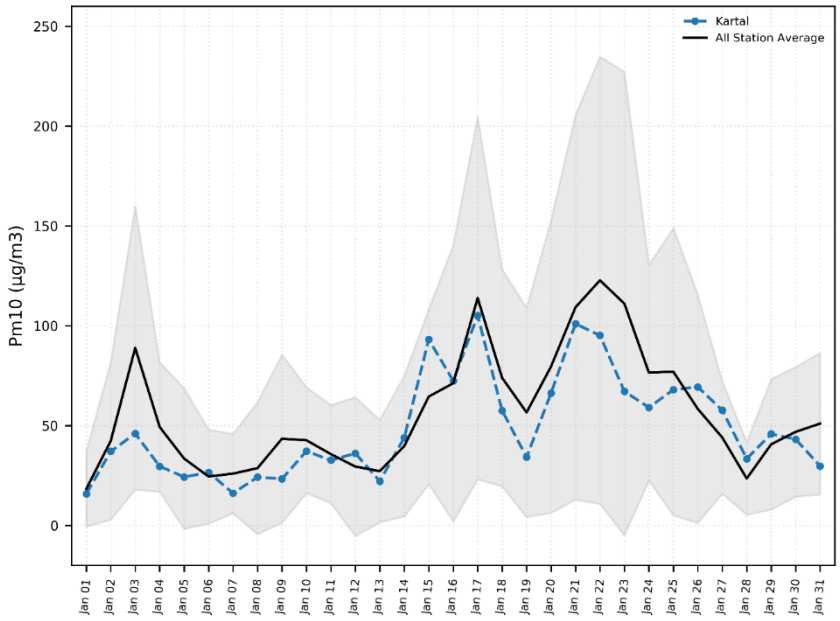

Figure 3.13 : Kartal station January 2015 observation values.

In Figure 3.14, ECDF plot of Kartal station shows that 83% of daily PM_{10} concentrations are under national daily PM_{10} limit. From the same figure it can be seen that 50th percentile is below European daily PM_{10} limit of 50 µg/m^3 meaning that for most days Kartal station has cleaner air compared to December 2014.

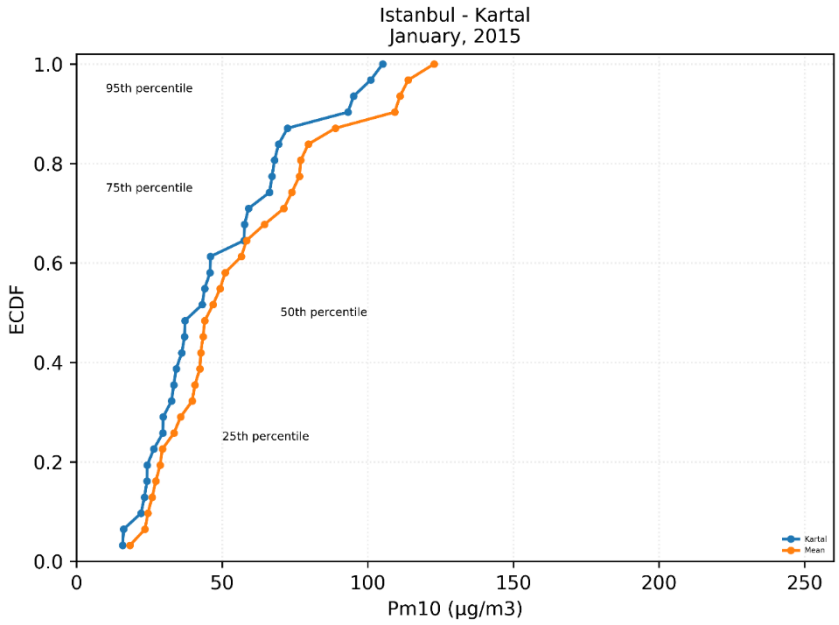

Figure 3.14 : ECDF values of Kartal station for January 2015.

3.2.4.3 February 2015:

Particulate matter concentrations exceeded national PM_{10} limit in six days. These days are February 1st, 2nd, 5th, 6th, 20th, 27th (Figure 3.11). Maximum PM_{10} value is on February 1st with 299.01 µg/m^3. The cleanest measured day was tenth day of the month with a concentration of 16.15 µg/m^3 (Figure 3.11). Particulate matter concentrations exceeded 100 µg/m^3 on four days. Monthly average of this station is 57.43 µg/m^3.

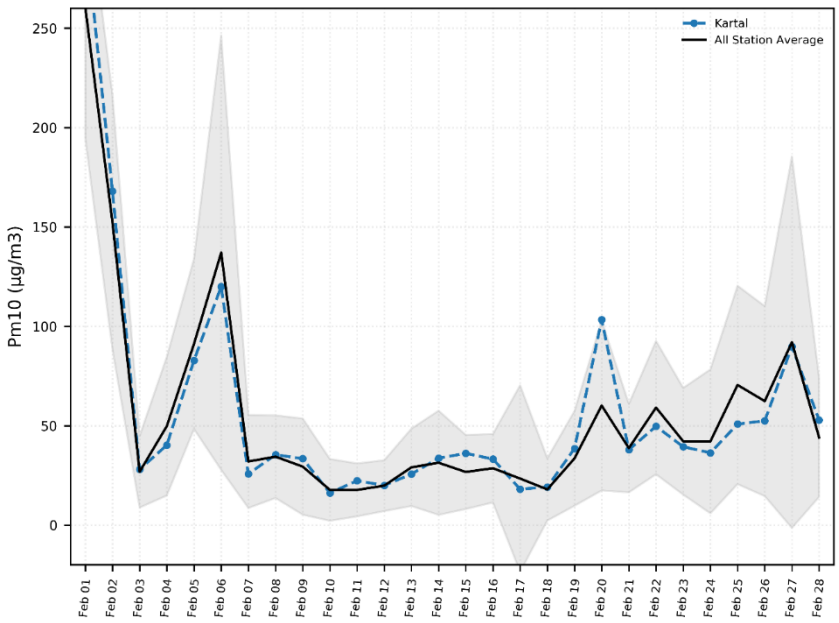

Figure 3.15 : Kartal station February 2015 observation values.

In Figure 3.16, ECDF plot of Kartal station shows that 79% of daily PM_{10} concentrations are under national daily PM_{10} limit. From the same figure it can be seen that 50th percentile is above European daily PM_{10} limit of 50 µg/m^3 meaning that for most days Kartal station has clean air in February 2015 with the exception of the first week of the month where particulate matter concentrations reached extreme levels, especially on the first day of the month.

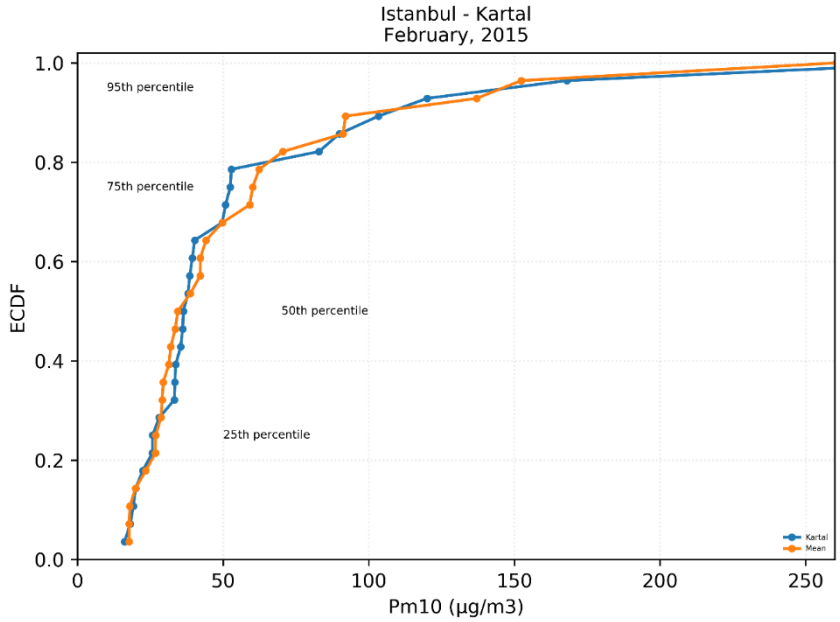

Figure 3.16 : ECDF values of Kartal station for February 2015

3.3 Meteorological Model

Meteorology ground observations and radiosonde observations were obtained from Turkish State Meteorological Service. Both ground observations and radiosonde data were recorded at Kartal station (40.91°N, 29.15°E) in Kartal province (Figure 3.17-a). Model performance was evaluated using these observation data. Statistical metrics that were used to assess the model performance are Mean Bias (MB) (equation (1)) to evaluate model bias, for model error evaluation Mean Absolute Gross Error (MAGE) (equation (2)) and Root Mean Square Error (RMSE) (equation (3)).

$$\text{MB} = \frac{1}{n}\sum(Model_i - Observation_i) \qquad (1)$$

$$\text{MAGE} = \frac{1}{n}\sum|Model_i - Observation_i| \qquad (2)$$

$$\text{RMSE} = \sqrt{\frac{1}{n}\sum(Model_i - Observation_i)^2} \qquad (3)$$

Meteorology outputs produced by the WRF model and comparisons with observations are given in Figure 3.17. For this study, the main focus of the evaluation is on model–observation comparisons of 2-m temperature. Temperature is an important factor for residential heating emissions since it is responsible for energy use for space heating and cooling.

Hourly comparison of temperature at 2-m (Figure 3.17-b) shows an agreement between model calculated values and Kartal station observations with a MB of 0.33 ^{o} C, MAE of 0.68 ^{o}C, and RMSE of 0.76 ^{o}C which is well within the benchmarks (-0.5 K < MB < 0.5 K and MAE < 2 K) proposed by (Emery, Edward, & Yarwood, 2001). Throughout the study period, daily mean temperature observations at 2-m are between 8.44 ^{o}C - 15.3 ^{o}C with a mean of 11.7 ^{o}C (Figure 3.17-b). Low temperature days were December 1st - 4th, December 10th and 11th, and December 13th - 17th.

Temperature measured by radiosonde at 1000 millibar for noon time (12Z) presented in Figure 3.17-c, values are between 7.78 ^{o} C and 13.2 ^{o} C with a mean of 19.4 ^{o} C. Comparison of radiosonde and the model showed that the meteorology model produced realistic temperature outputs (MB -0.60 ^{o}C, MAGE 0.84 ^{o}C, and RMSE 1.07 ^{o} C).

A comparison of potential temperature produced by the WRF model to potential temperature recorded by radiosonde observations is given in Figure 3.18. There is a high correlation between the observed and the modelled data for pressure levels between 1000 - 700 millibar with a correlation coefficient over 0.98 (Figure 3.18). These results suggest that the WRF model accurately estimated the potential temperature.

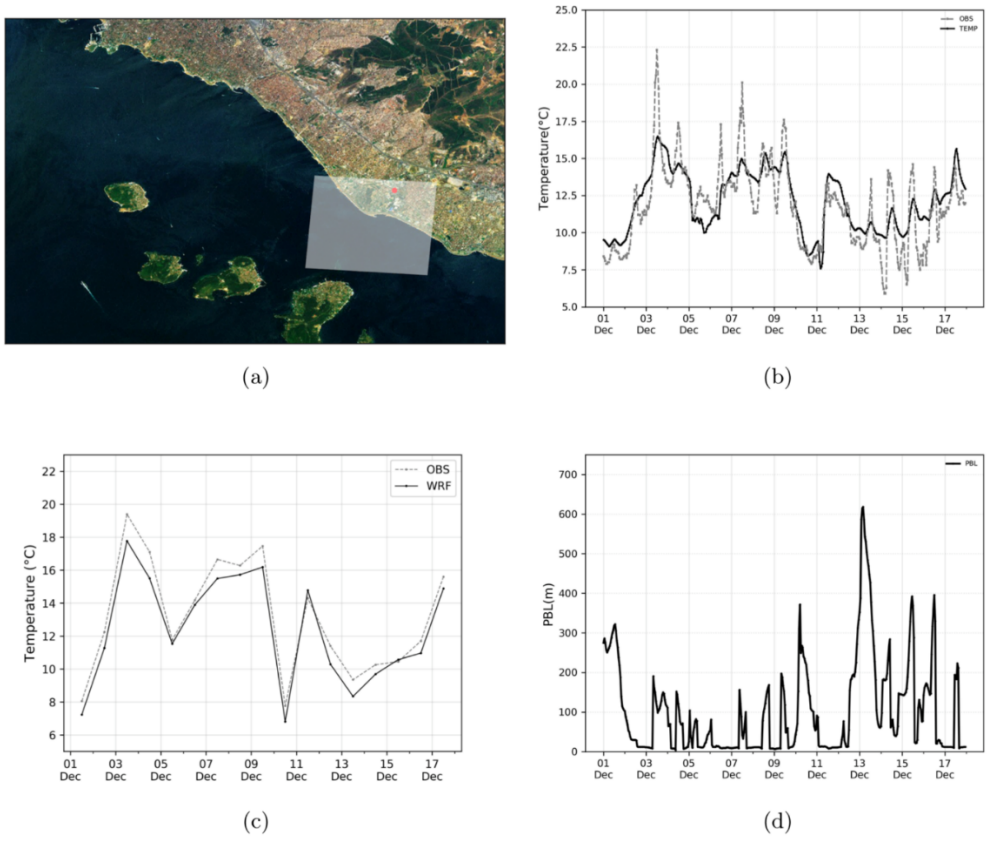

Figure 3.17 : Station Location and Meteorology Outputs.

The WRF model overestimates 10-m WSPD with a MB of 2.28 m/s, RMSE 2.55 m/s, MAGE 3.08 m/s. The Kartal observation site is near the Marmara Sea, meaning that the model grid cell is primarily water (Figure 3.17-a) which might be the reason for the large bias due to the model's usage of land fraction.

Previous studies showed similar overestimations in WSPD produced by the meteorology model; however, it should be noted that wind speed varies significantly depending on different terrain conditions and other physical parameters of the model. A common model performance criterion might not be applied to all modeling studies.

In order to assess the vertical mixing of the atmosphere PBLH was used and the WRF model produced hourly PBLH values given in (Figure 3.17-d). The PBL height throughout the study period only exceeded 400 m on one day (December 13th) (Figure 3.17-d) while the rest of the episode was mostly below 300 m which is considered low by air pollution perspective.

Low PBL heights for this episode means poor mixing of pollutants and high pollutant concentrations. Days with low PBLH are December 2nd - 10th, and December 12th.

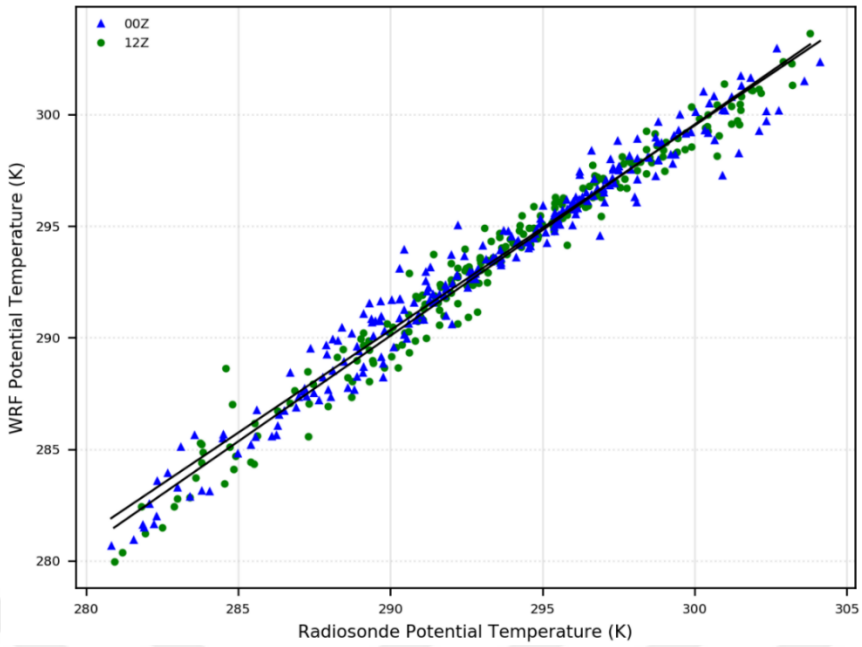

Figure 3.18 : Potential temperature comparison of the WRF model and Radiosonde observation.

Representation of weather phenomenon is crucial for air quality studies; overall the meteorology fields generated by WRF v3.8.1 meteorology model for CMAQ air quality model has been reasonable and well represented for the study period.

3.4 Emission Model

First part of this section is the base case emissions followed by the residential heating emissions results. As mentioned in previous sections modeling domain consist of three nested domains; 36-km, 12-km, and the 4-km domain. For the 36 and 12 km domains TNO emissions inventory are used.

In Figure 3.19 spatial distribution of sum of all sectors of particulate matter emissions for the 36-km domain is given. This domain is used primarily for boundary conditions. It can be seen from the figure that particulate matter emissions are higher on the Middle Eastern part of the domain. The outermost coarser 36-km emissions are beyond the scope of this study we have kept this domain brief while going in detail with inner domains.

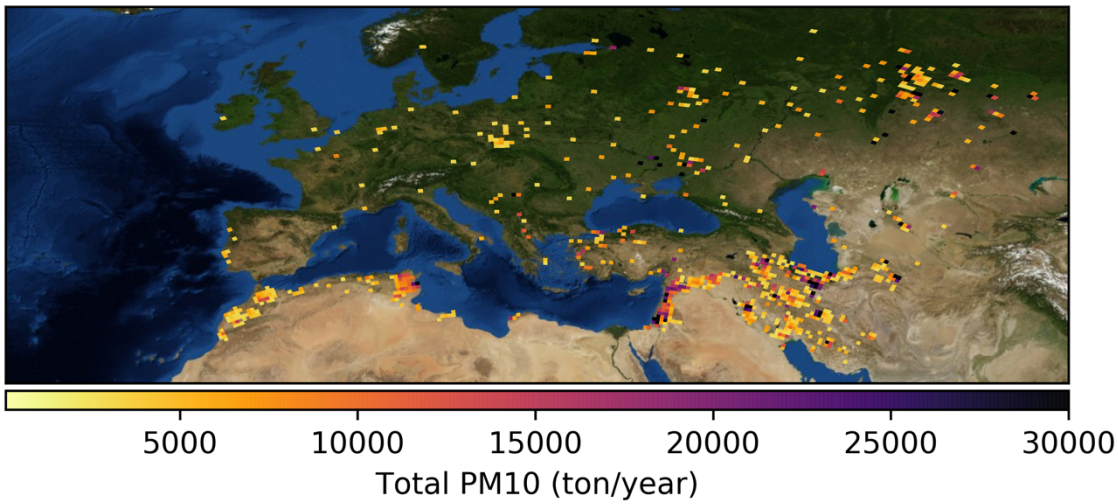

Figure 3.19 : Total PM_{10} emissions of the 36-km domain.

3.4.1 12-km domain emissions:

12-km domain covers entire Turkey, this domain is for evaluate air quality all over Turkey. For the selected pollutants (PM_{10}, SO_2, and NOx), sector specific distribution and annual totals are given in (Table 3.2). The major contributing sector of PM_{10} is Sector 6 with 34.6% followed by Sector 7 (14.8%) and Sector 9 (13.6%). For SO_2, both Sector 1 (36.1%) and Sector 10 (37.9%) contributes significantly compared to the rest of the sectors. For NO_x, the most significant contributor is Sector 1 (67.2%) which is emissions from energy industries (Table 3.2). Sector 2 consists 12.4% of PM_{10} emissions, 2.1% of SO_2 emissions, and 0.4% of NO_x emissions.

Table 3.2 : PM_{10}, SO_2, and NO_x Emission Totals and Sector Distribution of the 12-km domain.

12km	Sector 1	Sector 2	Sector 34	Sector 5	Sector 6	Sector 7	Sector 8	Sector 9	Sector 10	Sector Total (ton/year)
PM_{10}	5.7%	12.4 %	9.8%	0.1%	34.6 %	14.8 %	2.9%	13.6 %	5.9%	221,376
SO_2	36.1 %	2.1%	20.7%	0.0%	0.0%	1.0%	2.0%	0.0%	37.9%	422,964
NO_x	67.2 %	0.4%	1.1%	0.0%	0.4%	13.2 %	0.6%	0.0%	17.0%	415,620

In Figure 3.20 and 3.21, spatial distribution of sector total and sector specific emissions of NO_x emissions are given. In sector total figure (Figure 3.20) of NO_x, it can be seen that emissions are concentrated in mostly industrialized bigger cities.

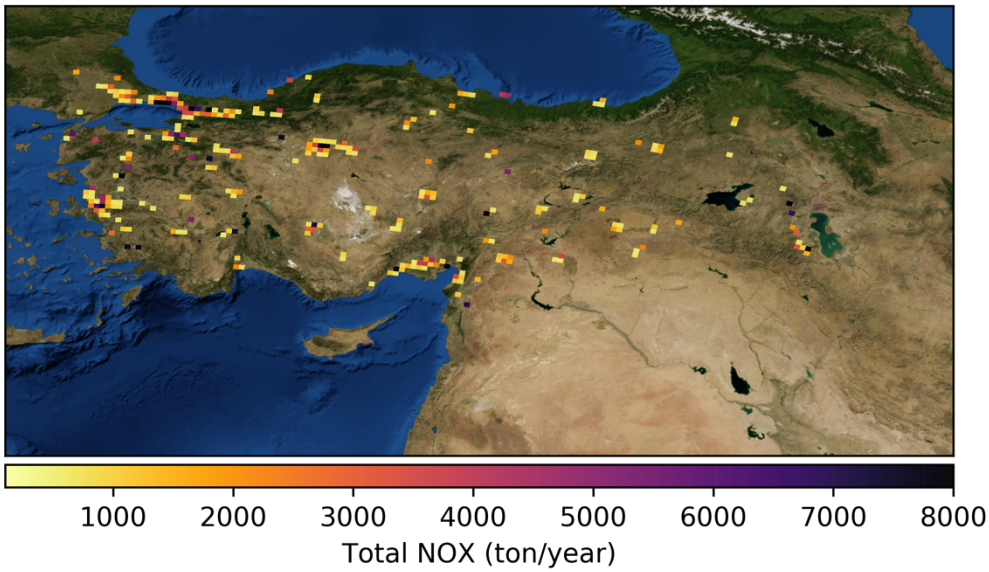

Figure 3.20 : Total NO_x emissions of the 12-km domain.

For the Sector 2 (Figure 3.21) specific emissions, emissions are from densely populated big cities; Istanbul, Ankara, Adana, İzmir, and generally industrialized western part of Turkey. The spatial distribution of NO_x emissions indicates the effect of residential heating, industry, and traffic emissions.

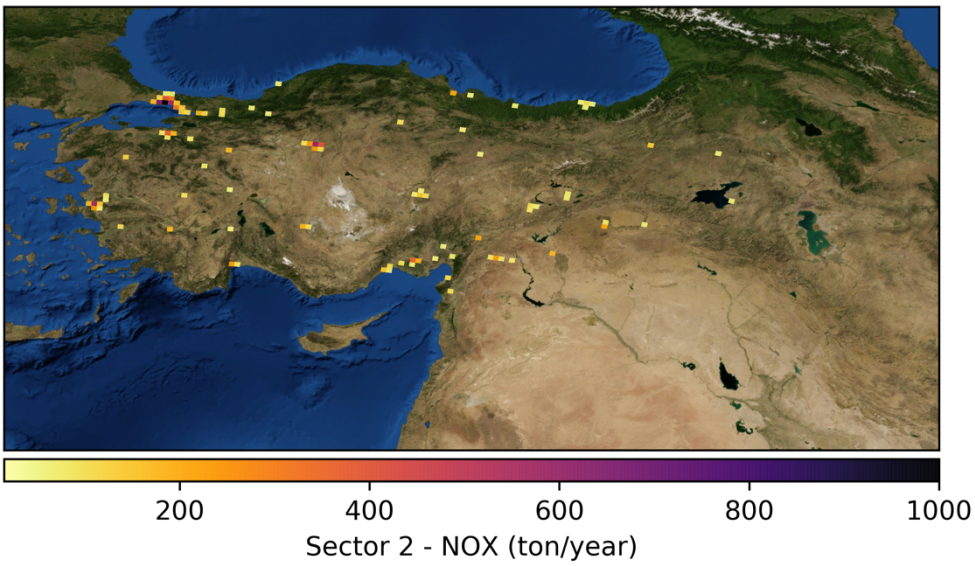

Figure 3.21 : Sector 2 - NO_x emissions of the 12-km domain.

In Figure 3.22 and 3.23, spatial distribution of sector total and sector specific emissions of PM_{10} emissions are given. In sector total figure (Figure 3.22) of PM_{10}, it can be seen that emissions are concentrated in mostly industrialized bigger cities, especially on western part of Turkey.

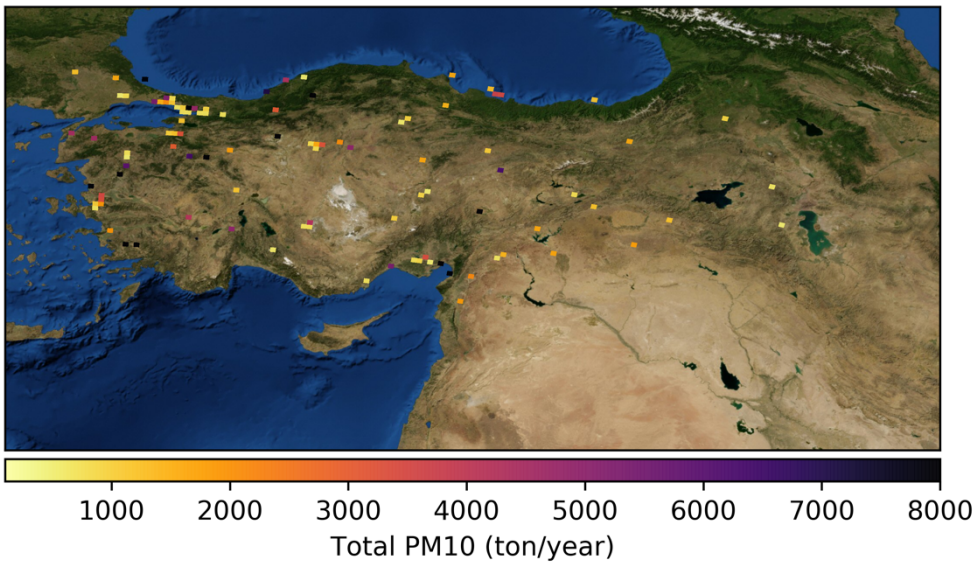

Figure 3.22 : Total PM_{10} emissions of the 12-km domain.

For the Sector 2 (Figure 3.23) specific emissions, emissions are from densely populated big cities; Istanbul, Ankara, and İzmir cities. The spatial distribution of PM_{10} emissions indicates the effect of residential heating and on road emissions since the highest emissions (over 900 ton/year) are found in Istanbul.

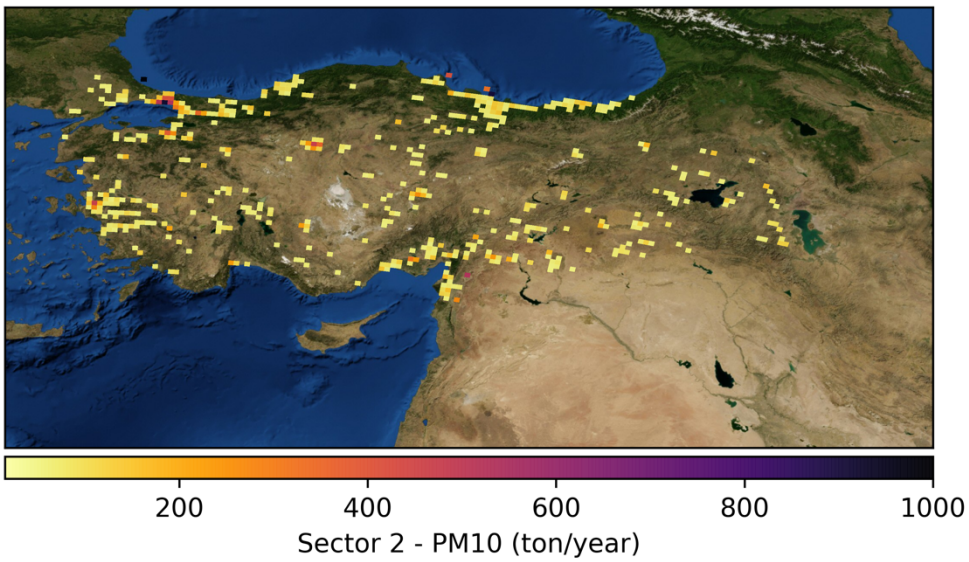

Figure 3.23 : Sector 2 - PM_{10} emissions of the 12-km domain.

In Figure 3.24 and 3.25, spatial distribution of sector total and sector specific emissions of SO_2 emissions are given. In sector total figure (Figure 3.24) of SO_2, it can be seen that emissions are concentrated in mostly industrialized bigger cities and mostly western part of Turkey, as with other pollutants.

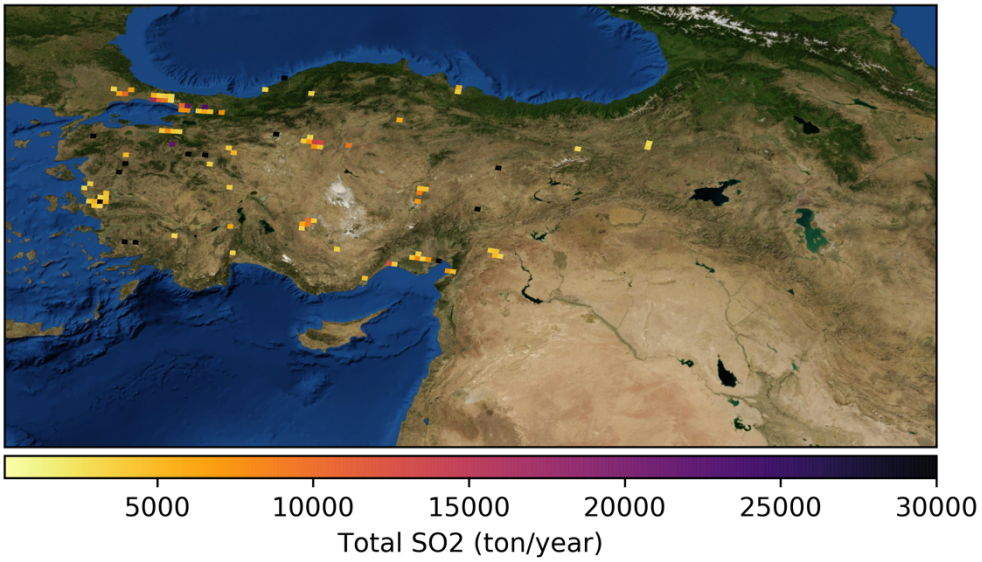

Figure 3.24 : Total SO_2 emissions of the 12-km domain.

For the Sector 2 (Figure 3.25) specific emissions, emissions are from densely populated big cities; Istanbul, Ankara. The spatial distribution of SO_2 emissions indicates the effect of residential heating emissions.

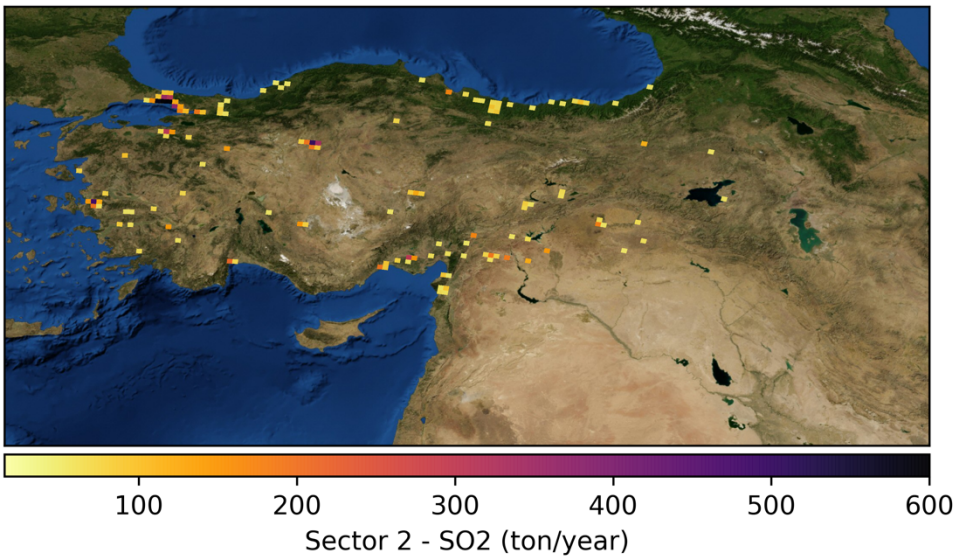

Figure 3.25 : Sector 2 - SO_2 emissions of the 12-km domain.

Spatial distributions of NO_x, PM_{10}, and SO_2 are inline with each other and support the previous literature. In Turkey, contribution of local sources, especially for big cities, are significantly higher than that of long-range transport. These results show that high-resolution emission inventories and air quality modeling is vital for policy makers to make healthy control strategies.

3.4.2 4-km domain emissions:

3.4.2.1 Base Case:

The innermost modeling domain is the 4-km domain that covers the Marmara Region. For the selected pollutants (PM_{10}, SO_2, and NOx), sector specific distribution and annual totals are given in (Table 3.3). The major contributing sector of PM_{10} is Sector 34 with 36.4% followed by Sector 1 (32.7%) and Sector 2 (14.3%). For SO_2, Sector 1 (69.3%) and Sector 34 (26.6%) contributes significantly compared to the rest of the sectors. For NO_x, the significant contributor is Sector 34 (31.7%) followed by Sector 1 and 7 with (24.3%) (Table 3.3). Sector 2 consists 14.3% of PM_{10} emissions, 1.6% of SO_2 emissions, and 3.4% of NO_x emissions.

Table 3.3: Emission Totals and Sector Distribution of the 4-km domain.

4km	Sector 1	Sector 2	Sector 34	Sector 5	Sector 6	Sector 7	Sector 8	Sector 9	Sector 10	Sector Total (ton/year)
PM_{10}	32.7 %	14.3 %	36.4%	0.3%	0.0%	1.5%	2.9%	2.3%	9.6%	179,946
SO_2	69.3 %	1.6%	26.6%	0.0%	0.0%	0.2%	2.1%	0.0%	0.1%	105,496
NO_x	24.3 %	3.4%	31.7%	0.0%	0.0%	24.3 %	16.1 %	0.0%	0.1%	384,041

In Figure 3.26 and 3.27, spatial distribution of sector total and sector specific emissions of NO_x emissions are given. In sector total figure (Figure 3.26) of NO_x, it can be seen that emissions are concentrated in mostly in Istanbul, Kocaeli, and Bursa.

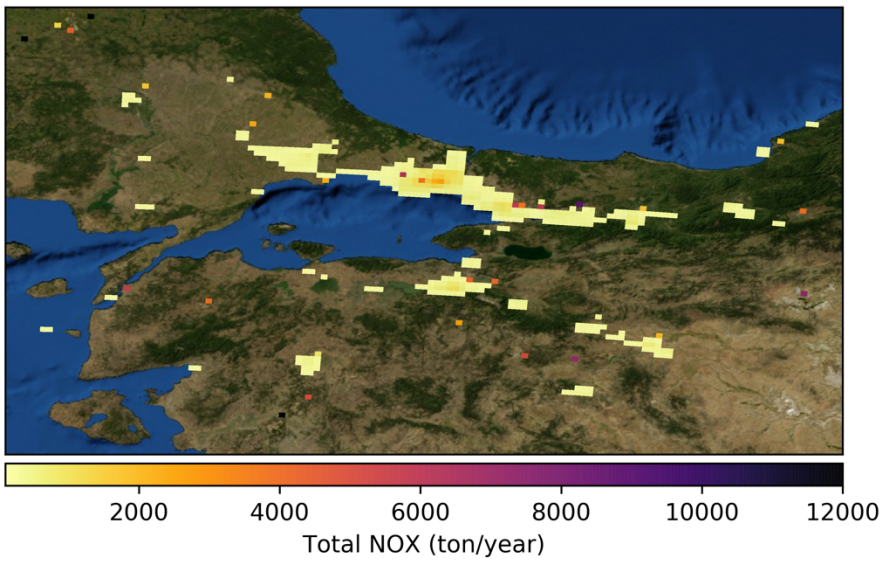

Figure 3.26 : Total NO_x emissions of the 4-km domain.

For the Sector 2 (Figure 3.27) specific emissions, emissions are from densely populated Istanbul. The spatial distribution of these pollutant emissions indicates the effect of residential heating and the surrounding industry. Emission hotspots are mainly residential areas. It is also seen from this figure that Bursa is another hotspot of NO_x emissions.

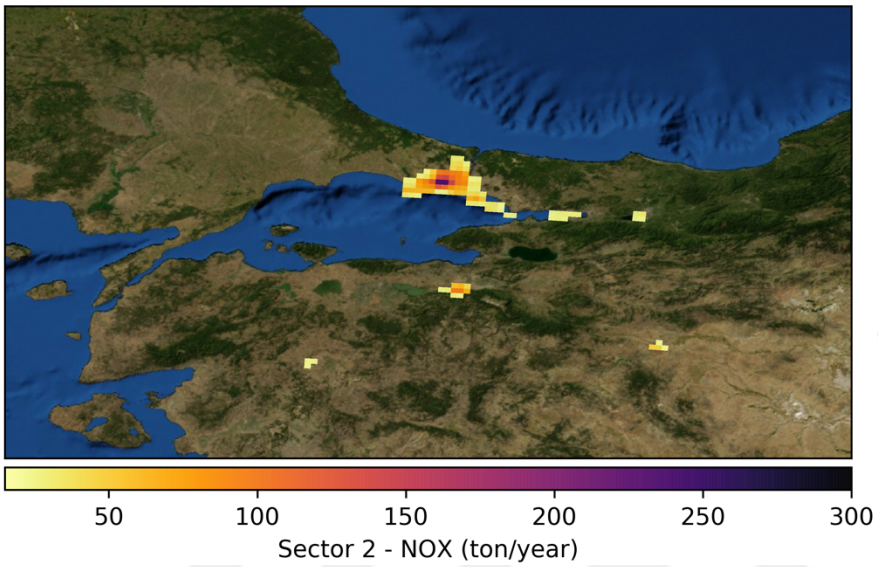

Figure 3.27 : Sector 2 - NO_x emissions of the 4-km domain.

In Figure 3.28 and 3.29, spatial distribution of sector total and sector specific emissions of PM_{10} emissions are given. In sector total figure (Figure 3.28) of PM_{10}, it can be seen that emissions are concentrated in industrialized areas, as high concentration point sources and in Istanbul in form of local area sources such as residential heating.

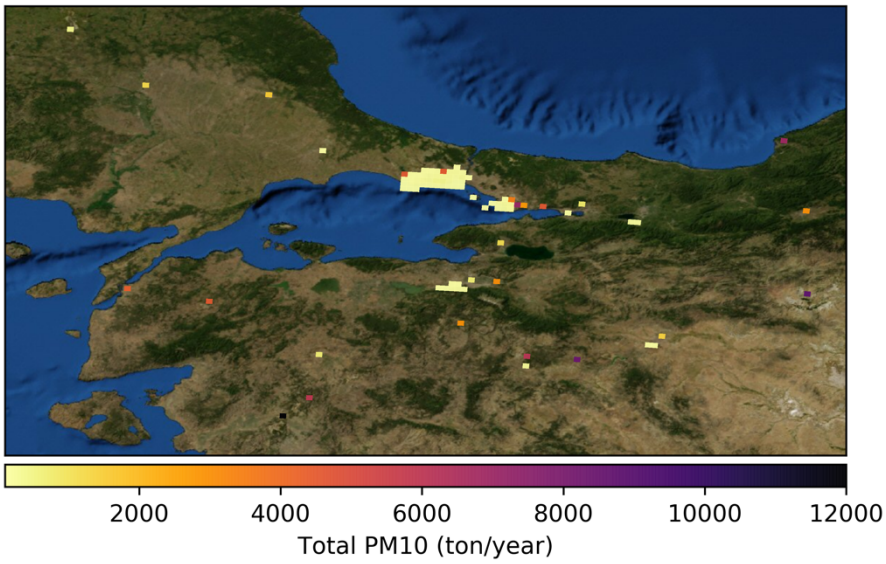

Figure 3.28 : Total PM_{10} emissions of the 4-km domain.

For the Sector 2 (Figure 3.29) specific emissions, emissions are from densely populated big cities; Istanbul, Kocaeli, and Bursa. The spatial distribution of PM_{10} emissions indicates the effect of residential heating and industry.

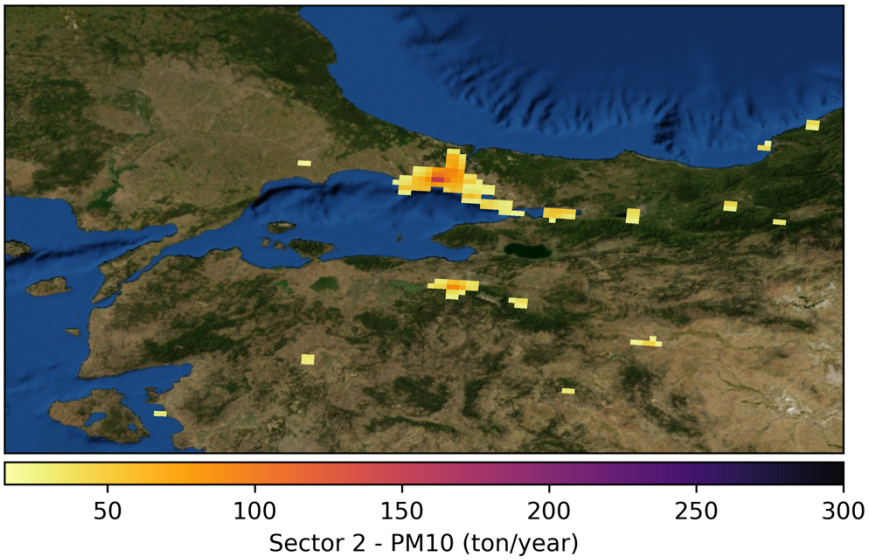

Figure 3.29 : Sector 2 - PM_{10} emissions of the 4-km domain.

In Figure 3.30 and 3.31, spatial distribution of sector total and sector specific emissions of SO_2 emissions are given. In sector total figure (Figure 3.30) of SO_2, it can be seen that emissions are spread over the modeling domain around industrial areas.

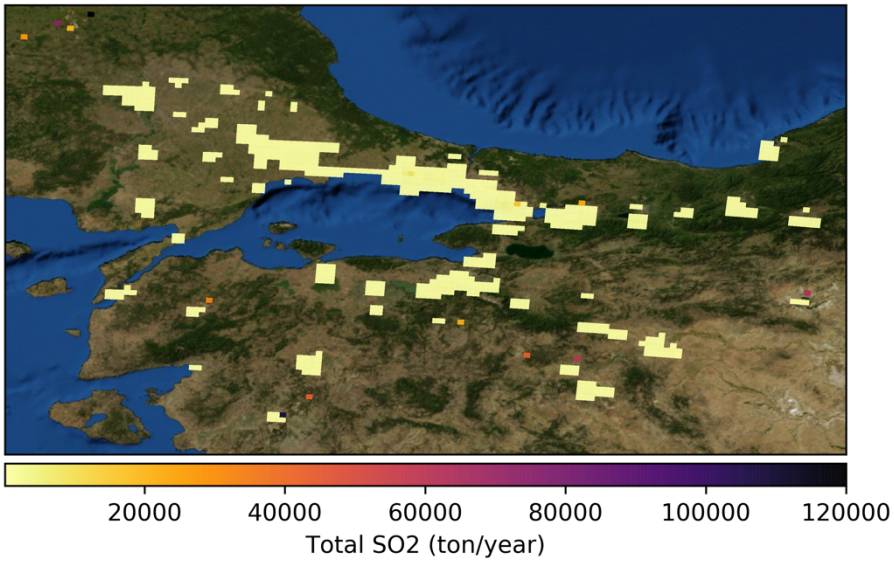

Figure 3.30 Total SO_2 emissions of the 4-km domain.

For the Sector 2 (Figure 3.31) specific emissions, emissions are from densely populated big cities; Istanbul and Bursa. The spatial distribution of SO_2 emissions

indicates the effect of residential heating since they are generally higher in Istanbul's residential areas.

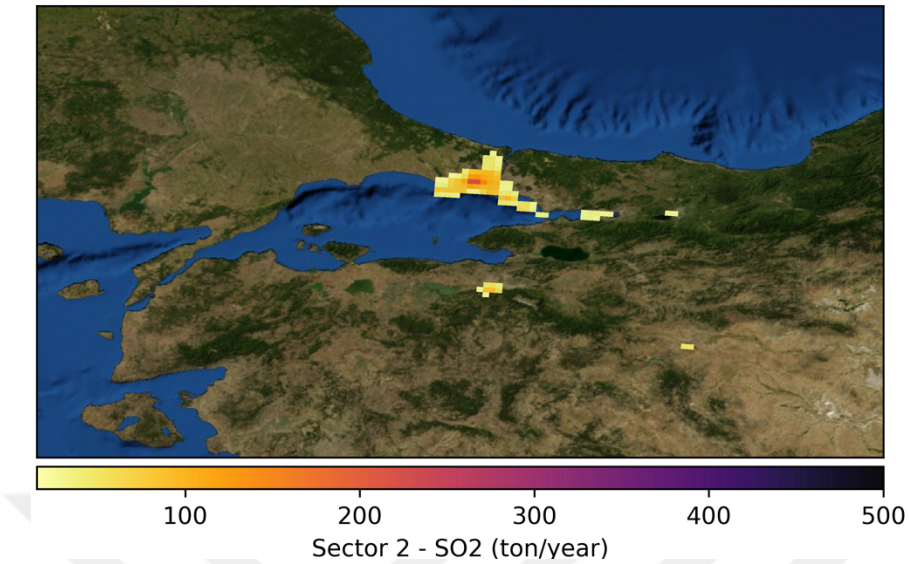

Figure 3.31 : Sector 2 - SO_2 emissions of the 4-km domain.

3.4.2.2 Residential Heating:

The innermost modeling domain is the 4-km domain that covers the Marmara Region. However, residential heating sector is replaced with a high-resolution emissions. From the figures it can been that spatial distrubtion and emission levels are improved significantly, given in the following section. For the selected pollutants (PM_{10}, SO_2, and NOx), sector specific distribution and annual totals are given in Table 3.4. The major contributing sector of PM_{10} is Sector 34 with 36.4% followed by Sector 1 (32.7%) and Sector 2 (14.3%). For SO_2, Sector 1 (69.3%) and Sector 34 (26.6%) contributes significantly compared to the rest of the sectors. For NO_x, the significant contributor is Sector 34 (31.7%) followed by Sector 1 and 7 with (24.3%) (Table 3.4). Sector 2 consists 14.3% of PM_{10} emissions, 1.6% of SO_2 emissions, and 3.4% of NO_x emissions.

Table 3.4 : Emission Totals and Sector Distribution of the 4-km domain.

4km	Sector 1	Sector 2	Sector 34	Sector 5	Sector 6	Sector 7	Sector 8	Sector 9	Sector 10	Sector Total (ton/year)
PM_{10}	31.4 %	17.7 %	35.0%	0.3%	0.0%	1.4%	2.8%	2.2%	9.2%	187,426
SO_2	67.9 %	3.7%	26.1%	0.0%	0.0%	0.2%	2.1%	0.0%	0.0%	107,700
NO_x	24.1 %	4.4%	31.4%	0.0%	0.0%	24.0 %	15.9 %	0.0%	0.1%	388,220

In Figure 3.32 and 3.33, spatial distribution of sector total and sector specific emissions of NO_x emissions are given. In sector total figure (Figure 3.32) of NO_x, it can be seen that emissions are concentrated in mostly in Istanbul, Kocaeli, and Bursa.

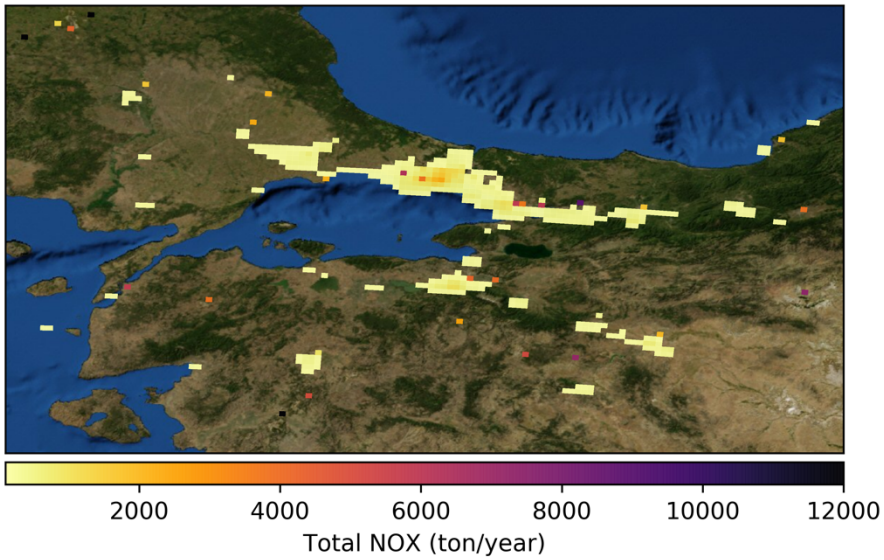

Figure 3.32 : Residential Heating Total NO_x emissions of the 4-km domain.

For the Sector 2 (Figure 3.33) specific emissions, emissions are from densely populated Istanbul. The spatial distribution of these pollutant emissions indicates the effect of residential heating and the surrounding industry. Emission hotspots are mainly residential areas. It is also can be seen from this figure that Bursa is another hotspot of NO_x emissions.

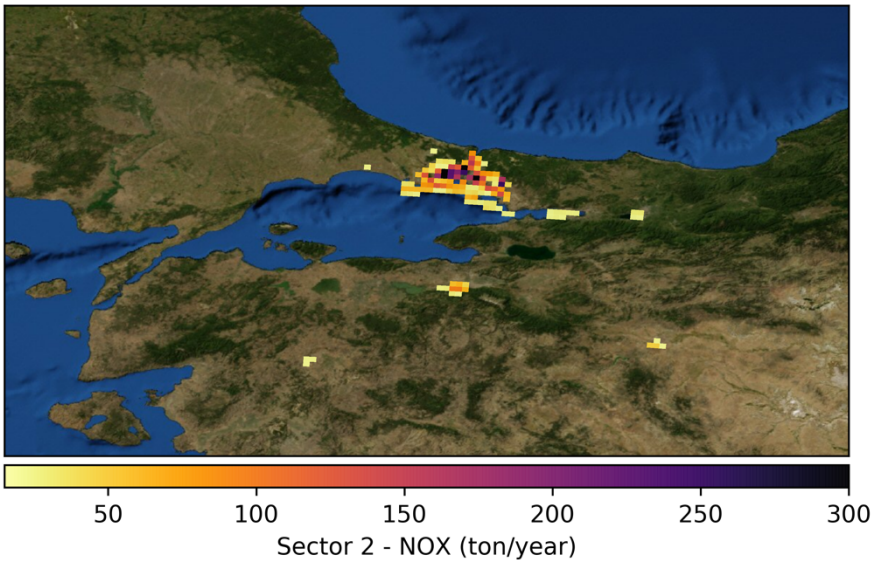

Figure 3.33 : Residential Heating Sector 2 - NO_x emissions of the 4-km domain.

In Figure 3.34 and 3.35, spatial distribution of sector total and sector specific emissions of PM_{10} emissions are given. In sector total figure (Figure 3.34) of PM_{10}, it can be seen that emissions are concentrated in industrialized areas, as high concentration point sources and in Istanbul in form of local area sources such as residential heating.

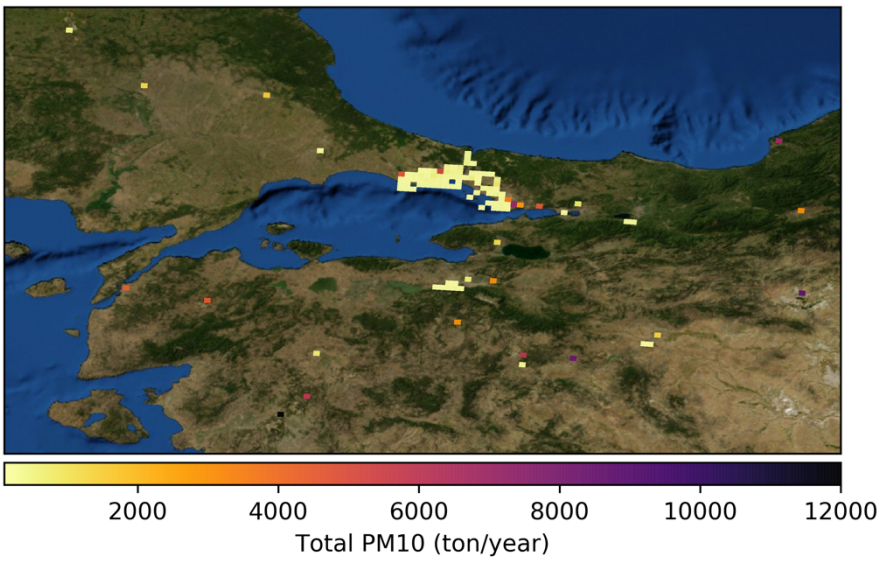

Figure 3.34 : Residential Heating Total PM_{10} emissions of the 4-km domain.

For the Sector 2 (Figure 3.35) specific emissions, emissions are from densely populated big cities; Istanbul, Kocaeli, and Bursa. The spatial distribution of PM_{10} emissions indicates the effect of residential heating and industry.

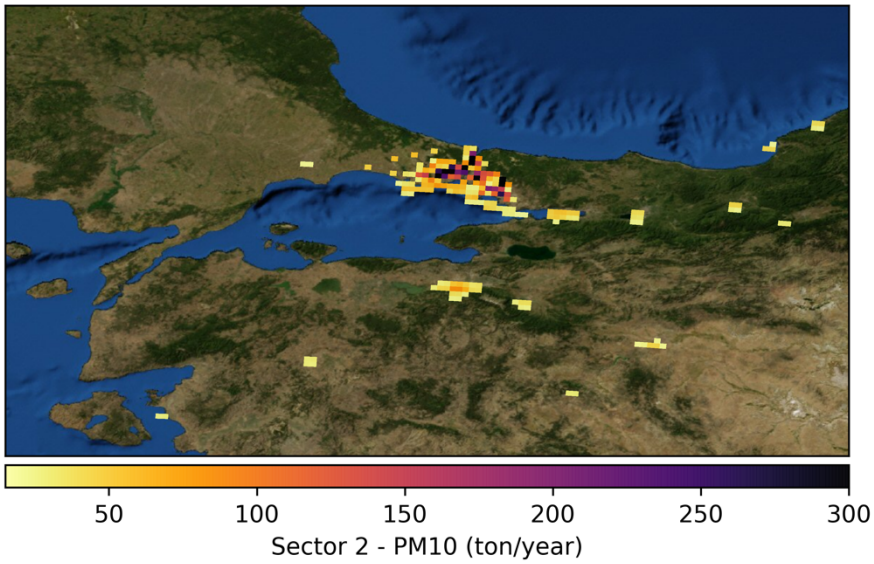

Figure 3.35 : Residential Heating Sector 2 - PM_{10} emissions of the 4-km domain.

In Figure 3.36 and 3.37, spatial distribution of sector total and sector specific emissions of SO_2 emissions are given. In sector total figure (Figure 3.36) of SO_2, it can be seen that emissions are spread over the modeling domain around industrial areas.

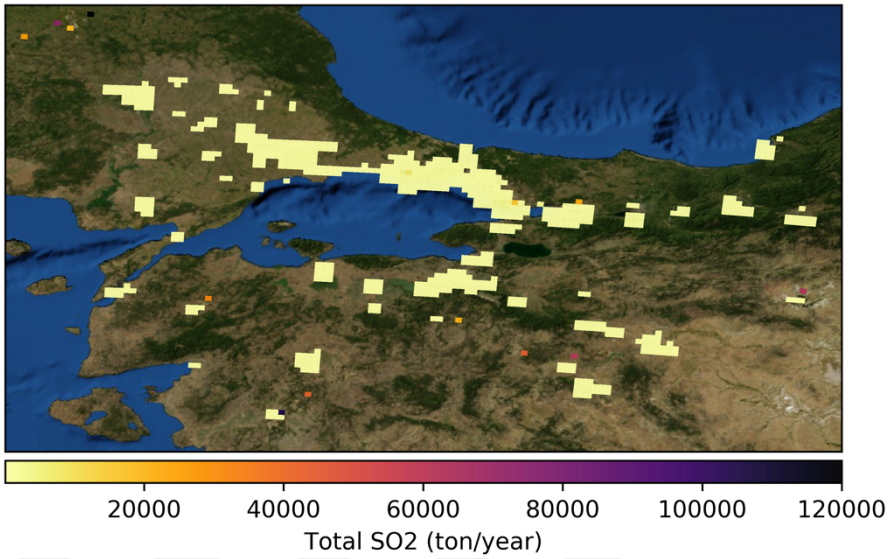

Figure 3.36 : Residential Heating Total SO_2 emissions of the 4-km domain.

For the Sector 2 (Figure 3.37) specific emissions, emissions are from densely populated big cities; Istanbul and Bursa. The spatial distribution of SO_2 emissions indicate the effect of residential heating since they are generally higher in Istanbul's residential areas. With the improvement of high resolution emissions spatial distribution of SO_2 emissions are clearly on residential areas.

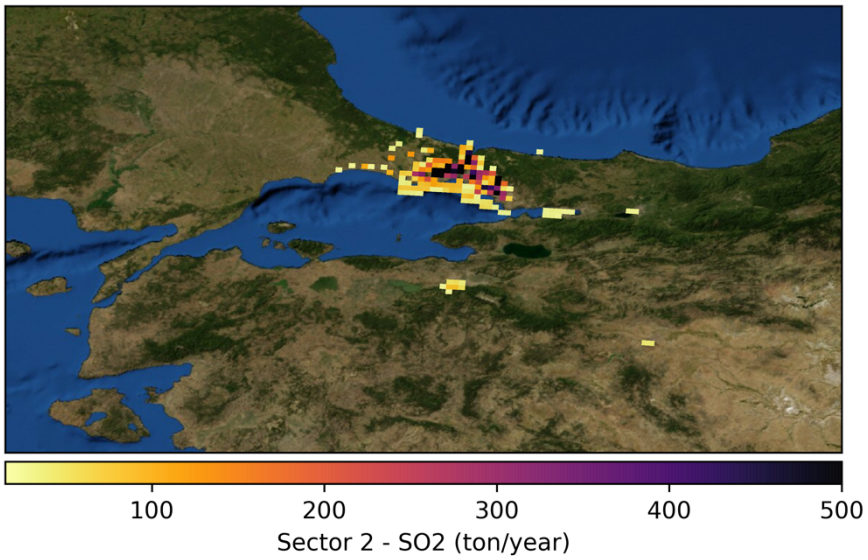

Figure 3.37 : Residential Heating Sector 2 - SO_2 emissions of the 4-km domain.

3.4.3 Residential Heating – Base Case Difference:

For the city of Istanbul both base case and residential heating results were compared. Annual emissions (ton/year) of gas phase species for both scenarios are given in Table 3.4. As it can be seen from this table, Residential Heating case had significantly higher emissions for all pollutants than the Base Case. Residentail Heating emissions of SO_2 were 55.4% higher than Base Case (Table 3.4). Residential Heating emissions of NO_x and PM_{10} were over 22% higher than Base Case emissions (Table 3.4).

Table 3.4 : Emissions of SO_2, NO_x, PM_{10} for the 4 km domain.

	Residential Heating	Difference (%)
NO_x	17,215	24.3
PM_{10}	33,238	22.5
SO_2	39,740	55.4

In Figure (3.38-a), all sector total emissions of Residential Heating case and its spatial distribution are given, while Figure (3.38-b) shows the difference between Base Case and Residential Heating cases.

The SO_2 emission peak for Istanbul was in the southwestern part of the city (3.38-a), Beylikdüzü - Esenyurt provinces, which accounted for 8% (over 5000 ton/year) of the SO_2 emissions in Istanbul. The southeastern part of Istanbul, Sultanbeyli - Kartal province, accounted for 13% (over 4000 ton/year) of the SO_2 emissions in Istanbul.

It should be noted that the other peak that is in the south easternmost part of the map, the grid cell which also has SO_2 emissions over 5000 ton/year, is Gebze province outside of Istanbul city. As it can be seen in Figure 3.38-b, there are no differences for that grid cell since emissions outside of Istanbul are not covered by our high-resolution emissions. From Figure 3.38-b, it can be seen that our inventory had significantly higher (up to 400 ton/year) SO_2 emissions. Distribution of these emissions were in line with residential areas (Figure 3.38-b) indicating that the contribution of SO_2, one of the major causes of particulate matter, was from the residential heating sector.

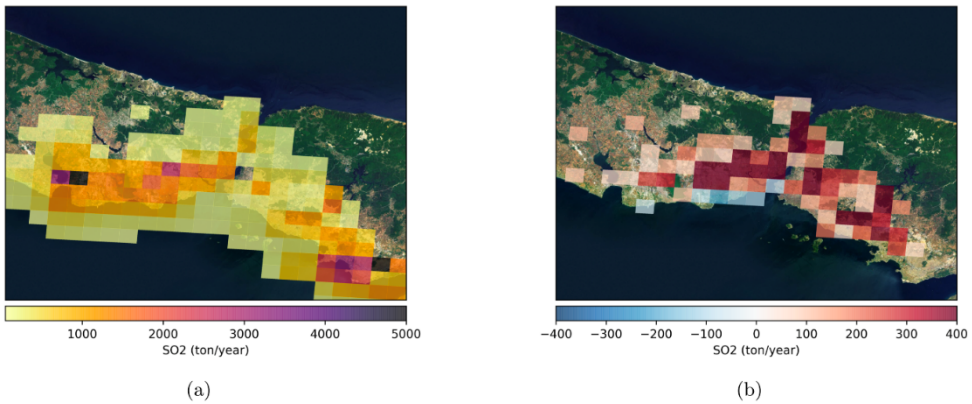

Figure 3.38 : SO_2 Emissions of a) Residential Heating run, b) Difference between two cases.

Difference in the southern part of the Istanbul where Base Case SO_2 emissions are higher than Residential Heating emissions can be attributed to the location. In Bakırköy - Zeytinburnu province, Atatürk Airport is located and base emissions inventory might be erroneously allocating more than the actual amount of emissions to these grid cells.

3.5 Chemical Transport Model

As mentioned in previous sections modeling domain consist of three nested domains; 36x36 km, 12x12 km, and the 4x4 km domain. For the 36 and 12 km domains TNO emissions inventory is used and for the 4-km residential heating run both TNO and our own high-resolution inventory is used with 4-km base case run uses only TNO emissions.

In Figure 3.39, spatial distribution of particulate matter concentrations for the 36-km domain is given. This domain is used primarily for boundary conditions as for the emissions. It can be seen from the figure that particulate matter concentrations are higher on the Middle Eastern part of the domain parallel to emissions. The outermost 36-km concentrations are beyond the scope of this study and we have kept this domain brief while going in detail with inner domains.

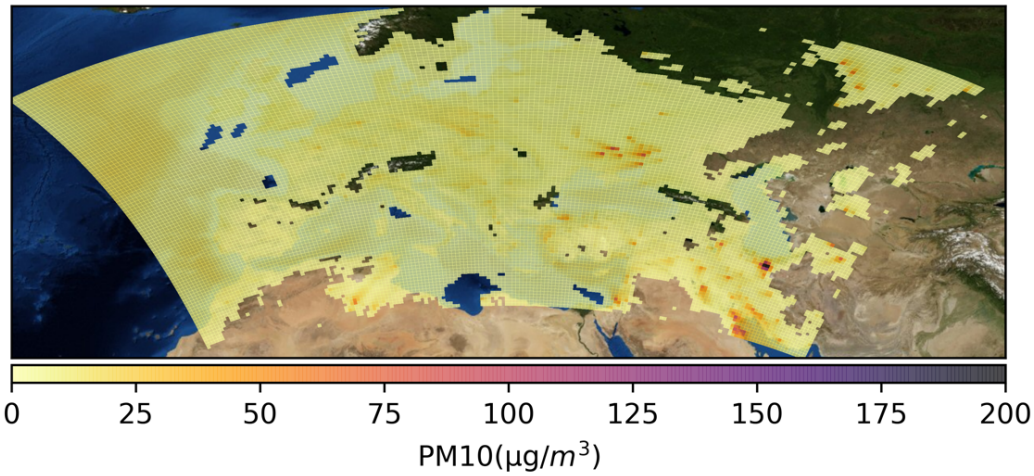

Figure 3.39 : PM_{10} concentrations of the 36-km domain December 4th.

3.5.1 Particulate matter concentrations of 12-km domain

Based on observation data, there are three peak days of particulate matter concentrations in the study period, December 4th, 11th, 15th, 2014. In Figure 3.40, December 4th particulate matter concentrations are given. Domain wide maximum PM_{10} concentration is 189.76 µg/m^3 while mean is 6.77 µg/m^3. Maximum value was in Adana from a point source. Istanbul has the overall highest particulate matter concentrations.

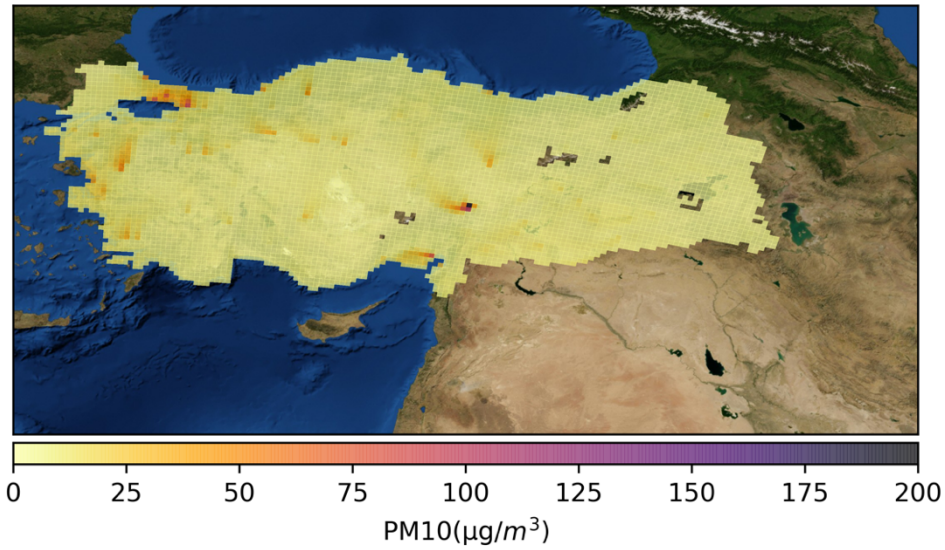

Figure 3.40 : PM_{10} concentrations of the 12-km domain December 4th.

December 11th particulate matter concentrations are given in Figure 3.41. Domain wide maximum PM_{10} concentration is 163.38 µg/m^3 while mean is 7.16 µg/m^3. Maximum

value was in Adana from a point source, same as December 4th. Istanbul has the overall highest particulate matter concentrations.

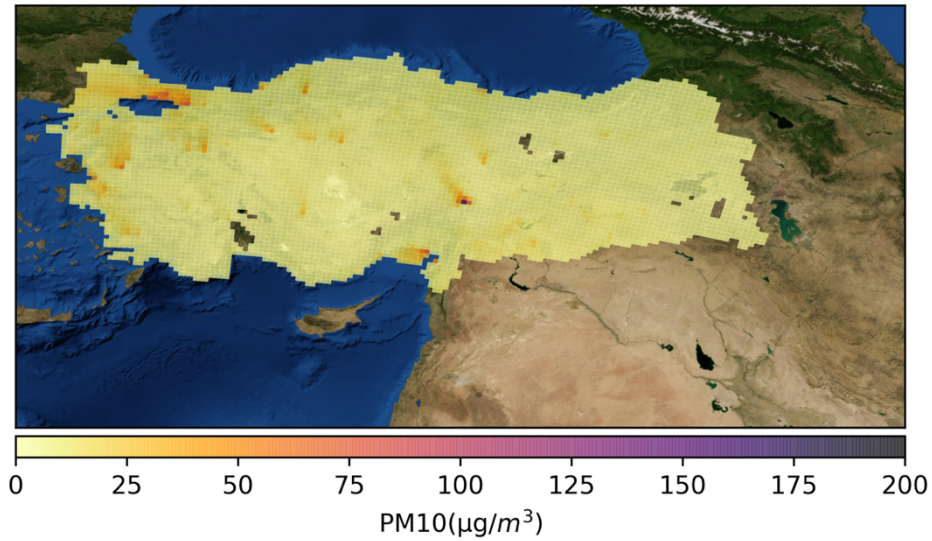

Figure 3.41 : PM_{10} concentrations of the 12-km domain December 11th.

December 15th particulate matter concentrations are given. Domain wide maximum PM_{10} concentration is 107.89 µg/m^3 while mean is 6.12 µg/m^3. Maximum value was in Istanbul and Istanbul has the overall highest particulate matter concentrations. However, on this day particulate matter concentrations are higher on western part of Turkey.

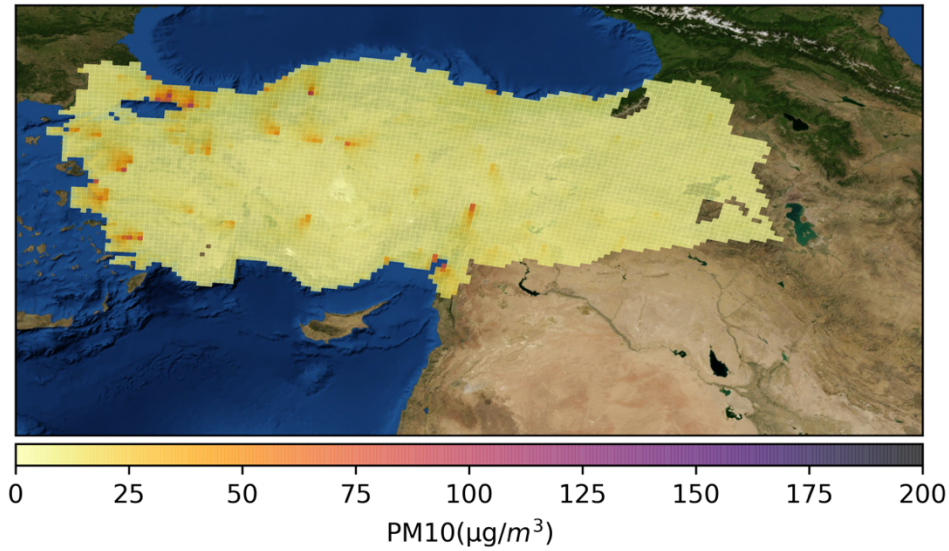

Figure 3.42 : PM_{10} concentrations of the 12-km domain December 15th.

3.5.2 Sub-grid variability of Base Case PM_{10} concentrations

In order to assess the model performance of different modeling domains and grid sizes on Marmara Region we have compared our three modeling domains with each other and observation data from Kartal Station. Reason for the comparison with Kartal station's observation data is this station is the model performance benchmark station for this study.

Firstly, 4x4km domain area and which grid cells they fall in 36x36km and 12x12 domains were found. In the next step, daily mean concentrations of PM_{10} for the duration of the study period was calculated. Finally grid cells that represent the Marmara Region in outer domains are compared to innermost 4-km real Marmara Region domain grid cells to evaluate the performance.

In Figure 3.43, comparison of particulate matter concentrations of outermost domain and innermost domain for Marmara Region. From this figure, it can be seen that compared to 4-km domain 36-km domain produce around 1 $\mu g/m^3$ less PM_{10} concentrations during the study period.

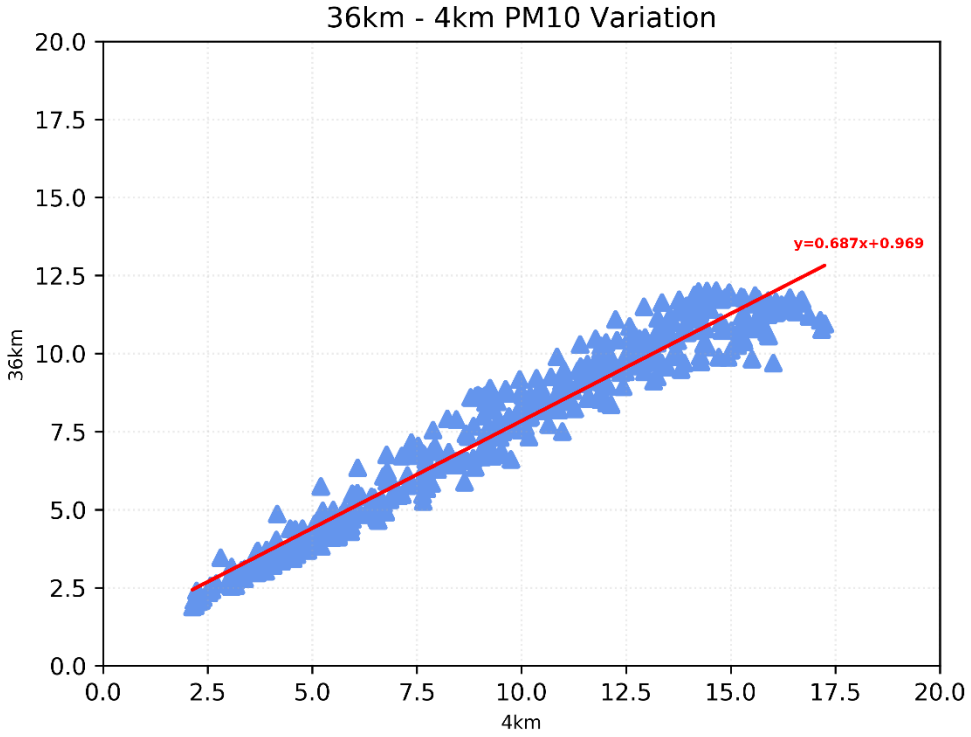

Figure 3.43 : PM_{10} concentrations of the 36 and 4-km domain.

In Figure 3.44, comparison of particulate matter concentrations of 12-km domain and innermost domain for Marmara Region. From this figure, it can be seen that compared

to 4-km domain 12-km domain produce around 0.76 µg/m^3 less PM_{10} concentrations during the study period. However, it should be noted that 12-km domain performs reasonably well for it is size.

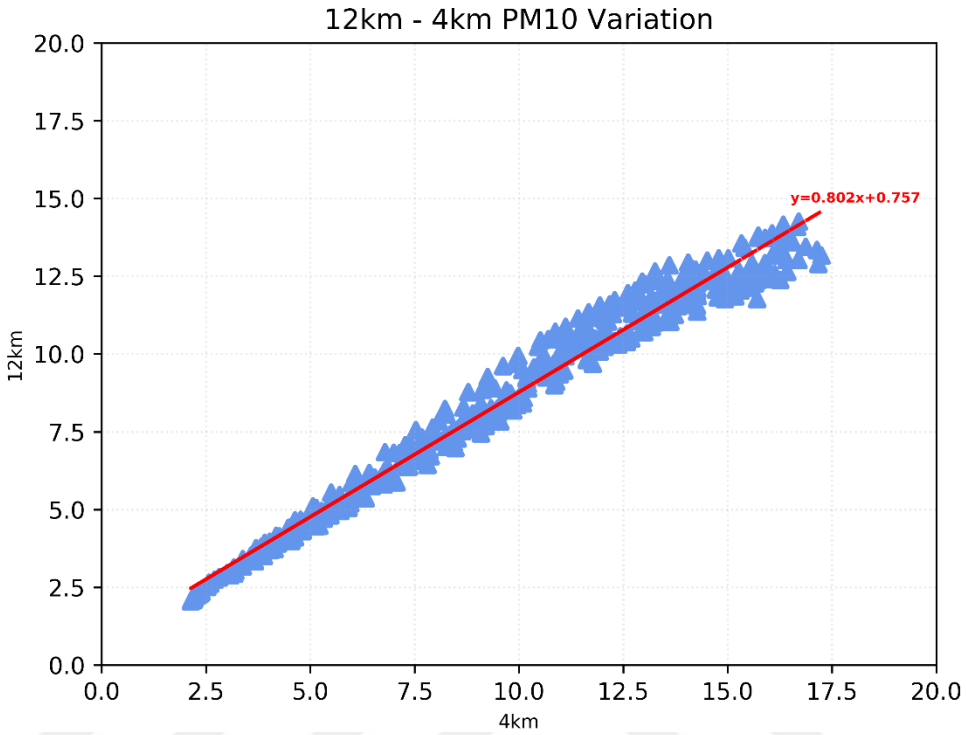

Figure 3.44 : PM_{10} concentrations of the 12 and 4-km domain.

In Figure 3.45, PM_{10} concentrations of all domains for Marmara Region along with Kartal station observation data is given. It can be seen from the figure that 36-km PM_{10} concentrations are always lower, except for the first day, than observed values. 12-km domain has higher concentrations than observations in five days 1st, 2nd, 6th, 8th, 14th. Only on the second day of the month that 12-km concentrations are close to observation. Although 12-km performed reasonably well, it should be noted that 12-km simulations missed all observed particulate matter concentration peaks except for the one on 11th.

Only in 4-km run has the same pattern as the observation and this domain got all the peaks. One reason for 12-km run to miss the observed patter can be attributed to 12x12 grid size and the location it covers. The 12-km domain grid cell that has the Kartal station in it has no water content, meaning it doesn't cover Marmara Sea, while 4-km domain has more than 60% of it is content being Marmara Sea. This is an important difference since CMAQ takes sea salt spray into consideration when it calculates particulate matter concentrations. It is well documented in previous studies that

aerosols from sea salt is a major contributor of particulate matter concentrations in coastal cities, especially megacities like Istanbul.

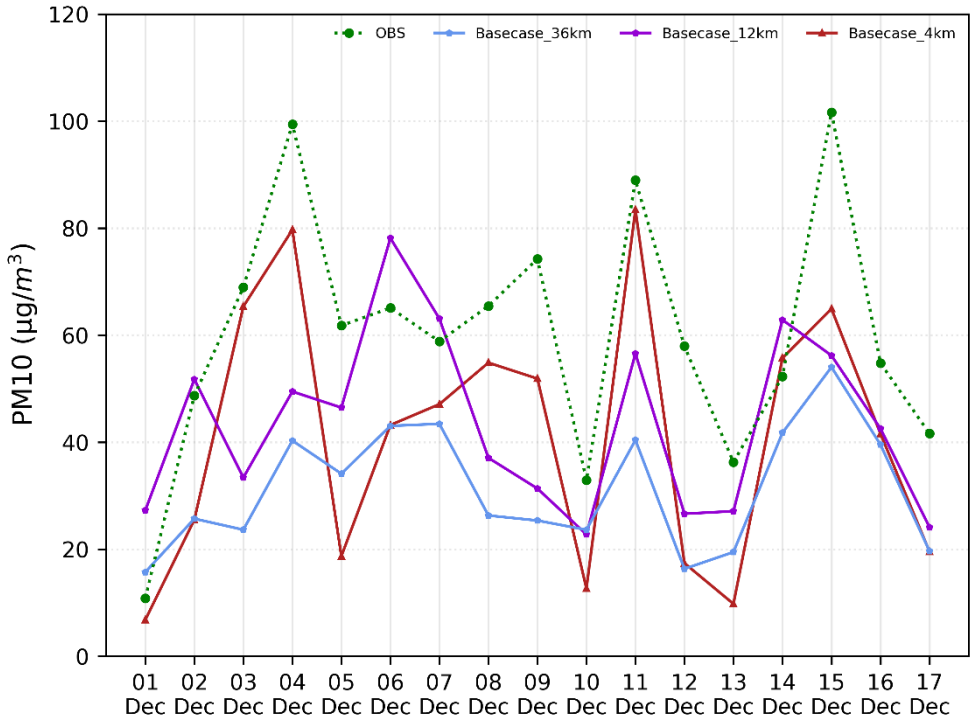

Figure 3.45 : PM_{10} concentrations of all domains and Kartal station observations.

Overall, it can be concluded from subgrid variability comparisons that 4-km domain performs best for its given domain area.

3.5.3 PM_{10} concentrations of 4-km domain

Particulate matter daily mean concentrations over Istanbul for both cases and observation are given in Figure 3.46. During the study period, daily mean PM_{10} concentrations ranged between 10 - 102 µg/m^3 with a mean of 59.9 µg/m^3 (Figure 3.46). Twelve out of seventeen days exceeded the European annual PM_{10} concentration limit value of 50 µg/m^3. The maximum value of 101.6 µg/m^3 occurred on December 15th and minimum of 10.8 µg/m^3 on the first day of December. As it can be seen from Figure 3.46, days with relatively high PBL height, December 1st, 10th, and 13th, had PM values lower than 40 µg/m^3. Days with 300 m and higher PBL value had better mixing and lower concentrations (< 40 µg/m^3). December 4th, 9th, 11th, and 15th were days with relatively higher PM_{10} concentrations (> 70 µg/m^3).

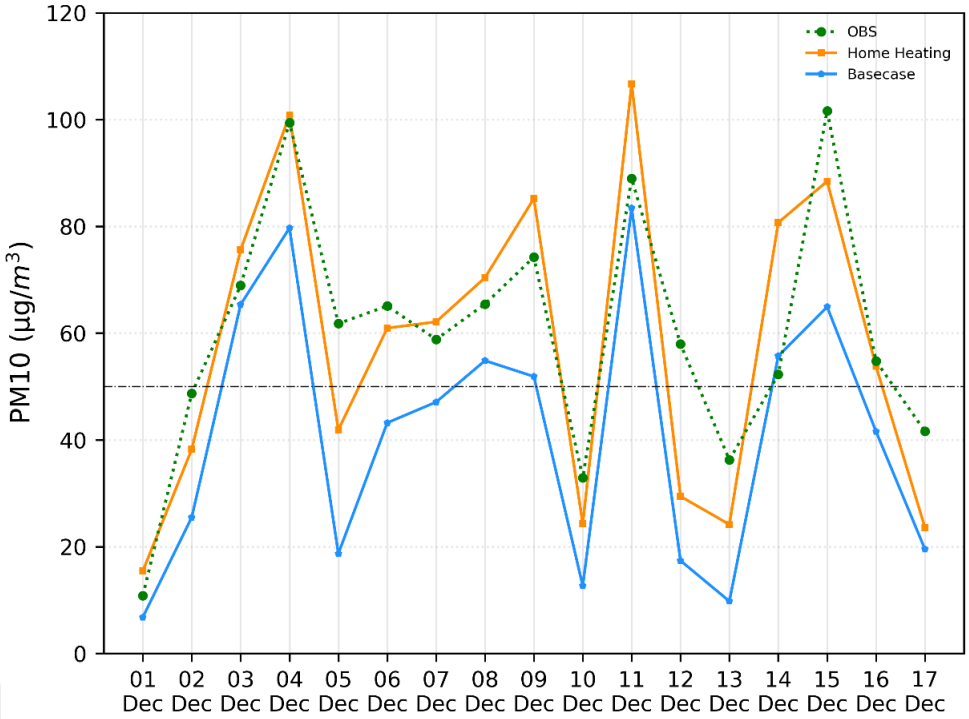

Figure 3.46 : PM_{10} Observation Data and Model Results.

It can be seen in Figure 3.46 that Base Case run underestimated PM_{10} concentrations (MB 18.91 µg/m^3, MAGE 19.32 µg/m^3, and RMSE 22.81 µg/m^3) throughout the study episode while Residential Heating run produced significantly more realistic results (MB 2.23 µg/m^3, MAGE 11.41 µg/m^3, and RMSE 14.15 µg/m^3) suggesting that our high-resolution emissions dramatically improved the performance of the air quality simulation for Istanbul.

Residential Heating model simulations underestimated PM_{10} concentrations throughout the study episode on average by 4.16% while Base Case underestimated PM_{10} concentrations on average by 35.1%. In the Residential Heating case, December 4th and December 16th, PM_{10} concentrations were only less than 2% different than observed PM_{10} values while in the Base Case the difference exceeded 20% for these days.

The highest difference for Residential Heating was on December 14th, which overestimated PM_{10} by 54.4%. The highest difference for Base Case was December 13th, which underestimated PM_{10} by 72.9%. In these days, PBLH was very high during December 13th (> 600 meter) but dropped under 100 meters at midnight and for the following day, December 14th, PBLH is mostly under 200 meters. PBLH might be one of the main reasons to explain the models' poor performance.

Figure 3.47 contains the air quality model output from particulate matter concentrations for December 4th. On this day PBLH and temperature is low and particulate matter concentrations are the second highest after December 15th (Figure 3.49-a).

In Figure 3.47-a, PM_{10} concentrations is given while Figure 3.47-b illustrates the main differences between particulate matter concentrations between two cases. Emissions of the Residential Heating case used local activity data and were spatially distributed using IMM's building information system (Figure 3.47-a) while the Base Case emissions by TNO mostly utilized information from production statistics, experts, international and national organizations and were distributed among the area coarsely due its original grid size.

The difference between these two cases is clear, especially in residential areas of Istanbul (Figure 3.47-b). The highest PM_{10} concentration (over 300 µg/m^3) was Küçükçekmece - Bağcılar provinces, which is a large residential area. The difference between two cases was also the highest in this location with a value of 90 µg/m^3 (Figure 3.47-b).

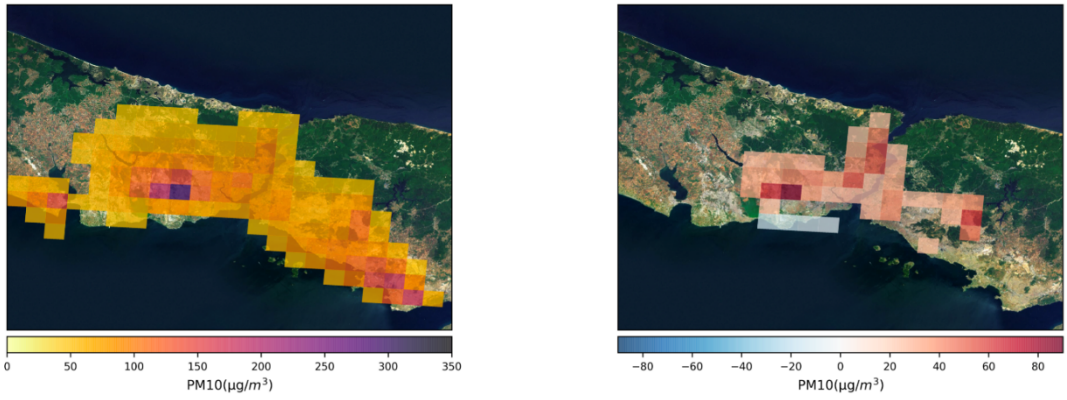

(a) (b)

Figure 3.47 : CMAQ PM_{10} outputs of a) Residential Heating run, b) Difference between two simulations for December 4th, 2014.

In Figure 3.48-a, PM_{10} concentrations is given for December 11th and Figure 3.48-b illustrates the main differences. The highest PM10 concentration (over 250 µg/m^3) was Küçükçekmece - Bağcılar provinces, which is a large residential area. In Figure 3.48-b, difference between two runs are most concentrated over dense residential areas of Istanbul.

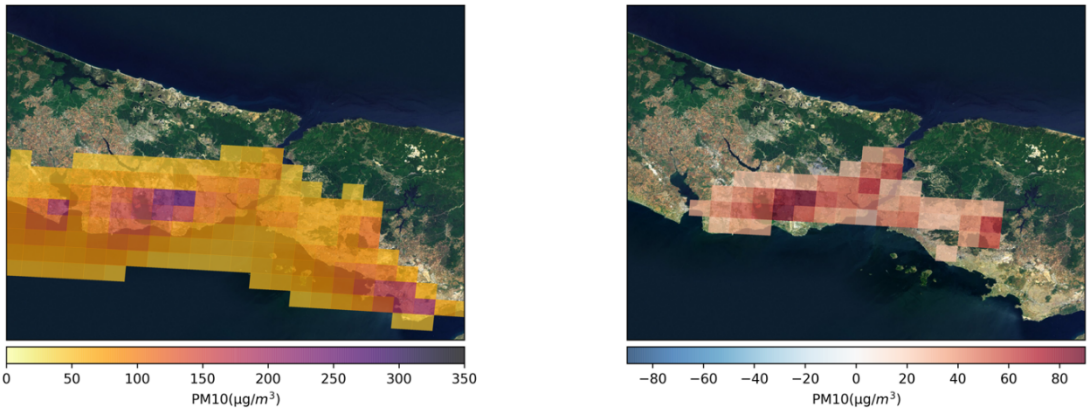

(a) (b)

Figure 3.48 : CMAQ PM_{10} outputs of a) Residential Heating run, b) Difference between two simulations for December 11th, 2014.

In Figure 3.49-a, PM_{10} concentrations is given while Figure 3.49-b illustrates the main differences between particulate matter concentrations between two cases. December 15th is the day with the highest particulate matter concentrations for the study period. The highest PM10 concentration (over 350 μg/m^3) was Küçükçekmece - Bağcılar provinces as with all other peak days. In difference figure (3.49-b), the difference high resolution emissions made is obvious. Spatial distribution of particulate matter concentration difference points at densely populated residential areas of the city.

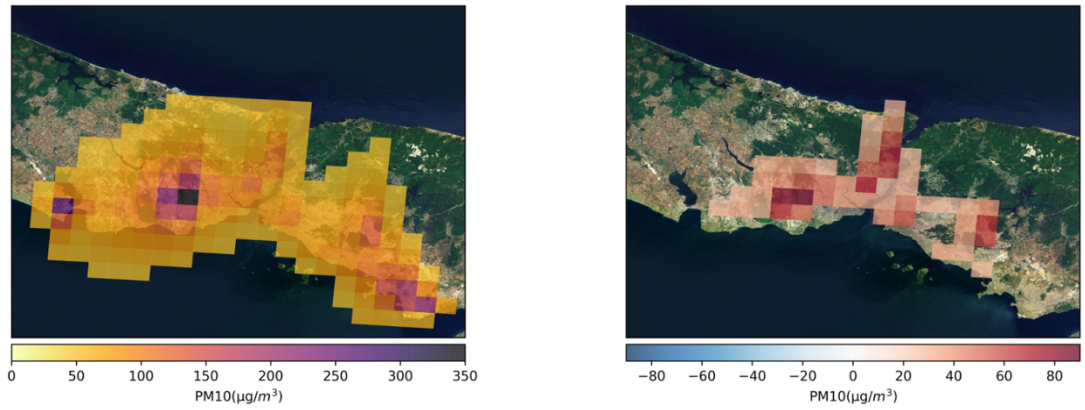

(a) (b)

Figure 3.49 : CMAQ PM_{10} outputs of a) Residential Heating run, b) Difference between two simulations for December 15th, 2014.

From these results, it can be concluded that all of the significant differences were in residential areas, including residential areas along the Bosphorus strait, which is in line with the spatial distribution of emissions. The Base Case run produced more PM_{10}

concentrations around Atatürk Airport only in December 4th, which is located in a less populated residential area. This shows the importance of high-resolution spatial distribution for emissions.

3.5.4 Particulate matter ($PM_{2.5}$) concentrations of 4-km domain

There are limited and only very recent observations of $PM_{2.5}$ concentration data available in Turkey. There are no observation data for $PM_{2.5}$ concentrations in Kartal station. However, air quality model-produced $PM_{2.5}$ values were compared (Figure 3.50) between two runs. As it can be seen in Figure 3.50, Residential Heating produced 69.5% higher $PM_{2.5}$ concentrations on average than Base Case.

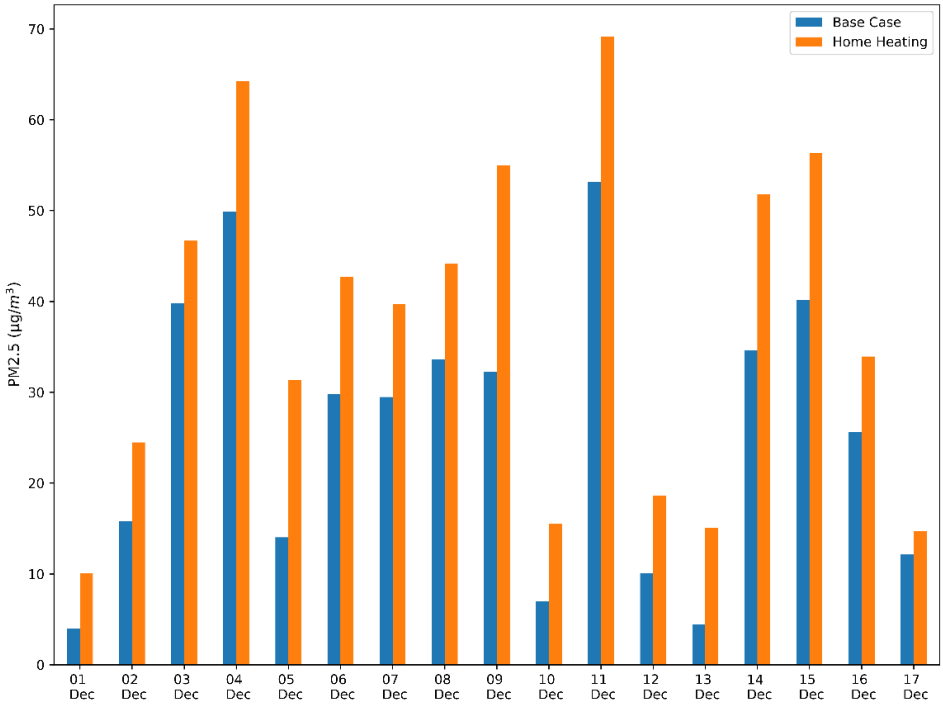

Figure 3.50 : Comparison of $PM_{2.5}$ values of Residential Heating and Base Case.

Chemical species that form $PM_{2.5}$ concentrations are given in Figure 3.51-a (Residential Heating) and in Figure 3.51-b (Base Case).

In the Residential Heating case, major components of $PM_{2.5}$ concentrations were; SO_4 (32.7%), NH_4 (11.0%), Organic Matter (11.0%), and Elemental Carbon (EC) (8.10%) (Figure 3.51-a) while for Base Case it is; SO_4 (33.8%), NH_4 (12.5%), Organic Matter (9.65%), and EC (7.27%) (Figure 3.51-b). Residential Heating produced 61.5% more SO_4 than Base Case.

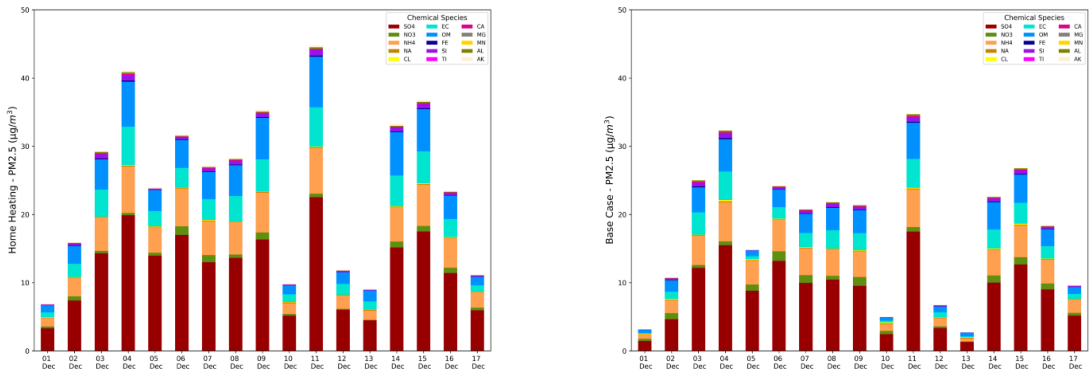

(a) (b)

Figure 3.51 : Chemical Species of PM2.5 of a) Residential Heating, b) Base Case.

The particulate matter and sulfate aerosol concentrations difference between two simulations can be attributed to the difference in SO_2 emissions. Concentrations were significantly higher for Residential Heating, which might be the result of residential heating emissions, mostly coal combustion. However, it should be noted that lack of observation and measurement data makes it difficult to reach solid conclusions about that origin of the difference between the scenario runs. Implication of the results of this study is that residential heating is influencing the concentration of particulate matter in Istanbul during winter time.

4. CONCLUSIONS

The PM_{10} levels in Turkey with a focus on megacity Istanbul are investigated using a mesoscale air quality modeling system, consisting of WRF v3.8.1 meteorological model, DUMANpy emission model, and CMAQ v5.2 model for the winter of 2015. Three nested domains are used; a 36x36 km European domain, 12x12 km Turkey domain, and 4x4 km Marmara domain. In order to assess the performance of modeling domains on one of the major area of interests of the study subgrid variability was analyzed. Results of this analysis showed that for Marmara Region the innermost 4x4 km domain performs better than the coarser domains.

In order to create model ready, temporal (hourly), spatial (at domain resolution), speciated, emissions an emission processor model (DUMANpy) similar to the US EPA SMOKE was written in Python programming langauge. This emissions model was used to create high resolution anthropogenic emissions for Turkey. Emissions of the Residential Heating case used local activity data and were spatially distributed using IMM's building information system.

Wintertime is when the residential heating sector is mainly a factor for regional air quality. The study period, first 17 days of December 2014, is below the HDD threshold temperature value, meaning increased residential heating sector activity and in turn increased SO_2 emissions from most likely coal combustion.

Our study showed that replacing the residential heating sector emissions, of available emissions inventories, with our high-resolution emissions would significantly improve the spatial distribution and concentration, specifically on December 4^{th}, 7^{th} 8^{th}, and 16^{th}, when the difference between observed PM_{10} concentrations were under 10% of air pollutants for Istanbul.

Air quality model simulations with our spatially distributed high-resolution emissions produced more realistic results (MB 2.23 $\mu g/m^3$, RMSE 14.15 $\mu g/m^3$) than the currently existing base emissions inventory, which underestimates PM_{10}

concentrations by 35.1% on average and 4.16% by our high-resolution inventory throughout the study period.

In country wide perspective, anthropogenic emission hotspots, in Turkey domain, indicate the importance of high resolution local emissions for anthropogenic emissions sectors for cities with high population, especially in western Turkey where contribution of industry to air pollution is significant.

Overall, WRF/CMAQ modeling system present satisfactory results for the Turkey and Marmara domain. However, it should be noted that air pollution is a complex problem with many components. Further studies using higher resolution anthropogenic emission inventories based on local activity data for different emission sectors and air quality model evaluation studies for longer periods are important to improve emission control and air quality strategies in Turkey.

REFERENCES

Akhtar, U. S., Rastogi, N., McWhinney, R. D., Urch, B., Chow, C. W., Evans, G. J., & Scott, J. A. (2014). The combined effects of physicochemical properties of size-fractionated ambient particulate matter on in vitro toxicity in human A549 lung epithelial cells. Toxicology Reports, 1(December), 145–156. https://doi.org/10.1016/j.toxrep.2014.05.002

Alapaty, K., Herwehe, J. A., Otte, T. L., Nolte, C. G., Bullock, O. R., Mallard, M. S., … Dudhia, J. (2012). Introducing subgrid-scale cloud feedbacks to radiation for regional meteorological and climate modeling. Geophysical Research Letters, 39(24), 1–5. https://doi.org/10.1029/2012GL054031

Atkinson, R. W., Anderson, H. R., Sunyer, J., Ayres, J., Baccini, M., Vonk, J. M., … Katsouyanni, K. (2001). Acute effects of particulate air pollution on respiratory admissions: Results from APHEA 2 project. American Journal of Respiratory and Critical Care Medicine, 164(10 I), 1860–1866. https://doi.org/10.1164/rccm2010138

Binkowski, F. S., & Shankar, U. (1995). The Regional Particulate Matter Model: 1. Model description and preliminary results. Journal of Geophysical Research, 100(D12), 26191. https://doi.org/10.1029/95JD02093

Brook, R. D., Franklin, B., Cascio, W., Hong, Y., Howard, G., Lipsett, M., … Tager, I. (2004). Air pollution and cardiovascular disease: A statement for healthcare professionals from the expert panel on population and prevention science of the American Heart Association. Circulation, 109(21), 2655–2671. https://doi.org/10.1161/01.CIR.0000128587.30041.C8

Chang, J. S., Brost, R. A., Isaksen, I. S. A., Madronich, S., Middleton, P., Stockwell, W. R., & Walcek, C. J. (1987). A three-dimensional Eulerian acid deposition model: Physical concepts and formulation. Journal of Geophysical Research, 92(D12), 14681–14700. https://doi.org/10.1029/JD092iD12p14681

Coats Jr, C. J. (1996). High-performance algorithms in the Sparse Matrix Operator Kernel Emissions (SMOKE) modeling system, 584–588.

Colette, A., Andersson, C., Manders, A., Mar, K., Mircea, M., Pay, M. T., … Wind, P. (2017). EURODELTA-Trends, a multi-model experiment of air quality hindcast in Europe over 1990-2010. Geoscientific Model Development, 10(9), 3255–3276. https://doi.org/10.5194/gmd-10-3255-2017

Crippa, M., Janssens-Maenhout, G., Dentener, F., Guizzardi, D., Sindelarova, K., Muntean, M., … Granier, C. (2016). Forty years of improvements in European air quality: Regional policy-industry interactions with global impacts. Atmospheric Chemistry and Physics, 16(6), 3825–3841. https://doi.org/10.5194/acp-16-3825-2016

Dai, L., Zanobetti, A., Koutrakis, P., & Schwartz, J. D. (2014). Associations of Fine Particulate Matter Species with Mortality in the United States: A Multicity Time-Series Analysis, 122(8), 837–842. https://doi.org/10.1289/ehp.1307568

Development, (2017). CMAQ. https://doi.org/10.5281/ZENODO.1167892

Dudhia, J. (1989). Numerical Study of Convection Observed during the Winter Monsoon Experiment Using a Mesoscale Two-Dimensional Model. Journal of the Atmospheric Sciences. https://doi.org/10.1175/1520-0469(1989)046<3077:NSOCOD>2.0.CO;2

EMEP/CEIP. (2014). EMEP database Retrieved from http://www.ceip.at/webdab_emepdatabase/reported_emissiondata/

Emery, C., Edward, T., & Yarwood, G. (2001). Enhanced meteorological modeling and performance evaluation for two Texas ozone episodes.

Franklin, M., Koutrakis, P., & Schwartz, P. (2008). The role of particle composition on the association between PM2.5 and mortality. Epidemiology (Cambridge, Mass.), 19(5), 680–9. Retrieved from http://www.ncbi.nlm.nih.gov/pubmed/18714438

Ghio, A. J., Carraway, M. S., & Madden, M. C. (2012). Composition of Air Pollution Particles and Oxidative Stress in Cells, Tissues, and Living Systems. Journal of Toxicology and Environmental Health, Part B, 15(1), 1–21. https://doi.org/10.1080/10937404.2012.632359

Guenther, A. B., Jiang, X., Heald, C. L., Sakulyanontvittaya, T., Duhl, T., Emmons, L. K., & Wang, X. (2012). The Model of Emissions of Gases and Aerosols from Nature version 2.1 (MEGAN2.1): an extended and updated framework for modeling biogenic emissions. Geoscientific Model Development, 5(6), 1471–1492. https://doi.org/10.5194/gmd-5-1471-2012

Haltiner, G.J. and Williams, R. T. (1980). Numerical Prediction and Dynamic Meteorology. 2nd Edition.

Herwehe, J. A., Alapaty, K., Spero, T. L., & Nolte, C. G. (2014). Increasing the credibility of regional climate simulations by introducing subgrid-scale cloud-radiation interactions. Journal of Geophysical Research, 119(9), 5317–5330. https://doi.org/10.1002/2014JD021504

Hong, S.-Y., Dudhia, J., & Chen, S.-H. (2004). A Revised Approach to Ice Microphysical Processes for the Bulk Parameterization of Clouds and Precipitation. Monthly Weather Review, 132(1), 103–120. https://doi.org/10.1175/1520-0493(2004)132<0103:ARATIM>2.0.CO;2

Hong, S.-Y., Noh, Y., & Dudhia, J. (2006). A New Vertical Diffusion Package with an Explicit Treatment of Entrainment Processes. Monthly Weather Review, 134(9), 2318–2341. https://doi.org/10.1175/MWR3199.1

Im, U., Markakis, K., Koçak, M., Gerasopoulos, E., Daskalakis, N., Mihalopoulos, N., … Kanakidou, M. (2012). Summertime aerosol chemical composition in the Eastern Mediterranean and its sensitivity to temperature. Atmospheric Environment, 50, 164–173.

Im, U., Markakis, K., Unal, A., Kindap, T., Poupkou, A., Incecik, S., … Mihalopoulos, N. (2010). Study of a winter PM episode in Istanbul using the high resolution WRF/CMAQ modeling system. Atmospheric Environment, 44(26), 3085–3094.

Im, U., Poupkou, A., Incecik, S., Markakis, K., Kindap, T., Unal, A., … Guler, M. (2011). The impact of anthropogenic and biogenic emissions on surface ozone concentrations in Istanbul. Science of the Total Environment, 409(7), 1255–1265. https://doi.org/10.1016/j.scitotenv.2010.12.026

Ito, K., Mathes, R., Ross, Z., Nádas, A., Thurston, G., & Matte, T. (2011). Fine particulate matter constituents associated with cardiovascular hospitalizations and mortality in New York City. Environmental Health Perspectives, 119(4), 467–73. https://doi.org/10.1289/ehp.1002667

Kindap, T. (2008). Identifying the trans-boundary transport of air pollutants to the city of Istanbul under specific weather conditions. Water, Air & Soil Pollution, 189, 279–289.

Kindap, T., Unal, A., Chen, S. H., Hu, Y., Odman, M. T., & Karaca, M. (2006). Long-range aerosol transport from Europe to Istanbul, Turkey. Atmospheric Environment, 40(19), 3536–3547. https://doi.org/10.1016/j.atmosenv.2006.01.055

Kuenen, J. J. P., Visschedijk, A. J. H., Jozwicka, M., & Denier Van Der Gon, H. A. C. (2014). TNO-MACC-II emission inventory; A multi-year (2003-2009) consistent high-resolution European emission inventory for air quality modelling. Atmospheric Chemistry and Physics, 14(20), 10963–10976. https://doi.org/10.5194/acp-14-10963-2014

Markakis, K., Im, U., Unal, A., Melas, D., Yenigun, O., & Incecik, S. (2012). Compilation of a GIS based high spatially and temporally resolved emission inventory for the greater Istanbul area. Atmospheric Pollution Research, 3(1), 112–125. https://doi.org/10.5094/APR.2012.011

Middleton, N., Yiallouros, P., Kleanthous, S., Kolokotroni, O., Schwartz, J., Dockery, D. W., & Demokritou, P. (2008). A 10-year time-series analysis of respiratory and cardiovascular morbidity in Nicosia, Cyprus: the effect of short-term changes in air pollution and dust storms. Environmental Health, 7(1), 39. https://doi.org/10.1186/1476-069X-7-39

Mlawer, E. J., Taubman, S. J., Brown, P. D., Iacono, M. J., & Clough, S. A. (1997). Radiative transfer for inhomogeneous atmospheres: RRTM, a validated correlated-k model for the longwave. Journal of Geophysical Research: Atmospheres, 102(D14), 16663–16682. https://doi.org/10.1029/97JD00237

Ozdemir, H., Pozzoli, L., Kindap, T., Demir, G., Mertoglu, B., Mihalopoulos, N., … Unal, A. (2014). Spatial and temporal analysis of black carbon aerosols in Istanbul megacity. Science of the Total Environment, 473–474, 451–458. https://doi.org/10.1016/j.scitotenv.2013.11.102

Ozdemir, H., Unal, A., Kindap, T., Turuncoglu, U. U., Durmusoglu, Z. O., Khan, M., … Karaca, M. (2012). Quantification of the urban heat island under a changing climate over Anatolian Peninsula. Theoretical and Applied Climatology, 108(1–2), 31–38.

Pleim, J. E., & Chang, J. S. (1992). A non-local closure model for vertical mixing in the convective boundary layer. Atmospheric Environment. Part A. General Topics, 26(6), 965–981. https://doi.org/10.1016/0960-1686(92)90028-J

Powers, J. G., Klemp, J. B., Skamarock, W. C., Davis, C. A., Dudhia, J., Gill, D. O., … Duda, M. G. (2017). The weather research and forecasting model: Overview, system efforts, and future directions. Bulletin of the American Meteorological Society, 98(8), 1717–1737. https://doi.org/10.1175/BAMS-D-15-00308.1

Puett, R. C., Hart, J. E., Yanosky, J. D., Spiegelman, D., Wang, M., Fisher, J. A., … Laden, F. (2014). Particulate Matter Air Pollution Exposure, Distance to Road, and Incident Lung Cancer in the Nurses' Health Study Cohort. Environ Health Perspect, 122(9), 926–932. https://doi.org/10.1289/ehp.1307490

Skamarock, W. C., Klemp, J. B., Dudhi, J., Gill, D. O., Barker, D. M., Duda, M. G., … Powers, J. G. (2008). A Description of the Advanced Research WRF Version 3. Technical Report, (June), 113. https://doi.org/10.5065/D6DZ069T

Spinoni, J., Vogt, J., & Barbosa, P. (2015). European degree-day climatologies and trends for the period 1951-2011. International Journal of Climatology, 35(1), 25–36. https://doi.org/10.1002/joc.3959

Status Report 1/2016, E. (2016). Transboundary particulate matter, photo-oxidants, acidifying and eutrophying components, EMEP Status Report 2016; September 13, 2016.

Tewari, M., Chen, F., Wang, W., Dudhia, J., LeMone, M. A., Mitchell, K., … Cuenca, R. H. (2004). Implementation and verification of the unified noah land surface model in the WRF model. Bulletin of the American Meteorological Society, 2165–2170. https://doi.org/10.1007/s11269-013-0452-7

Theodosi, C., Im, U., Bougiatioti, A., Zarmpas, P., Yenigun, O., & Mihalopoulos, N. (2010). Aerosol chemical composition over Istanbul. Science of the Total Environment, 408(12), 2482–2491. https://doi.org/10.1016/j.scitotenv.2010.02.039

US EPA. (1996). Air Quality Criteria for Particulate Matter Volume II of III. Environmental Protection, II(April), 1148. https://doi.org/10.1039/b007792p

Yarwood, G., Jung, J., Whitten, G. Z., Heo, G., Mellberg, J., & Estes, M. (2010). Updates to the Carbon Bond Mechanism for Version 6 (CB6). Presented at the 9th Annual CMAS Conference, Chapel Hill, NC, October 11-13, 6(415), 1–4.

Ye, D., Klein, M., Mulholland, J. A., Russell, A. G., Weber, R., Edgerton, E. S., … Ebelt Sarnat, S. (2018). Estimating Acute Cardiovascular Effects of Ambient PM2.5 Metals. Environmental Health Perspectives, 126(2), 027007. https://doi.org/10.1289/EHP2182

Zheng, Y., Alapaty, K., Herwehe, J. A., Del Genio, A. D., & Niyogi, D. (2016). Improving High-Resolution Weather Forecasts Using the Weather Research and Forecasting (WRF) Model with an Updated Kain–Fritsch Scheme. Monthly Weather Review, 144(3), 833–860. https://doi.org/10.1175/MWR-D-15-0005.1

CURRICULUM VITAE

Name Surname **:** Metin BAYKARA

Place and Date of Birth **:** 29.10.1987, Şişli / İstanbul

E-Mail **:** baykara@itu.edu.tr

EDUCATION **:**

- **B.Sc.** **:** 2011, Karadeniz Technical University, Forestry
- **M.Sc.** **:** 2013, Karadeniz Technical University, Soil Science

PUBLICATIONS, PRESENTATIONS AND PATENTS ON THE THESIS:

- **Baykara M.,** Im, U., and Unal, A. (2018). Evaluation of impact of residential heating on air quality of megacity Istanbul by CMAQ. Science of the Total Environment. 651. 10.1016/j.scitotenv.2018.10.091.

OTHER PUBLICATIONS, PRESENTATIONS AND PATENTS:

- Kara Ö. and **Baykara M**., 2014, "Changes in Soil Microbial Biomass and Aggregate Stability Under Different Land Uses in the Northeastern Turkey", Environmental Monitoring and Assessment, vol.186, pp.3801-3808, DOI: 10.1007/s10661-014-3658-0
- **Baykara, M.** 2015, Evaluation of Impact of Biogenic Emissions on Secondary Organic Aerosols and Ozone Using MEGAN v2.1 and NEMO over Europe, CMAS Conference, North Carolina